Fall 12-18-2015

Acute Methamphetamine Exposure Affects Histone Modifying Enzymes and Cytokine Production in Macrophages

Ariel Burns
University of Nebraska Medical Center

Tell us how you used this information in this short survey.

Follow this and additional works at: https://digitalcommons.unmc.edu/etd

Part of the Cell Biology Commons

Acute Methamphetamine Exposure Affects Histone Modifying

Enzymes and Cytokine Production in Macrophages

by

Ariel Burns

A DISSERATION

Presented to the Faculty of the

University of Nebraska Graduate School

In Partial Fulfillment of the Requirements for the

Degree of Doctor of Philosophy

Pharmacology and Experimental Neuroscience

Graduate Program

Under the Supervision of Professor Pawel Ciborowski

University of Nebraska Medical Center

Omaha, Nebraska

November, 2015

Supervisory Committee

Howard Fox, M.D., Ph.D.   David McMilan, Ph.D.

Keshore Bidasee, Ph.D.   Michael Belshan, Ph.D.

ACKNOWLEDGEMENTS

Neuroscience department and chose my application for an interview to which I was accepted and able to fulfill my dream. He is also a great listener when courses were not going well or I needed advice on how to navigate through difficult graduate school situations. Obviously, I am in debt to the great instructors and all the mentors here at UNMC. Although there are too many to mention, they provided me with the foundation needed to prepare me for my graduate research work.

At the beginning of this adventure was fellow department recruits Pavan Puligujja and Aditya Bade. While there were other students who joined with us, some did not make it but the three of us stuck together making sure that we would be successful in classes, in research, in accomplishing the necessary graduate requirements, and even encouraging in each other about our future endeavors and aspirations. Thousands of hours spent at school and outside, so many laughs, tears (all from me), and most importantly support from these two was a blessing. Without a doubt, I can admit that I would not have made it through my Ph.D. without these two lifting my spirits up and pushing me forward. Other great people that I spent almost every day with were my "lunch buddies". The group changed many times over the years as people moved away, got different jobs, or started medical school but most notably is Jacklyn Hollinger and Dr. Shantanu Balkundi.

Another large part of my time at UNMC was spent in the laboratory and I can honestly say that I joined the Proteomics Lab because of the members that were in it: Jayme Weiderin, Teena Jagadish, Dr. Gwenael Pottiez, and fellow graduate student Nicole Haverland. All of them were and are so friendly, helpful, and fun, making the decision of which lab to join quite easy. Next, a warm thank you goes out to all of the administration staff in the Pharmacology and Experimental Neuroscience department: Theresa Grutel, Sandy Mahoney, Kim Morrison, Robin Taylor, Connie, Leticia Tran, Johna Belling, and Julie Ditter. These women are extremely supportive and take pride in

helping the students succeed in any way they can. They work so hard and well that I think they should get a raise. I believe that they are the best administration staff in the entire UNMC and I know for certain that they are the best administration staff of all the graduate departments. It was always a pleasure to spend time in the office chatting and catching up with these ladies.

Last but not least are my friends from before UNMC. Psychologist claim that if you have a friend more than seven years that you will remain friends for life. That is the case for my friends Jackie Frank (19 year friendship), Tamara Allred (15 years), Katie Clowers (11 years), Amanda Roodhouse (11 years), and Monica Washington (6 years). I am so proud to call them my friends and the fact that they are proud of me and my accomplishments is energizing. Many of these women helped shaped me into the person I am and also accepted the crazy person I was. Interestingly, one my newer friends, Jessica Wooden, I met while at UNMC and we became best friends instantly. Our relationship is so strong that people mistake us as sisters. We are so much alike that although I have only known her for about two years it feels like I have known her my whole life. Just so all you lovely ladies know and it is now written and forever documented, I love you dearly!

Finally, to anyone I may have missed, I apologize. I appreciate everyone who has supported, encouraged, and motivated me to fulfill this dream. Thank you so much.

Ariel Burns

University of Nebraska Medical Center

November 2015

Acute Methamphetamine Exposure Effects Histone Modifying Enzymes and Cytokine Production in Macrophages

Ariel Burns, Candidate for the Doctor of Philosophy Degree

University of Nebraska Medical Center, 2015

ABSTRACT

The effects of methamphetamine (Meth) in the periphery are not well studied and a comprehensive investigation on the effects and molecular mechanism will give insight into why Meth users are at an increased risk of infections. For this reason, we use macrophages as a model for the immune system dysregulation seen in Meth abusers and also because macrophages are a long-lived cell that HIV infects and persists in. We aimed to determine the effects of Meth on the cytokine production, histone modifying enzymes and the corresponding histone post-translational modifications, and the molecular mechanism in HIV-infected human macrophages treated with combination antiretroviral therapy.

We measured a total of six histone deacetylases (HDACs) and found that Meth decreases HDAC1 but not in HIV or HIV and Meth. Combinational antiretroviral therapy also did not seem to have an effect on any HDACs measured. The decrease in HDAC1 correlated to an increase in acetylation of HDAC1 histone targets, histone 4 lysine 5 and histone 3 lysine 18. Next, we determined that Meth induces a time-dependent and concentration dependent change in cytokine expression. Furthermore, Meth generated a rapid induction of pro-inflammatory cytokines at two hours and maintained until 6 hours post exposure. Subsequently, we expanded on where Meth could be affecting the TLR9 signaling pathway to support the result of altered cytokine production by looking at DNA methylation, presence of transcription factors, and TLR9-mediated signaling mediators.

In conclusion, Meth decreases HDAC1, modifies cytokine production in macrophages leading to a pro-inflammatory phenotype.

TABLE OF CONTENTS

LIST OF FIGURES

LIST OF TABLES

LIST OF ABBREVIATIONS

AIDS	Acquired immunodeficiency syndrome
ATV	Atazanavir
BBB	Blood-brain barrier
cART	Combinational antiretroviral therapy
CCL	Chemokine (C-C motif) ligand
cDNA	Complementary deoxyribonucleic acid
CNS	Central nervous system
CpG	Cytosine phosphodiester guanine
CT	Cycle threshold
DAT	Dopamine transporters
DNA	Deoxyribonucleic acid
FTC	Emtricitabine
GAPDH	Glyceraldehyde 3-phosphate dehydrogenase
HAT	Histone acetyltransferase
HDAC	Histone deacetylase
HEPES	4-(2-hydroxyethyl)-1-piperazineethanesulfonic acid
HIV	Human immunodeficiency virus
HRP	Horseradish peroxidase
IFN	Interferon
IL	Interleukin
IRAK	Interleukin-1 receptor-associated kinase
LPS	Lipopolysaccharide
MALDI-TOF	Matrix assisted laser desorption/ionization-time of flight
MCSF	Macrophage-colony stimulating factor
MDM	Monocyte-derived macrophages

Meth	Methamphetamine
mRNA	Messenger ribonucleic acid
MTT	3-(4,5-dimethylthioazol-2-yl)-2,5-diphenyl tetrazolium bromide
NF-κB	Nuclear factor-kappa B
ODN	Oligodeoxynucleotides
PBS	Phosphate buffer saline
PTM	Post-translational modifications
PCR	Polymerase chain reaction
PCT	Pressure cycling technology
PVDF	Polyvinylidene fluoride
RNA	Ribonucleic acid
RP-HPLC	Reverse phase high pressure liquid chromatography
RT	Reverse transcriptase
TDF	Tenofovir
TCA	Trichloroacetic acid
TLR	Toll-like receptor
TNF	Tumor necrosis factor
WCL	Whole cell lysate
WHO	World Health Organization

Chapter 1

General Introduction

1.1. Brief History of Meth

Methamphetamine hydrochloride (Meth), or crystal meth, was synthesized by a Japanese pharmacologist, Akira Ogata, in 1919 via reduction of ephedrine using red phosphorus and iodine [1]. Throughout the years, it was manufactured in pill form by pharmaceutical companies all over the world and had many names: Philopon (Japan), Pervitin (Germany), Obetrol (United States), and is still manufactured and prescribed as Desoxyn (United States) [2]. It has been prescribed for asthma and narcolepsy, and used as an alertness aid and an appetite suppressant to regulate weight [3]. The use of Meth skyrocketed during World War II when both the German and Japanese soldiers used it to enhance their performance and to prevent depression on the frontlines. The Japanese Kamikaze pilots also reportedly used it before suicide missions [4]. It was not until the 1960's that the abuse worsened when doctors in California began administering an injectable form of Meth to treat heroin addicts [5]. Eventually, as the addictive qualities of the drug became apparent, governments began to regulate the production and distribution of prescription Meth more strictly. The United States made Meth a schedule II controlled substance under the Controlled Substances Act in 1970. Soon after the illicit underground the market for Meth grew, manufacturing of Meth starting in California and eventually moving eastward. In the Midwest rural areas Meth labs became popular because of the ease and accessibility of anhydrous ammonia tanks, an ingredient to needed to produce Meth.

During the 1990's and the early 2000's, as illicit Meth manufacturing and abuse became endemic throughout the states, Meth research rose exponentially. Studies found it to be very dangerous and highly addictive compound, associated with permanent brain damage in long-term users [8, 9]. Furthermore, Meth use is correlated with an increase in mortality, as well as a dramatic rise in the violent crimes [10]. In addition, studies

found a positive correlation of Meth use with lowered sexual inhibitions and poor judgment, possibly contributing to the spread in transmission of Human Immunodefiency Virus type 1 (HIV-1) [11-13]. Due to the devastating effects of Meth on individuals and in the communities, Congress passed the Comprehensive Meth Control Act in 1996. This law regulated mail order and chemical companies selling precursor chemicals, such as red phosphorous, iodine and hydrochloric gas and required that companies show a legitimate use for the chemicals. The law also limited the quantity of the over-the-counter cold medications containing pseudoephedrine, another precursor chemical, and for the sale of these medications be a documented transaction. In conclusion, Meth is a very popular (over an estimated 1.4 million people used within the last year in the United States) and has become the drug of choice over other illicit psychostimultant drugs, including cocaine, heroin, and crack since Meth is cheaper and has longer lasting effects [14].

1.2. Chemistry of Meth

The chemical formula of Meth is $C_{10}H_{15}N$ and its molecular weight 149.23 g/mol. It structurally similar to other abused drugs like amphetamine, ephedrine, and MDMA (ecstasy), as well as monoamine neurotransmitters like dopamine, epinephrine, and norepinephrine (Fig. 1.1.). Pharmacokinetic properties help explain how the body responds after Meth is administered and are measured by bioavailability (how easily the body absorbs a drug), volume of distribution (where in the body the drug will be located), and the half-life (how quickly half the dose is eliminated). Bioavailability, by definition, is the percentage of an administered non-metabolized drug that reaches the systemic system and therefore, 100% of a drug reaches the blood stream for intravenous doses. But when a drug is given orally the drug is metabolized or not absorbed thus decreasing
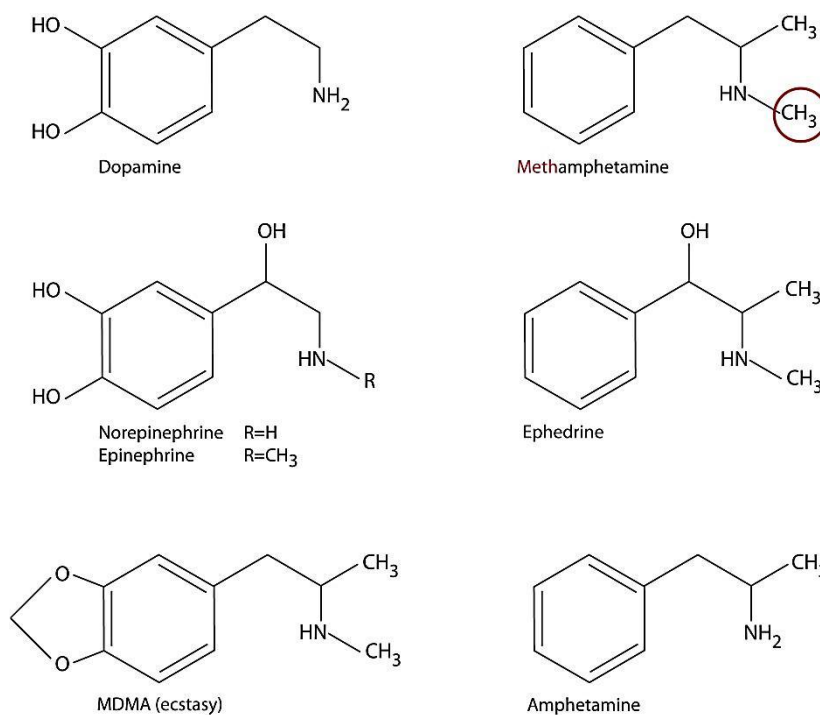
Figure 1.1. Similarities of chemical structures to methamphetamine

The bioavailability. Meth has a high bioavailability regardless of ingestion route whether smoked (90.3%) or swallowed (67.2%) [15]. The volume of distribution (V_d) is a measurement of how much of the dose is in the tissues versus retained in the plasma. Drugs with low plasma binding capabilities have higher V_d and Meth has a moderate V_d of 5.8 L/kg for a 10 mg oral dose [16]. There are no known proteins that bind Meth in the plasma. The secondary amine group on Meth makes it more lipophilic, suggesting why Meth is distributed in tissues, including the brain, rather than the blood [17]. The last important property is half-life. The half-life is the amount of time it takes for the concentration of drug in blood plasma to reach one-half the original amount. The plasma half-life for Meth is an average of 12 h, significantly longer than cocaine which has half-life of 90 min [15, 18]. Taken together these properties show that Meth is easily distributed throughout the body tissues and is retained for long periods of time [18-20].

1.2. Cellular Mechanism of Meth Addiction

Meth affects the regions of the central nervous system (CNS) that control judgment, reward-seeking behavior, and memory. Meth activates the prefrontal cortex, amygdala, and the nucleus accumbens [21, 22]. The prefrontal cortex is responsible for making decisions and cognition and innervates to the amygdala that is associated with emotional control and memory formation [22]. The nucleus accumbens processes the understanding of pleasure, reward, and reinforcing behaviors [23]. To this extent, these brain regions help elucidate the behavioral changes seen in Meth users like decreased inhibition, grandiosity, increased libido and ease of becoming addicted to the feeling of well-being.
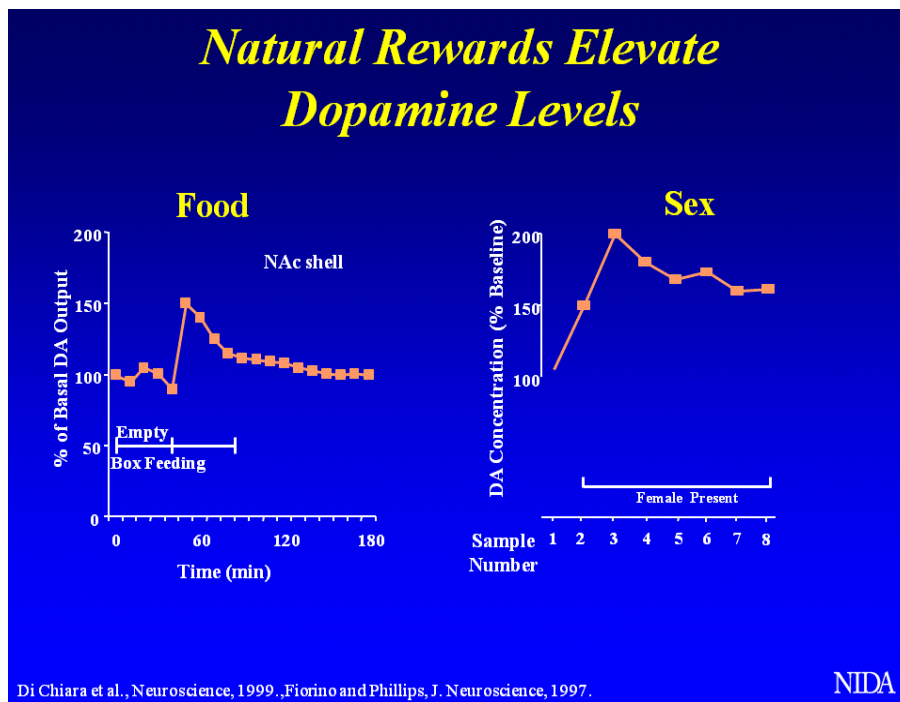
Figure 1.2. Dopamine Released as a Result of Natural Stimuli (Source: Di Chiara et al.) [24]

The main cell type in the brain regions that affect Meth and addiction is dependent on dopaminergic neurons. Due the neurotoxicity of Meth, and a loss of
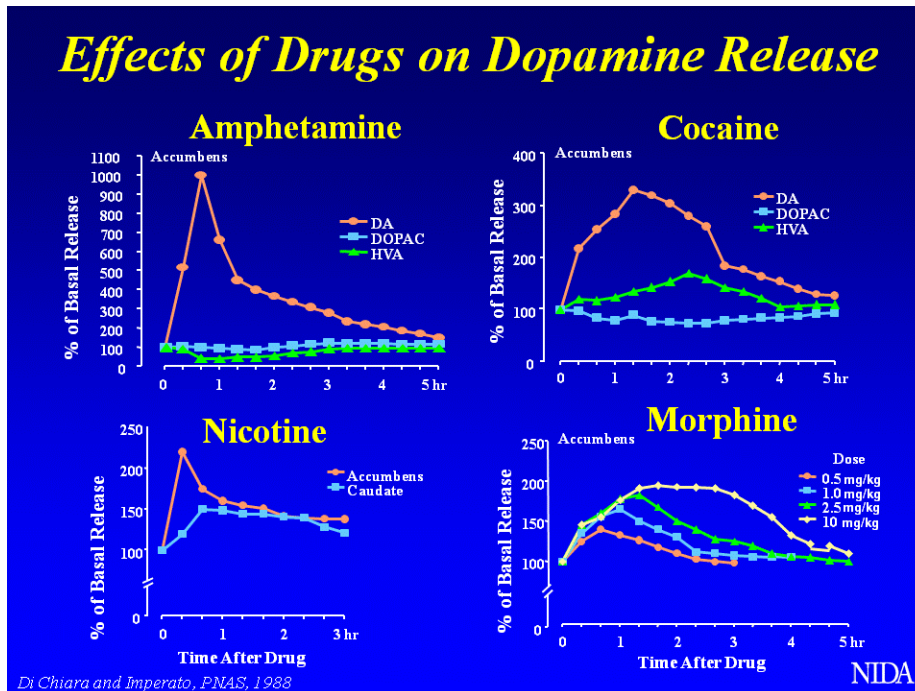
Figure 1.3. Dopamine Levels Released After Addictive Drugs Over Time (Source: Di Chiara et al.) [24]

dopaminergic neurons, chronic users develop a tolerance to Meth. The increased tolerance makes users actively seek out higher doses (drug-seeking behavior), increase frequency of ingestion. The exact mechanism or mechanisms causing neurotoxicity from Meth is not known but many have been proposed, including inflammation, reactive oxygen species disrupting mitochondria function, disruption of the blood brain barrier, free radicals causing DNA damage, and/or glutamate toxicity [25-28]. Dopaminergic neurons are the main source of dopamine. Dopamine is a neurotransmitter released as a result of rewarding experiences such as food, sex, and natural stimuli (Fig. 1.2.). Meth releases magnitudes more dopamine than natural stimuli or other drugs making it very pleasurable and those feelings desired to be repeated by users and abusers [24] (Fig 1.3.). Dopamine is a member of the catecholamine family and readily degraded in

19

neurons by enzymes such as monoamine oxidase and catechol-O-methyl transferase. Dopamine is naturally stored in vesicles until a stimulus induces its release. When Meth crosses the blood brain barrier and the cell membrane of neurons, it replaces the dopamine inside the vesicles [29]. Once dopamine is displaced, there is a higher concentration gradient inside the cytosol than outside the cell triggering an efflux of dopamine into the synaptic clefts [30]. Dopamine activating receptors on the post-synapse in the brain regions mentioned previously propagates the chemical transmission and gives the effect of euphoria after Meth. The other cellular mechanism giving rise to the euphoria effect is the prolonged duration of dopamine in the clefts. Meth accomplishes this by inhibiting the reuptake of dopamine from the clefts by blocking the extracellular dopamine transporter on the exon terminals of the presynaptic neurons [31, 32]. Therefore, Meth is so addictive because it causes a large quantal release of dopamine for sustained periods of time.

1.4.   Health and Social Impact of Meth

The physical effects of Meth are similar whether the drug is snorted, smoked, injected, or swallowed. The short term effects of Meth are due to the activation of sympathetic nervous system and are therefore, similar to the fight-or-fight responses, including increased wakefulness, decreased appetite, increased breathing, heart rate, and blood pressure [33]. Due to the lipophilic nature of Meth, Meth can pass through the placenta to the fetus and cause premature delivery, separation of the placenta from the uterus, low birth weight, and heart and brain problems in the child [34]. Long term effects of chronic Meth use include weight loss, kidney failure, brain damage, depression, hallucinations, permanent psychological problems, persistent ticks, violent and aggressive behavior, "meth mouth" or dental disease and teeth rot, insomnia, behavior resembling paranoid schizophrenia, increased susceptibility to infections, liver damage,

and stroke (because of increases in blood pressure, heart rate, and body temperature) [8, 35, 36]. Chronic use can damage the cardiovascular system, lungs, liver, and muscles [37-39]. Psychological addiction or dependence is when the user gets high to avoid the negative effects or withdraw symptoms of Meth include such symptoms as cravings, depression, irritability, shaking, and a loss of energy.

Clearly, Meth has many short term and long term physical and psychological effects on the individual user but there are societal concerns and policies being set against the illegal use of Meth that have a huge monetary price. The social problems associated with Meth addiction come from crime and incarcerations, death, treatment facilities, and educational programs. In the most recent RAND study, the total economic cost of Meth is estimated at an average $23.4 billion [40]. Each estimate discussed will go further into detail of the actual break down included in the amount but will always have intangible cost and therefore, should be considered as a conservative estimate. Here, only the average cost will be reported, whereas the lower and upper limits are outlined in the study.

In order to pay for their habit, addicts are tempted to rob, steal, or burglarize. This type of crime is just one category grouped under property damage and violent crimes. Another example of violent crimes committed by Meth abusers is physical violence. As mentioned previously, Meth use can lead to irritability, violent and aggressive behavior and according to one study Meth users reported violence against their partner, friends, family, or strangers at least once [41]. The other categories are arrests for Meth possession or sales and parole or probation revocation. More details contributing to the cost are the length of the prison sentence and cost associated per day per person and cost of drug testing of parolees. The best estimate for all of these expenses is $4.2 billion, noticeably a huge portion of total economic cost of $23.4 billion.

A Meth related death is defined by the World Health Organization as a death caused by mental or behavioral disorders due to psychoactive substance use or poisoning of accidental, intentional, or undetermined intent. It is not just death but also injuries caused by Meth lab mishaps, chemical fires, and or hospitalization from inhalation of toxins from the ingredients of manufacturing Meth. Also, when explosions happen in the Meth labs there is a societal cost accompanying professionals to cleanup, process, properly dispose of chemical and hazardous waste. The cost of deaths was an average of $31.5 million and injuries added an additional $1 million while, the cost of cleaning up labs was $29.2 million. Yet, these estimates do not include the cost of pollution caused by the dumping, burying, or burning of the hazardous waste manufactured by each pound of Meth. Nor does the estimate include the cost of decontamination of individuals on the Meth lab sites or evacuation of nearby neighbors.

Methamphetamine is a highly addictive drug and requires intense, long-term treatment. Treatment cost in the United States can be split between the community based treatment facilities (hospitals and specialty) and the federally provided treatment programs, which include Department of Defense, Veterans Affairs, Federal Bureau of Prisons, and IHS. The cost breakdown is $506 and $545 million for community based and federally provided treatment facilities, respectively [40]. According to the Alcohol and Drug Services Study, the average daily cost of inpatient treatment (community based facility) was about $76.13 per day in 2002, and the cost of outpatient treatment was about $26.72 per day [42]. Most private Meth rehab centers offer financing options for qualified patients or cost might be covered by insurance companies. Although, uncompensated treatment can place a huge burden on the national budget in the range of hundreds of millions of dollars [43].

Education campaigns against the use of Meth significantly raises awareness of consequences and effects, influence users to use less Meth, and practice safe sex more

often in order to prevent sexually transmitted diseases [44]. And although, these marketing campaigns are less expensive and more cost-effective for raising awareness on important health and psychosocial issues than the cost associated with other methods, it is still costly to the public and government associations, between $20 million for one state and upper bounds of $448 million for the nation [40, 45].

1.5.   Effects of Meth on Innate Immunity

Interestingly, Meth addicts are more susceptible to infections, including, HIV-1, Methicillin-resistant staphylococcus aureus (MRSA), genital herpes, fungal infections, and bacterial meningitis [46-50]. Infections are fought by the innate immune system, which is the rapid but non-specific first response to foreign pathogens and injuries in the body. There are many cell types that facilitate the innate immune response, among them macrophages are important because they are long-lived cells, harbor cryptoccal neoformans, facilitate fungal dissemination, and are an HIV reservoir [51]. Macrophages possess many functions to accomplish its role in both innate and adaptive immunity. In innate immunity, macrophages act as scavengers or surveyors of the surrounding tissue and rid the body of dead or dying cells and foreign particles by phagocytosis. In addition, macrophages have a critical role in initiating and regulating inflammation. Macrophages secrete cytokines and chemokines as a chemical signal to recruit other immune cells to the site of infection. Macrophages are the foremost cell type that process and present antigens, which plays a crucial role in initiating the adaptive immune response, or production of antibodies. After digesting a pathogen, a macrophage will present a part of the antigen to a corresponding T cell.

Studies have demonstrated that Meth alters many functions of macrophages. Research on the effects of Meth on macrophage functions and their molecular mechanisms can help elucidate why Meth users are at an increased risk to infections,

hopefully leading to the development of immune boosting treatments that can offset the deleterious effects. Various studies show Meth alone alters cytokine production. For example, TNF-α, IL-8, IL-1β, MIP-1α (CCL3), MIP-1β (CCL4), IFN-α and other cytokines in monocyte-derived macrophages (MDM), THP-1 macrophages, and dendritic cells (another immune phagocyte) [50, 52-54]. It is not just cytokines that are altered but other small chemical signals are found to be decreased like nitric oxide and superoxide [46, 55]. Another study showed that Meth reduces the ability of macrophages to rid the body of tumor cells compared to the stimulation of gram negative bacteria (LPS) and double stranded RNA viruses (poly I:C). Meth also decreased the expression of CD14, the co-receptor for TLR4, which detects LPS. [55]. Moreover, Meth treatment decreases the ability of macrophages to clear HIV and worsens viral load in infected cells [56]. The mechanism of increased viral load was attributed to the down-regulation of anti-viral cytokine, IFN-α, and the increased expression of the HIV entry co-receptor, CCR5 in primary human MDM [50]. Lastly, Meth prevents the phagocytosis of Candida albicans and Cryptococcus neoformans, two major AIDS-related fungus pathogens [56, 57]. In conclusion, Meth is immunosuppressive by decreasing the ability of macrophages to respond normally to viruses, bacteria, and fungal infections.

1.6.   Effects of Meth on TLR Signaling

Since the discovery of the first mammalian toll-like receptor (TLR) in 1997, 11 have now been identified in humans. Functional analysis of TLRs revealed that they recognize specific patterns or PAMPs (pathogen-associated molecular patterns) of microbial components and the homodimers or heterodimers of the receptors then activate specific signaling mechanisms. Although different TLRs recognize different PAMPs, a majority of the signaling pathways converge to a common factor, MyD88 (myeloid differentiation factor 88) (Fig. 1.4.).
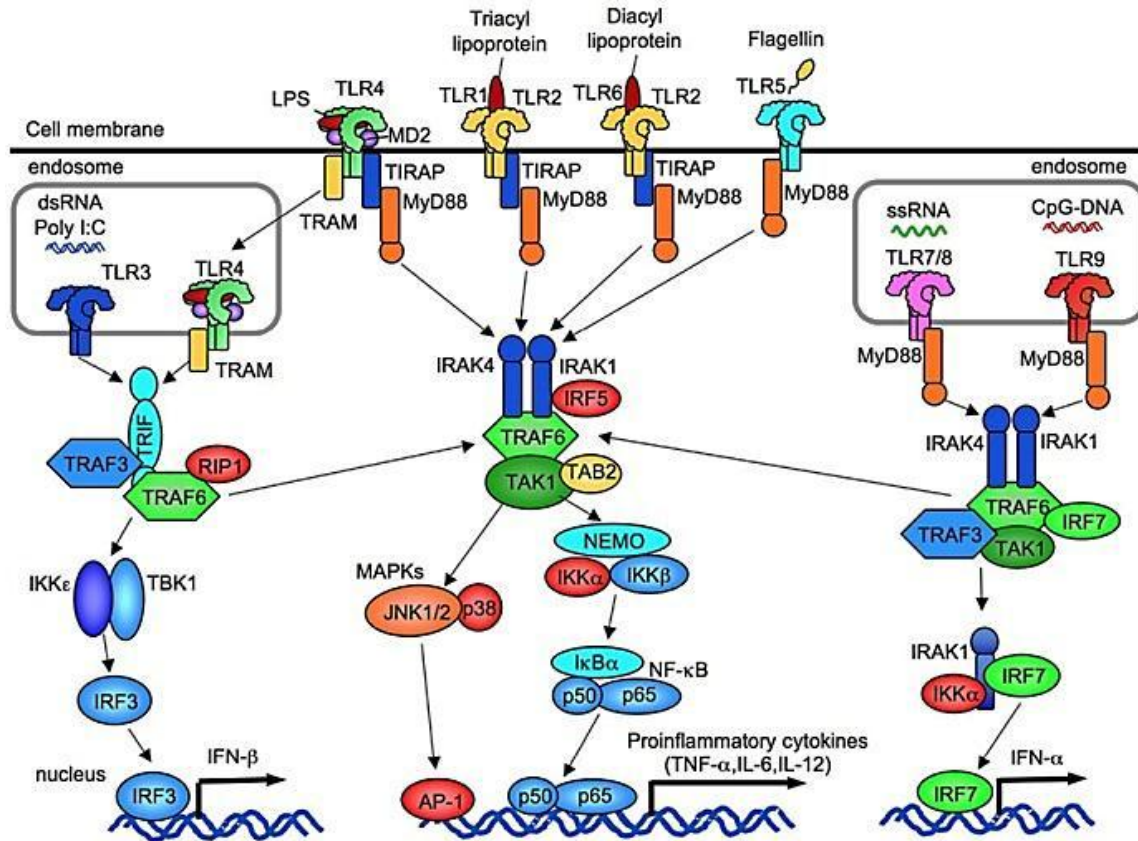
Figure 1.4. Mechanisms of Toll-like Receptors

MyD88 contains a TIR (Toll/IL-1 receptor) domain in the C-terminal portion and a death domain at the N-terminal portion. The C-terminal domain of MyD88 associates with an activated TLR (referred to as TIRAP or TIR domain containing adaptor protein) while the death domain at the N-terminal of MyD88 recruits the linker protein IRAK (IL-1 receptor-associated kinases) 1, 2 and 4. IRAK4 phosphorylates IRAK1, which in turn binds the TRAF (tumor-necrosis factor-receptor associated factor) domain of TRAF6 to IRAK1 and activates TRAF6. Ubiquitinated TRAF6 serves as a scaffold protein with TAK1 (TGF-β activated kinase 1) and TAB2 (TAK1- binding protein 2). TAK1 then couples to the IKK (inhibitor of NF-κB kinase) complex, which includes the scaffold protein NEMO (NF-κB essential modulator). Once TAK1 phosphorylates IKK, IKK phosphorylates the IκBα

protein (inhibitor of NF-κB alpha) and results in the dissociation of IκBα from NF-κB allowing NF-κB to translocate to the nucleus and mediate an increase in inflammatory cytokine genes such as TNF-α, IL-1 and IL-12 [58-61].

The effects of Meth on macrophage function, especially altered cytokine production and decreased defense against bacterial and viral infections, have been implicated to be a consequence of deregulated TLR signaling. One such study showed that activation of TLR9 by its agonist CpG ODN up-regulates the expression of TLR9, IFN-α, IRF-7, and MyD88. These anti-viral factors boost the immune response and reduce the HIV viral load in macrophages *in vitro*. However, METH treatment of macrophages greatly inhibited the anti-HIV effect mediated by TLR9 signaling by inhibiting the expression of TLR9 and downstream signaling factors [62]. Upon activation of TLR4 with LPS, that Meth exacerbated the TNF-α mRNA expression and protein levels however, in conjunction with an IKK inhibitor TNF-α levels decreased suggesting the common pathway of MyD88-dependent signaling in Meth-induced effects [63]. Taken together, further studies need to be conducted to determine the molecular mechanism of Meth in macrophages.

1.7. Bibliography

1.   *Brief history of methamphetamine - methamphetamine prevention in Vermont.* 2015 [cited 2015 September 28].

2.   *Obetrol.* July 15, 2015 [cited 2015 September 28].

3.   Rasmussen, N., *America's first amphetamine epidemic 1929-1971: a quantitative and qualitative retrospective with implications for the present.* Am J Public Health, 2008. **98**(6): p. 974-85.

4.   *Desoxyn prescribing information*, 2013, United States Food and Drug Administration.

5.   Weisheit, R. and W. White, *Methamphetamine: its history, pharmacology and treatment*2009: Hazelden Publishing. 296.

6.   *History of methamphetamine: early methamphetamine use.*   [cited 2015 September 28].

7.   *Meth awareness: how is meth made?*

8.   Gold, M.S., et al., *Methamphetamine- and trauma-induced brain injuries: comparative cellular and molecular neurobiological substrates.* Biol Psychiatry, 2009. **66**(2): p. 118-27.

9.   Theodore, S., et al., *Progress in understanding basal ganglia dysfunction as a common target for methamphetamine abuse and HIV-1 neurodegeneration.* Curr HIV Res, 2007. **5**(3): p. 301-13.

10.   Dobkin, C. and N. Nicosia, *The War on Drugs: Methamphetamine, Public Health, and Crime.* Am Econ Rev, 2009. **99**(1): p. 324-349.

11.   Potula, R. and Y. Persidsky, *Adding fuel to the fire: methamphetamine enhances HIV infection.* Am J Pathol, 2008. **172**(6): p. 1467-70.

12. Ellis, R.J., et al., *Increased human immunodeficiency virus loads in active methamphetamine users are explained by reduced effectiveness of antiretroviral therapy.* J Infect Dis, 2003. **188**(12): p. 1820-6.

13. Toussi, S.S., et al., *Short communication: Methamphetamine treatment increases in vitro and in vivo HIV replication.* AIDS Res Hum Retroviruses, 2009. **25**(11): p. 1117-21.

14. Prevention, C.f.D.C.a., *Methamphetamine use and risk for HIV/AIDS*, C.f.D.C.H.A.F. Sheet, Editor 2007.

15. Cook, C.E., et al., *Pharmacokinetics of methamphetamine self-administered to human subjects by smoking S-(+)-methamphetamine hydrochloride.* Drug Metabolism and Disposition, 1993. **21**(4): p. 717-23.

16. Schepers, R.J.F., et al., *Methamphetamine and amphetamine pharmacokinetics in oral fluid and plasma after controlled oral methamphetamine administration to human volunteers.* Clinical Chemistry, 2003. **49**(1): p. 121-32.

17. Kirkpatrick, M.G., et al., *Comparison of intranasal methamphetamine and d-amphetamine self-administration by humans.* Addiction, 2012. **107**(4): p. 783-91.

18. Riviere, G.J., W.B. Gentry, and S.M. Owens, *Disposition of methamphetamine and its metabolite amphetamine in brain and other tissues in rats after intravenous administration.* Journal of Pharmacology and Experimental Therapeutics, 2000. **292**(3): p. 1042-7.

19. Volkow, N.D., et al., *Distribution and pharmacokinetics of methamphetamine in the human body: clinical implications.* PLoS ONE, 2010. **5**(12): p. e15269.

20. Dietrich, J.B., *Alteration of blood-brain barrier function by methamphetamine and cocaine.* Cell Tissue Res, 2009. **336**(3): p. 385-92.

21. Broening, H.W., C. Pu, and C.V. Vorhees, *Methamphetamine selectively damages dopaminergic innervation to the nucleus accumbens core while sparing the shell.* Synapse, 1997. **27**(2): p. 153-60.

22. Coutinho, A., et al., *Chronic methamphetamine induces structural changes in frontal cortex neurons and upregulates type I interferons.* J Neuroimmune Pharmacol, 2008. **3**(4): p. 241-5.

23. Kartikeyan, S., et al., *HIV and AIDS: basic elements and priorities*2007: Springer.

24. Chiara, G.D. and A. Imperato, *Drugs abused by humans preferentially increase synaptic dopamine concentrations in the mesolimbic system of freely moving rats.* Proceedings of the National Academy of Sciences, 1988. **85**: p. 5274-8.

25. Shah, A., et al., *Involvement of metabotropic glutamate receptor 5, AKT/PI3K signaling and NF-kappaB pathway in methamphetamine-mediated increase in IL-6 and IL-8 expression in astrocytes.* J Neuroinflammation, 2012. **9**: p. 52.

26. Mahajan, S.D., et al., *Methamphetamine alters blood brain barrier permeability via the modulation of tight junction expression: Implication for HIV-1 neuropathogenesis in the context of drug abuse.* Brain Res, 2008.

27. Cadet, J.L. and I.N. Krasnova, *Molecular bases of methamphetamine-induced neurodegeneration.* Int Rev Neurobiol, 2009. **88**: p. 101-19.

28. Davidson, C., et al., *Methmphetamine neurotoxicity: necrotic and apoptotic mechanisms and relevance to human abuse and treatment.* Brain Research Reviews, 2001. **36**: p. 1-22.

29. Sulzer, D., et al., *Amphetamine redistributes dopamine from synaptic vesicles to the cytosol and promotes reverse transport.* Journal of Neuroscience 1995. **15**(5): p. 4102-8.

30. Kahlig, K.M., et al., *Amphetamine induces dopamine efflux through a dopamine transporter channel.* Proc Natl Acad Sci U S A, 2005. **102**(9): p. 3495-500.

31. Rothman, R.B. and M.H. Baumann, *Monoamine transporters and psychostimulant drugs.* European Journal of Pharmacology, 2003. **479**(1-3): p. 23-40.

32. Han, D.D. and H.H. Gu, *Comparison of the monoamine transporters from human and mouse in their sensitivities to psychostimulant drugs.* BMC Pharmacol, 2006. **6**: p. 6.

33. *Methamphetamine.* 2014 January 2014 [cited 2015 June 30].

34. Chomchai, C., et al., *Methamphetamine abuse during pregnancy and its health impact on neonates born at Siriraj Hospital, Bangkok.* Southeast Asian Journal of Tropical Medicine and Public Health, 2004. **35**(1): p. 228-31.

35. Hussain, F., R.W. Frare, and K.L.P. Berrios, *Drug abuse identification and pain management in dental patients: a case study and literature review.* Substance Abuse, 2011: p. 334-47.

36. *Methamphetamine.* 2014 [cited 2015 January].

37. Darke, S., et al., *Major physical and psychological harms of methamphetamine use.* Drug Alcohol Rev, 2008. **27**(3): p. 253-62.

38. Wells, S.M., et al., *Acute inhalation exposure to vaporized methamphetamine causes lung injury in mice.* Inhal Toxicol, 2008. **20**(9): p. 829-38.

39. Kamijo, Y., et al., *Acute liver failure following intravenous methamphetamine.* Vet Hum Toxicol, 2002. **44**(4): p. 216-7.

40. Nicosia, N., et al., *The economic cost of methamphetamine use in the United States, 2005.* RAND, 2009.

41. McKetin, R., et al., *Does methamphetamine use increase violent behaviour? Evidence from a prospective longitudinal study.* Addiction, 2014. **109**(5): p. 798-806.

42. *Alcohol and drug services study (ADSS) cost study*, D.a.A.S.I. System, Editor 2002, Substance Abuse and Mental Health Services Administration

43. Cretzmeyer, M., et al., *Treatment of methamphetamine abuse: research findings and clinical directions.* Journal of Substance Abuse Treatment, 2003. **24**(3): p. 267-277.

44. Nanin, J.E., et al., *Community reactions to campaigns addressing crystal methamphetamine use among gay and bisexual men in New York City.* Journal of Drug Education, 2006. **36**(4): p. 297-315.

45. Kemmick, E. *$20M spent in anti-meth campaign.* 2009.

46. Martinez, L.R., et al., *Methamphetamine enhances histoplasmosis by immunosuppression of the host.* J Infect Dis, 2009. **200**(1): p. 131-41.

47. Cohen, A.L., et al., *Methamphetamine use and methicillin-resistant Staphylococcus aureus skin infections.* Emerg Infect Dis, 2007. **13**(11): p. 1707-13.

48. Valencia, F., et al., *Influence of methamphetamine on genital herpes simplex virus type 2 infection in a mouse model.* Sexually Transmitted Diseases, 2012. **39**(9): p. 720-5.

49. Patel, D., et al., *Methamphetamine enhances Cryptococcus neoformans pulmonary infection and dissemination to the brain.* MBio, 2013. **4**(4).

50. Liang, H., et al., *Methamphetamine enhances HIV infection of macrophages.* Am J Pathol, 2008. **172**(6): p. 1617-24.

51. Koppensteiner, H., R. Brack-Werner, and M. Schindler, *Macrophages and their relevance in Human Immunodeficiency Virus Type 1 infection.* Retrovirology, 2012. **9**(82).

52.   Mahajan, S.D., et al., *Methamphetamine modulates gene expression patterns in monocyte derived mature dendritic cells: implications for HIV-1 pathogenesis.* Mol Diagn Ther, 2006. **10**(4): p. 257-69.

53.   Nair, M.P., et al., *Methamphetamine enhances HIV-1 infectivity in monocyte derived dendritic cells.* J Neuroimmune Pharmacol, 2009. **4**(1): p. 129-39.

54.   Burns, A. and P. Ciborowski, *Acute exposure to methamphetamine alters TLR9-mediated cytokine expression in human macrophage.* Immunobiology, 2015.

55.   In, S.-W., et al., *Modulation of murine macrophage function by methamphetamine.* Journal of Toxicology and Environmental Health, 2004. **67**: p. 1923-37.

56.   Talloczy, Z., et al., *Methamphetamine inhibits antigen processing, presentation, and phagocytosis.* PLoS Pathog, 2008. **4**(2): p. e28.

57.   In, S.W., et al., *Methamphetamine administration produces immunomodulation in mice.* J Toxicol Environ Health A, 2005. **68**(23-24): p. 2133-45.

58.   Akira, S. and K. Takeda, *Toll-like receptor signalling.* Nat Rev Immunol, 2004. **4**(7): p. 499-511.

59.   Takeda, K. and S. Akira, *TLR signaling pathways.* Seminars in Immunology, 2004. **16**(1): p. 3-9.

60.   McCoy, C.E. and L.A.J. O'Neil, *The role of toll-like receptors in macrophages.* Frontiers in Bioscience, 2008. **13**: p. 62-70.

61.   O'Neill, L.A., D. Golenbock, and A.G. Bowie, *The history of Toll-like receptors - redefining innate immunity.* Nat Rev Immunol, 2013. **13**(6): p. 453-60.

62.   Cen, P., et al., *Methamphetamine inhibits Toll-like receptor 9-mediated anti-HIV activity in macrophages.* AIDS Res Hum Retroviruses, 2013. **29**(8): p. 1129-37.

63.   Liu, X., et al., *Methamphetamine increases LPS-mediated expression of IL-8, TNF-alpha and IL-1beta in human macrophages through common signaling pathways.* PLoS One, 2012. **7**(3): p. e33822.

Chapter 2

Effects of Meth on Macrophage Function and Signaling

2.1. Introduction

2.1.1. Toll-like receptor signaling in macrophages

Macrophages are key elements of the innate immune system that rapidly respond to various stimuli such as bacterial, viral, fungal or parasitic infections, tissue injury as well as other insults. Macrophages detect viral and bacterial infections by utilizing Toll-like Receptors (TLRs). TLRs 1, 2, and 4 are expressed on the cell surface and detect bacterial components like lipopolysaccharide (LPS), whereas intracellular TLRs 3, and 7-9 sense viral RNA and DNA. TLR signaling consists of two pathways, the MyD88-dependent and MyD88-independent pathways. The MyD88-independent pathway leads to the activation of IRF3 (interferon regulatory factors 3) and IRF7 to induce Type I interferons. In the MyD88-dependent TLR signaling pathway, MyD88 (myeloid differentiation primary response gene 88) recruits IRAK4 (IL-1 receptor-associated kinase 4) and activates IRAK1. Activated IRAK1 interacts with TRAF6 (TNF-receptor associated factor 6) to activate TGF-β–activated kinase 1 (TAK1). The TAK1-TRAF6 complex simultaneously phosphorylates and polyubiquitinates IKK (I kappa B kinase). Post-translational modifications of IKK relieve inhibition of NF-κB (nuclear factor kappa-light-chain-enhancer of activated B cells) and allow NF-κB to translocate to the nucleus and regulate the production of pro-inflammatory cytokines and chemokines [1]. If TLR signaling is impaired, the host becomes susceptible to an invading microorganism by failing to recruit other immune cells and not eliciting the proper adaptive immune response.

2.1.2. Epidemiology of Meth and opportunistic infections

Methamphetamine (Meth) is one of the most addictive and destructive illicit drugs and its use is on the rise [2]. Epidemiology data demonstrates that chronic Meth users are at an increased risk of acquiring infections such as Methicillin Resistant Staphylococcus aureus (MRSA) and HIV-1 [3-5]. Moreover, *in vivo* and *in vitro* studies show histoplasmosis, cryptococcal

neoformans, HIV-1, as well as other sexually transmitted infections, tend to progress more rapidly with the use of Meth [6-11]. This suggests that Meth has the ability to profoundly interfere with the cell-mediated immune response. However there remains a lack of understanding as to how Meth impairs immune cell function at the molecular level.

2.1.3. Delineating the mechanism of Meth-exposed macrophages

It has been shown in macrophages that Meth exacerbates LPS-mediated expression of IL-8, TNF-α and IL-1β mediated by p38 MAPK and PI3-AKT signaling pathways [12]. Other studies show that phagocytosis, antigen processing, and antigen presenting in macrophages is diminished by Meth exposure [13]. These studies indicate that Meth exposure impairs macrophage functions; however the exact mechanism is unknown. Several possibilities include alterations in signaling mediators, transcriptional factors, histone post-translational modifications and DNA methylation [13, 14]. In this study, we investigated how exposure to Meth affects macrophage cytokine production and subsequent observations of the impairment of cytokine responses due to TLR9 signaling by recognition of DNA.

2.2.   Materials and Methods

2.2.1. Cell culture and treatments

THP-1 monocytes, a human monocytic cell line derived from an acute monocytic leukemia patient, were obtained from ATCC (Manassas, VA), and plated at a concentration of 10^6 cells per mL. They were differentiated into macrophages in the presence of 200 nM phorbol 12-myristate 13-acetate (PMA, Sigma-Aldrich; St. Louis, MO) in complete media, which consisted of RPMI-1640 medium (HyClone; Logan, UT) supplemented with 10% fetal bovine serum (Atlanta Biologicals; Norcross, GA) and 50 µM of beta-mercaptoethanol (Gibco; Grand Island, NY). All of the media was exchanged every other day for four days and cells were allowed to rest

in complete media without PMA for an additional two days, at which point cells assumed a macrophage-like phenotype (Fig. 2.1). On day six, media was either replaced with 100 µM methamphetamine (Sigma-Aldrich) in complete media or control media for the specified times. In a separate series of experiments macrophages were treated with either 1µg/mL of mock CpG oligodeoxynucleotides 2243 (CpG ODN) or TLR9-stimulatory CpG ODN 2216 (both from Invivogen; San Diego, CA) for specified times.

2.2.2. Cell viability assay

Both time-dependent and concentration-dependent experiments on the viability of THP-1 macrophages were performed according to the MTT assay protocol. Macrophages were seeded onto 96-well plates at a density of 5×10^4 cells/well and treated with 0, 1, 10, 100, 500, and 1000 µM methamphetamine for two hours. In parallel experiments cells were seeded at the same density and propagated for 2, 6, 24, and 48 hours of 100 µM Meth along with the appropriate time control (RPMI media). Positive and negative controls consisted of 100% killed macrophages or wells with only MTT reagent, respectively. The positive control macrophages were treated with 1% Triton X-100 (Fisher Scientific; Fair Lawn, NJ) to permeabilize the cell membrane. The cell viability was assessed using the MTT assay (Life Technologies; Carlsbad, CA). Absorbance at 490 nm was quantitated using a SpectraMax M3 microplate reader (Molecular Devices, Sunnyvale; CA, USA). Eight parallel replicates were measured for each condition.

2.2.3. Human cytokines and chemokines RNA PCR array

Total RNA was extracted using Trizol (Life Technologies) and cleaned using the RNeasy Mini Kit according to manufacturer's protocol (Qiagen; Germantown, MD). Only RNA that had a 260/280 ratio greater than 1.8 and a RIN value greater than 7 was used for reverse transcription (RT) to synthesize cDNA using the RT2 First Strand Kit (SABioscience; Frederick, MD). Reverse transcription and PCR was executed by following the SABioscience's protocol with a total of 5 µg

of RNA being reverse transcribed and DNA contamination eliminated by incubating with genomic DNA elimination mix supplied by the manufacturer. RNA was converted to cDNA using the RT Cocktail mixed with the DNA-free samples and incubated at 42ºC for 15 min followed by heating at 95ºC for 5 minutes. Samples were diluted with the 2X RT2 SYBR Green Mastermix before performing PCR on the Applied Biosystems StepOnePlus Real-Time PCR System using the default settings. Every sample was loaded in triplicate by the fully automated Corbett Robotics (San Francisco, CA) to provide uniformity across all plates. Relative abundance was calculated using the comparative CT method [16].

2.2.4. RNA extraction and quantitative PCR

Cells were lysed directly in the culture dish with Trizol Reagent (Life Technologies). RNA was resuspended in 10 mM Tris (Pro-Pure, Solon, OH) and 1 mM EDTA (Fisher Scientific), pH 8.0 in RNase free water. One microgram of RNA was converted to cDNA using the High Capacity cDNA Reverse Transcription Kit (Life Technologies) per the manufacturer's protocol. The primers used to detect IL-8, TNF-α, CCL7, CXCL1, IFN-α, and TLR9 were purchased from Integrated DNA Technologies (Coralville, IA); human GAPDH primers were obtained from Applied Biosystems (Warrington, UK). The relative abundance of each gene was calculated using the comparative CT method [15].

2.2.5. Harvest and protein extraction

THP-1 macrophages were washed thrice with phosphate-buffered saline (PBS, HyClone), and collected for either protein or RNA. To obtain protein from whole cell lysates, cells were scraped in PBS and pelleted by centrifugation at 1000 x g for 5 min at 4°C and re-suspended in 300 µL per 106 cells of lysis buffer. Lysis buffer contained 2% (w/v) SDS (Bio-Rad; Hercules, CA), in 0.1 M Tris-HCl (Fisher Scientific), 0.1 M DTT (Promega; Madison, WI) and 1X Protease Inhibitor Cocktail (Sigma-Aldrich). Cells were heated at 95°C for 5 min, allowed to cool, and 100 units/mL

Benzonase Nuclease (Merck KGaA; Darmstadt, Germany) were added. Protein was quantified using Pierce 660 Assay as per the manufacturer's protocol using 50 mM ionic detergent compatible reagent (Thermo Scientific; Rockford, IL). Twenty micrograms of whole cell lysate from each condition were loaded onto a 4-12% bis-tris gel (Life Technologies) and separated at 100 V for 90 min and transferred to a PVDF membrane at 25 V for 90 min. Membranes were blotted with antibodies recognizing the following antigens: NF-κB/p65 [Cat# 8242] (New England Biolabs, Ipswich, MA), TLR9 [Cat# ab85860] (Abcam, Cambridge, United Kingdom), and IRAK1 [Cat# ab238] (Abcam) all at 1:1000 concentration overnight in 4°C.

2.2.6. Immunocytochemistry

THP-1 cells were plated and differentiated as described above. Methamphetamine and CpG ODN treatment was for 2 hours on day 6 post-plating. Macrophages were washed three times with PBS (HyClone), scraped, pelleted and resuspended in PBS to obtain a final concentration of $1x10^5$ cells per ml for cytospin. After cells were spun at 1000 rpm for 10 min on glass microscope slides, cells were fixed to the slide with 4% paraformaldehyde (Sigma-Aldrich) at room temperature for 30 min and rinsed once with PBS. Cells were blocked and permeabilized simultaneously by using 0.5% Tween 20 (Fisher Scientific) in PBS (PBST) supplemented with 10% normal goat serum (Invitrogen; Carlsbad, CA) for one hour at room temperature and rinsed once with PBST. Slides were stained with TLR9 [Cat# Ab85860] (Abcam) at 1:500 for 1 hour and rinsed three times with PBST for 5 min each before secondary antibody was added at a concentration of 1:500 for 45 min at room temperature in the dark. Slides were washed three times in PBST to remove secondary antibody and incubated with 1 µg/mL of DAPI (Invitrogen) for 5 min. After one wash, one drop of Prolong Gold (Invitrogen) was added and a cover slip was placed over cells prior to being visualized using Zeizz Axio Observer inverted

microscope at 40X oil immersion and capturing images using AxioVision Release software version 4.8.

2.2.7. Methylation pyrosequencing

DNA was extracted using the DNeasy Blood and Tissue Kit (Qiagen) according to manufacturer's protocol. Samples were treated with mock CpG, Meth, or Meth and CpG as previously mentioned in Cell Culture and Treatments. Bisulfite treatment was carried out using 1000 ng of sample genomic DNA and the EZ DNA Methylation-Direct kit (Zymo Research, Orange, CA). This process deaminates unmethylated cytosine residues to uracil leaving methylated cytosine residues unchanged. To perform PCR reactions, 42 ng of bisulfite-modified DNA was used as template. The PCR reactions were performed in a total volume of 50 µl for 35 cycles using Roche Diagnostic Corporation (Indianapolis, IN) FastStart Taq DNA Polymerase (1.0U), MgCl2 solution (3.5 mM), dNTP's (0.2 mM), sense primer (0.24 µM), antisense primer (0.18 µM), with denaturation at 95 ºC for 30 seconds, annealing temperature for 45 seconds at annealing temperatures specific to the primer and extension at 72 ºC for 1 minute (Table 2.1). For a positive (high methylation level) control, Roche Diagnostic Corporation (Indianapolis, IN) human lymphocyte genomic DNA was methylated using M. SssI (CpG) methylase kit (New England Biolabs, Ipswich, MA). Methylated DNA (1000 ng) was treated with sodium bisulfite as described above. Sodium bisulfite treated Roche human lymphocyte genomic DNA (1000 ng) served as a negative (low methylation level) control. All PCR products were electrophoresed on 0.8% agarose gel, stained with ethidium bromide, and visualized for appropriate and pure product before proceeding with all analyses using a Bio-Rad Laboratories (Hercules, CA) Gel-Doc UV illuminator. Methylation percentage of each CpG was determined using a Qiagen (Valencia, CA) Pyromark Q96 pyrosequencer and sequencing primer according to manufacturer's recommendations (Table 2.2.).

2.3. Results

2.3.1. Meth exposure affects the mRNA expression profile of cytokines and chemokines

Macrophages were exposed to 100 μM Meth for 2, 6, or 24 h and profiled for a broad set of 84 immune mediators including cytokines, chemokines, interleukins and growth factors. An RT kit was optimized for the downstream real-time PCR-based gene expression analysis with the Human Cytokine and Chemokine RT² Profiler PCR Arrays (SABiosciences), which is a 96-well plate format that includes 84 immune mediators and the appropriate controls. The mRNA expression profile resulted in identification of 58 differentially expressed mediators with more than two-fold up or down regulation in at least one time point (Table 2.3). Meth elicited a strong (more than 10-fold) up-regulation of CXCL16 and CXCL2, a moderate (5- to 10-fold) up-regulation of IL-7, CCL20, CXCL1, CCL24, and IL-8, and a strong (more than 10-fold) down-regulation of CCL7 (also called monocyte-specific chemokine 3 (MCP-3) at the 2 h time point. TNF-α maintained moderate transcript levels at 2 and 6 h of Meth exposure. In addition, IL-10 became highly up-regulated at 6 h. Similarly, CXCL13 was up-regulated between 6 h and 24 h. Some cytokine responses to Meth exposure were dynamic. For example, while CXCL16 was strongly up-regulated at 2 h of exposure, at the 6 h time point the levels subsided back to control level. Notably, by 24 h the majority of the cytokines returned back to control levels. In accordance with previous studies, we performed viability assays of Meth-treated macrophages for up to 48 h (Fig. 2.2). There was a slight trend of decreased viability however, we did not observe significant changes in any of the time points.

2.3.2. Meth promotes a pro-inflammatory macrophage phenotype

Based on the classification of pro-inflammatory and anti-inflammatory functions of cytokines, the pattern of cytokine expression after Meth exposure shifted the phenotype of macrophages towards pro-inflammatory (Fig. 2.3) [16-18]. Overall, the changes in cytokines expression peaked at 2 h after exposure to a single dose of Meth and persisted for 6 h, eventually subsiding by 24 h (Table 2.3). Next, we focused our study on TNF, CXCL1 and IL-8. Each was up-regulated in an increasing manner at stepwise concentrations of Meth (Fig. 2.4). The effect of Meth at higher concentrations such as 500 μM or 1 mM, was masked, possibly due to a small yet significant decrease in cell viability, which was not observed in concentrations up to 100 μM (Fig. 2.2). Therefore, to prevent the cytotoxic effects of Meth and cytokine-induced cytokine expression, all further experiments were conducted at 2 h of Meth exposure at 100 μM.

2.3.3. Meth down-regulates CCL7 expression

Based on our array results showing a robust down-regulation of CCL7 by Meth and given the importance of CCL7 in innate immunity we further looked at signaling pathway upstream of CCL7 expression [13, 21]. CCL7 is induced by TLR9 activation in a MyD88-dependent pathway and utilizes AP-1 and NF-κB as transcription factors [21]. First, to confirm the array data we performed RT-qPCR to investigate whether CCL7 is down-regulated by Meth exposure in a concentration dependent manner. Indeed, increased concentrations of Meth from 1 to 100 μM at 2 h of exposure led to a statistically significant reduction in CCL7 mRNA expression (Fig. 2.5 A). It has been shown *in vivo* that the expression of CCL7 and INF-α is dependent on activation of TLR9 [21]. Therefore, we performed experiments to see if Meth would block TLR9 mediated signaling. To do this we used CpG ODN, an agonist of TLR9, which is also used as a surrogate for an infection model of bacterial DNA. We measured the expression of CCL7 in the presence of

Meth and CpG ODN for 2 h, and used INF-α as a positive control. As expected, treatment with the TLR9 agonist (CpG ODN) up-regulated expression of CCL7 and IFN-α. CCL7 was down-regulated when macrophages were treated with only Meth, at similar levels to our time-dependent profiling experiment. Meth also attenuated the CpG ODN-induced expression of both, CCL7 and IFN-α (Fig. 2.5 B-C).

2.3.4. Meth affects TLR9 signaling pathway

The attenuation of CCL7 and IFN-α expression by Meth during TLR9 activation suggested that Meth reduces viral defense. CCL7 and IFN-α utilize several of the same signaling components downstream of TLR9, but the expression of each is dependent on different transcription factors, NF-κB and IRF7 respectively [22, 23]. Thus, we hypothesized that in order for both CCL7 and IFN-α to be differently expressed, the inhibition caused by Meth was occurring at or upstream the common TRAF3/6 signaling factors that are used by both cytokines (Fig. 2.8.). First we investigated if the levels of TLR9 changed upon Meth exposure. Neither mRNA expression nor protein levels of TLR9 were significantly changed compared to mock CpG treatment, but there was a trend of reduced TLR9 expression after Meth treatment alone (Fig. 2.6). Meth did, however, decrease the expression of TLR9 in CpG ODN treated cells to the level of control cells.

2.3.5. Effect of Meth on the transcriptional regulator NF-κB

There are several putative binding sites in the promoter region of CCL7 for the transcription factors, AP-1 and NF-κB. A possible mechanism of how Meth down-regulates the expression of CCL7 is Meth reduces the abundance of the transcription factors for CCL7. Therefore, we measured the protein levels of the NF-κB subunit, p65, from Meth exposed macrophages up to 48 h and observed no change over time (Fig. 2.7). Although these results informed us that overall levels of NF-κB do not change in Meth treated cells, it could still

interfere by preventing the translocation of NF-κB and making it less available at the promoter. The nuclear localization signal of NF-κB is masked by IκB and the inhibition of NF-κB by IκB is released when IκB is phosphorylated and degraded. Meth preventing the phosphorylation or the degradation of IκB warrants further investigation as well as the availability of the other CCL7 transcription factor, AP-1.

2.3.6. DNA methylation in the promoter region of CCL7 does not contribute to suppression

Changes in DNA methylation might be one potential mechanism that Meth induces to alter gene expression. To investigate whether such a mechanism is occuring on CCL7 expression, we measured the DNA methylation status of two CpG islands in the promoter region of CCL7. These islands are located on chromosome 17:(hg19) at positions 32596886 and 325971103. One CpG island is located at -349 relative to the promoter start site while second one is located at position -132. We have found that in mock treated macrophages for 2 h at the -349 position is hypermethylated at the level of 96% while -132 position is hypomethylated at the level of 2% (Table 2.2). The levels of methylation of both CpG islands were not affected by addition of Meth or treatment with CpG ODN, indicating that Meth does not regulate the methylation status of CCL7.

Gene	Sense Primer (5' to 3')	Anti-sense Primer (5' to 3')	Sequencing Primer (5' to 3')	PCR (bp)	Anneal °C
CCL7-1	AAGTTATTAGGATTTAAGATA GTGAAGAA	TATATAAAAAATATTCCCCTTTTC CCTTT	AAGTTTGAATGTTTTTTTGT GGAT	133	58
CCL7-2	TGATAATAGTTATAGATTATAT ATTGTGG	TCTACTAAACCAATACACTTCAA TAAAAA	GTTTTAGTTGAAAAATAGG TTAGTT	147	58

Table 2.1. Parameters for DNA pyrosequencing. Primers for CCL7 around two CpG islands (CCL7-1 and CCL7-2), the size of the PCR product, and optimal annealing temperature.

chr17: (hg19)	32596886	32597103
Relative to Transcription Start Site	-349	-132
Sample	CpG Percent Methylation	
Mock	93	3
Meth	97	2
CpG	96	2
M+C	96	2
Lymphocyte DNA	87	3
SSS1 methylated DNA	100	96

Table 2.2. Percentage of methylated DNA around both CpG islands for CCL7 promoter. Macrophages were either mock treated with 1 µg/mL of non-stimulatory CpG (ODN 2243), 100 µM of methamphetamine, or 1 µg/mL of stimulatory CpG (ODN 2216) for two hours. Then harvested for DNA and analyzed for methylation. Sss1 methylated and lymphocyte DNA served as the positive and negative control, respectively

	2	6	24
CXCL16	12.1	-1.7	-1.2
CXCL2	11.5	2.4	1.7
TNF	8.7	5.2	1.1
IL7	8.6	1.9	2.4
CCL20	7.2	3.4	3.6
CXCL1	7.1	3.3	1.9
CCL24	6.2	3.7	3.3
IL8	5.9	2.6	2.9
IL16	4.6	2.4	1.2
CCL1	4.5	1.4	1.6
OSM	4.3	-1.2	-1.2
CXCL12	4.3	4.1	3
IL5	4	-2	-1.7
CSF2	4	1.5	1.2
NODAL	3.7	3.5	1.1
IL10	3.6	13.9	1.5
BMP6	3.5	3.5	2.2
CXCL10	3.1	2.1	1.9
CSF3	2.5	-1.8	-1.4
CCL5	2.4	-2	-1.6
VEGFA	2.1	2.9	2
THPO	2	-5.9	-1.9
IL1A	1.9	-2	1.5
CCL21	1.8	-3	-1.4
CXCL5	1.7	-4.1	-3.7
IL6	1.6	1.6	2.8
CCL19	1.6	3.7	2.9
MIF	1.2	-2.3	-1.5
IL4	1.2	-4.3	-1.2
SPP1	1.1	7.7	7.7
IL27	1.1	-3	-2.2
CCL2	1.1	-2.4	-1.3
CXCL13	1	6	11.1
MSTN	-1	-2.3	-1
IL23A	-1.1	-3.3	-2.1
LIF	-1.2	-6.6	0
IL24	-1.4	-3.1	-1.4
IL1RN	-1.4	-1.9	-1.2
IL12A	-1.4	-3.4	-1.2
CXCL9	-1.5	-2.7	-1.8
LTB	-1.6	-7.5	-1.3
IFNG	-1.6	2.6	1.3
CSF1	-1.6	-2.1	1.3
LTA	-1.7	-5	-3
IL12B	-1.7	1.6	2.3
CCL18	-1.9	-4.8	-4.8
CCL17	-1.9	-2	-2.2
C5	-2	-2.5	1.4
IL13	-2.1	-3.9	-4.2
FASLG	-2.4	-1.3	-2.2
IL22	-2.5	-1.1	-2.3
BMP4	-3.2	-2.8	1
CD40LG	-3.3	-1.7	1.2
TNFRSF11B	-3.7	-1.1	-1.3
TNFSF13B	-4.1	-2.6	-1.5
IL11	-4.3	-3.9	-1.7
CCL13	-4.7	-1.1	1.9
CCL7	-13.6	-2.5	1.5

Table 2.3. RNA expression profile of immune mediators over time from Meth-exposed macrophages. RT-qPCR analysis of mediators that illicit an immune response including receptors, growth factors, interleukins, and cytokines were measured after

macrophages were exposed to Meth for either 2, 6, or 24 hours. The average fold change represented in each box is from Meth treated macrophages relative to corresponding time control from 3 biological replicates. Red positive box indicates an up-regulation while a green negative box indicates a down-regulated gene. Fold changes are normalized to the housekeeping gene GAPDH.
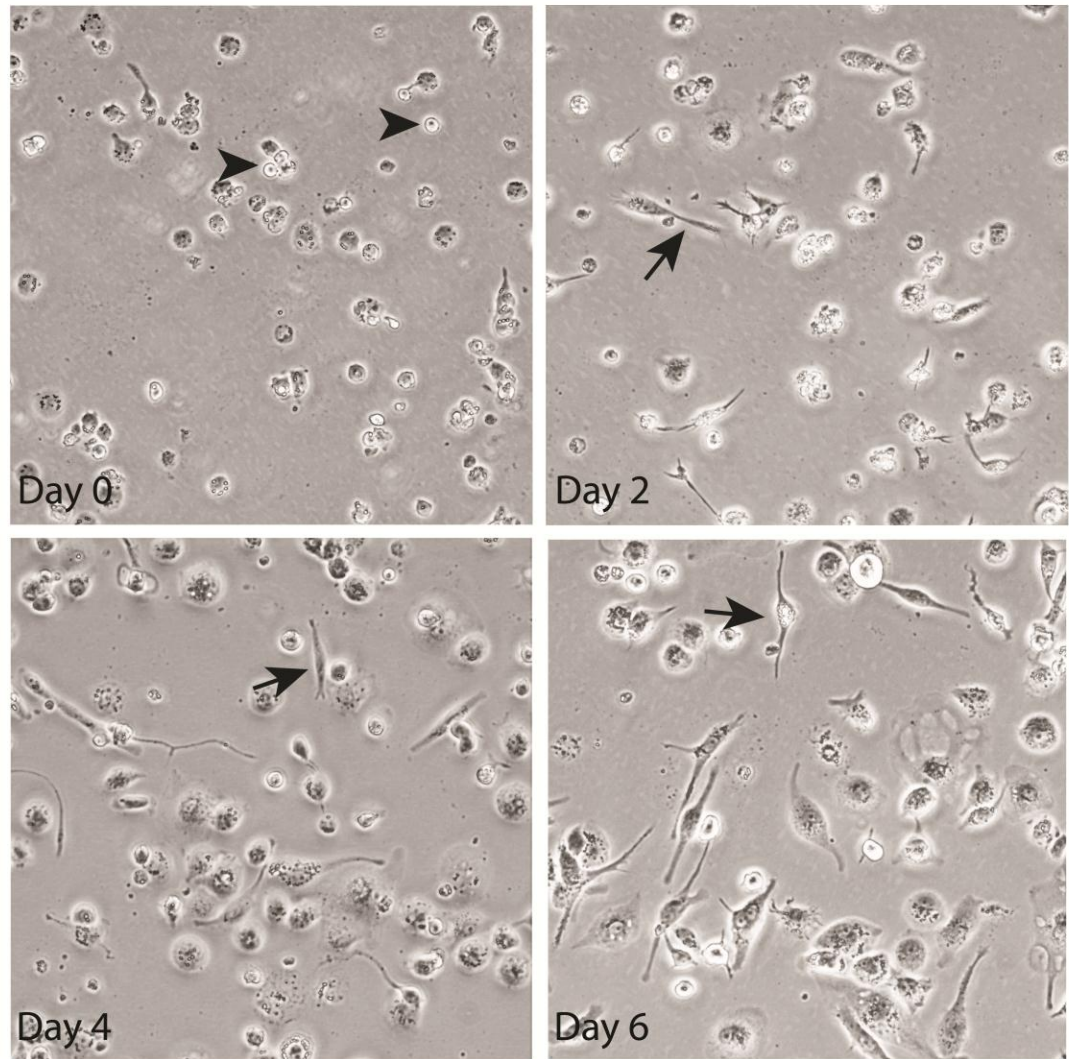
Figure 2.1. THP-1 monocyte to macrophage differentiation. THP-1 monocytes, a human monocytic leukemia cell line, were differentiated according to ATCC guidelines with 200 nM of PMA on days 0 and 2 until day 4. Cells rest in PMA-free media from day 4 to 6, after which they are considered macrophage-like and exposed to treatments. Similar to in-vivo macrophages, THP-1 macrophages are terminally differentiated and do not proliferate. 10X objective. Arrowhead (➤) symbolize spherical, round monocytes. Arrows (↑) point to processes of macrophages.
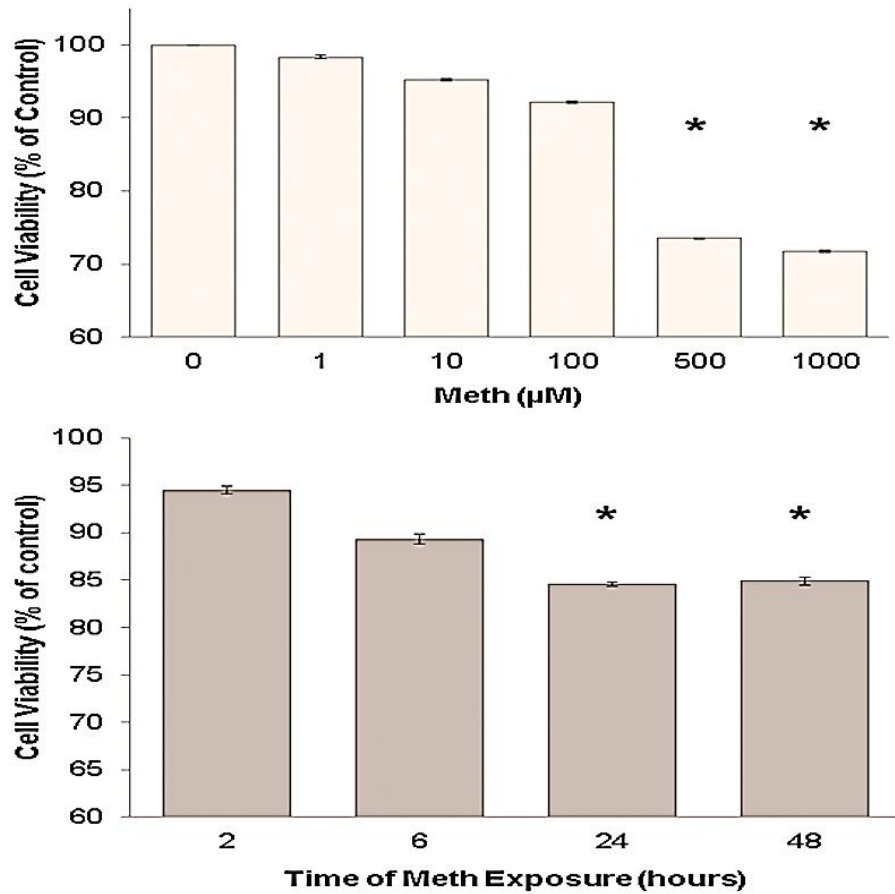
Figure 2.2. Viability of macrophages at different times and concentrations of Meth exposure. (a) Macrophages treated with either control (complete RPMI media) or 100 µM of Meth for 2, 6, 24, and 48 hours. Viability assessed by MTT assay and normalized to the respective time control and to a positive control. (b) Macrophages were treated with varying concentrations of Meth (1-1000 µM) for 2 h. Viability assessed by MTT assay and normalized to control (0 µM). Positive control cells were treated with 1% Triton X-100. Data are represented as the mean ± SD. An asterisk (*) indicates $p < 0.05$ by a Student's t-test.
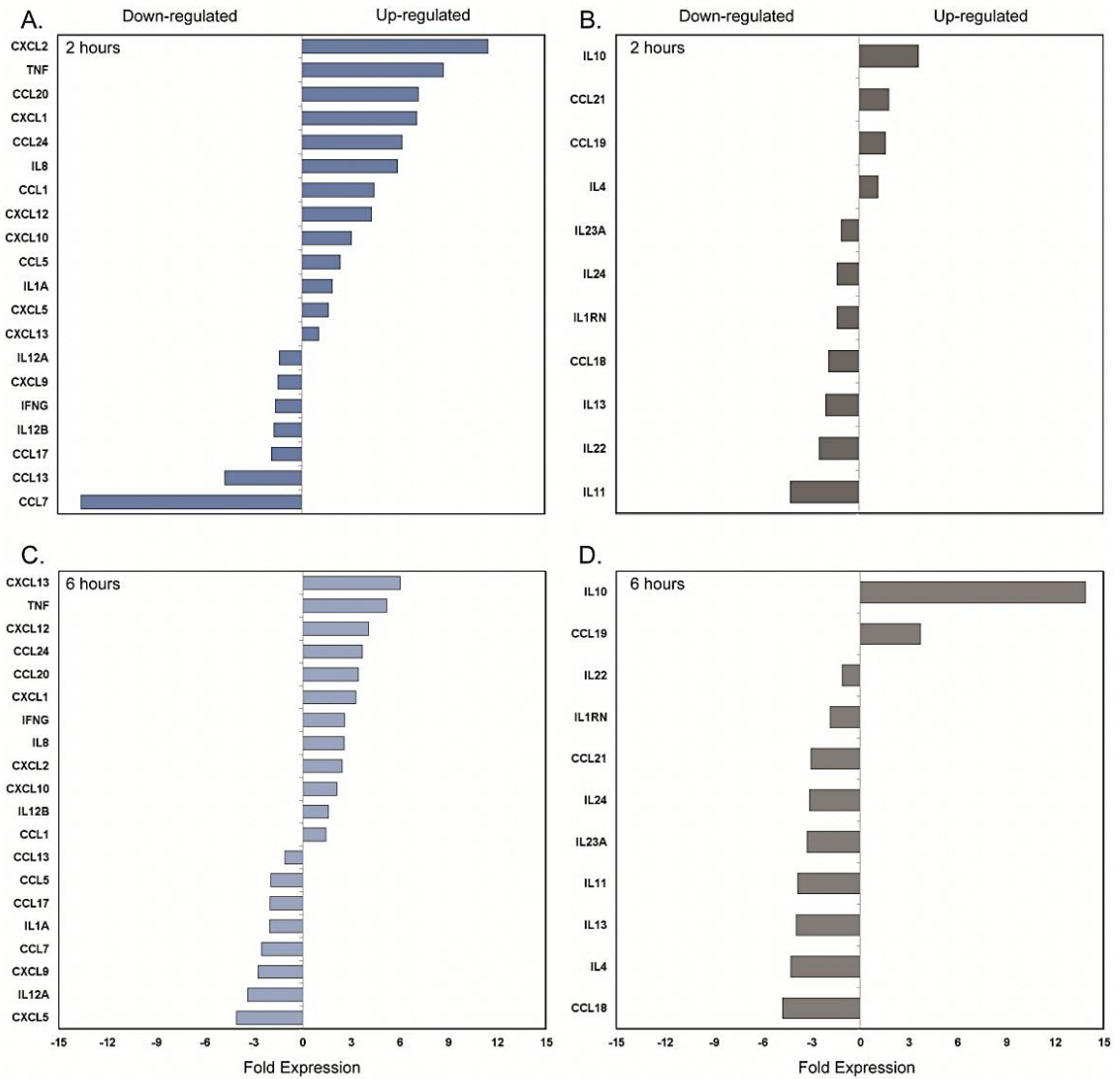
Figure 2.3. Characterization of immune mediators from Meth-exposed macrophages. Macrophages were treated with 100 μM Meth for either 2 or 6 h. After treatment, total RNA was isolated and expression of chemokines, interluekins, and cytokines was profiled by RT-qPCR. Cytokines are defined as either pro-inflammatory (a, c) or anti-inflammatory (b, d) and organized in decreasing order of regulation levels. Fold changes are normalized to the housekeeping gene GAPDH.
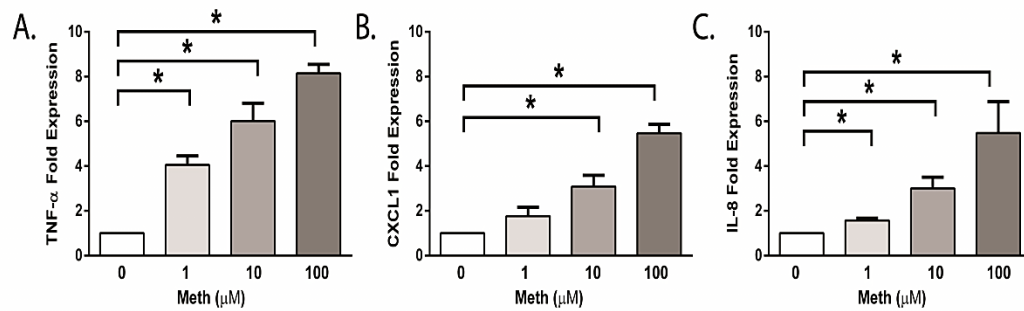
Figure 2.4. Concentration dependence on mRNA cytokine expression. Macrophages were exposed to 0-100 µM methamphetamine for 2 h and select cytokines were chosen for relative quantification by RT-qPCR. Baseline expression of each cytokine corresponds to control (0 µM) and represents a fold expression of 1. Data are represented as the mean±SD fold expression of 3 independent experiments. An asterisk (*) indicates $p < 0.05$ by a Student's t-test. All fold change is normalized to the housekeeping gene GAPDH.
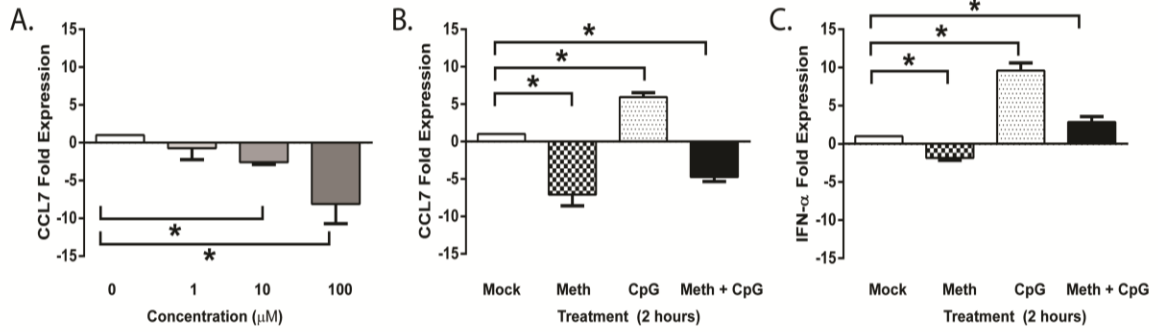
Figure 2.5. Methamphetamine inhibits the expression of CCL7. (a) RNA expression of CCL7 was measured by RT-qPCR in macrophages treated with varying concentrations of methamphetamine (0-100 μM) for 2 h. (b, c) Macrophages were exposed to 100 μM or 1 μg/mL CpG (CpG oligodeoxynucleotides) for 2 h. Expression of IFN-α is induced by activation of TLR9 by CpG and used as a positive control. Data are represented as the mean±SD fold expression of 3 independent experiments. An asterisk (*) indicates p<0.05 by a Student's t-test. Fold changes are normalized to the housekeeping gene GAPDH.
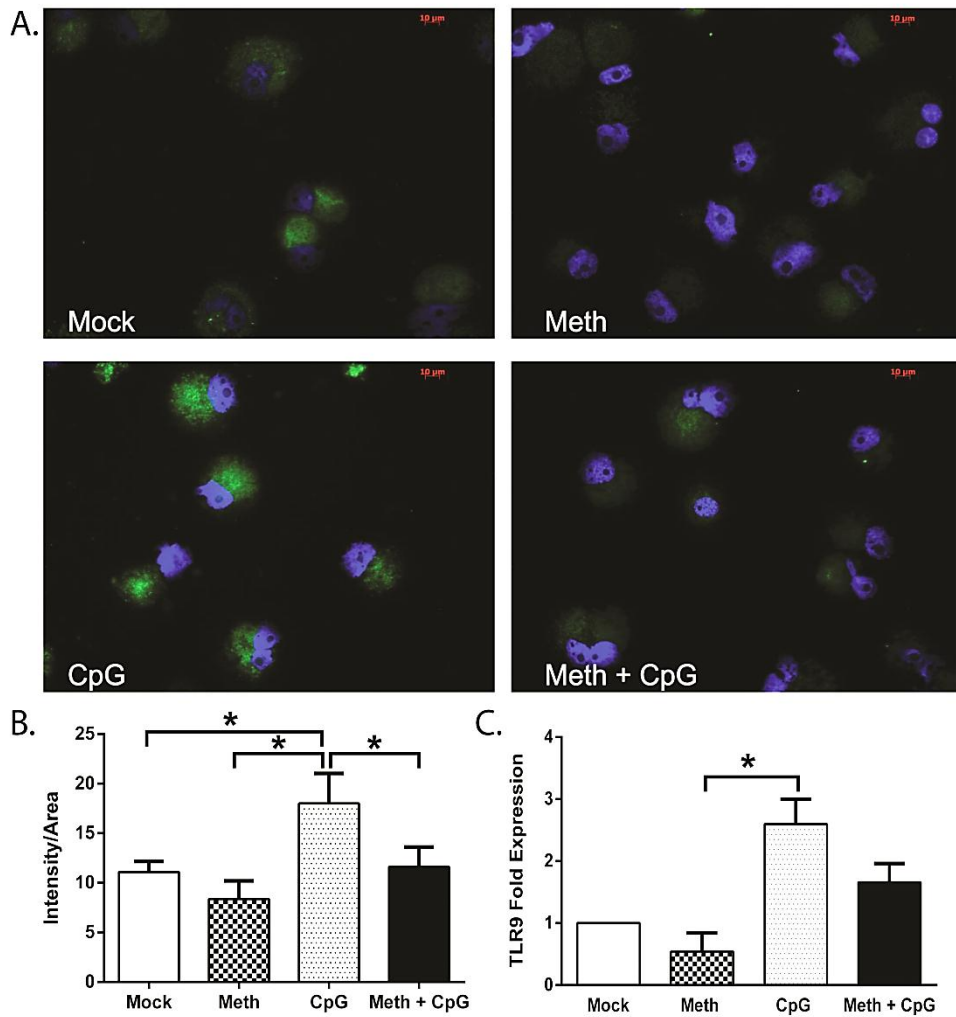
Figure 2.6. Methamphetamine attenuates the CpG-induced expression of TLR9. (a) Representative image of immunocytostained macrophages for TLR9 (green) at 1:500 and DAPI (blue) at 1 μg/mL that were either mock treated with 1 μg/mL non-stimulatory CpG (ODN 2243), 100 μM of methamphetamine, or 1 μg/mL of stimulatory CpG (ODN 2216) for 2 h. 40X oil immersion fluorescent microscope (b) Immunostaining for TLR9 antibody protein were quantified using Image J. Data are represented as the mean±SD fluorescent intensity per area of 3 independent experiments. (c) Total RNA from treated

macrophages was converted to cDNA and the levels of TLR9 determined by RT-qPCR relative to the mock treated macrophages. An asterisk (*) indicates $p<0.05$ by a Student's t-test. Quantification was normalized to the housekeeping gene GAPDH, n=3.
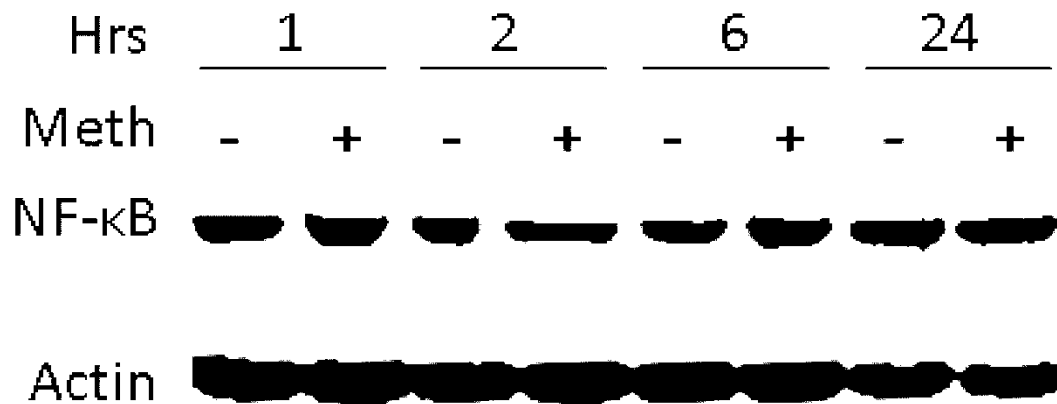
Figure 2.7. Methamphetamine does not alter protein levels of the pro-inflammatory transcription factor, NF-κB. Macrophages were either mock treated (RPMI media) or treated with 100 µM methamphetamine for 1, 2, 6, and 24 h. Western blots from whole cell lysates were blotted for anti- p65 (1:1000) or anti-actin (1:2000) for a loading control. This figure is a representative Western blot of 3 biological replicates.
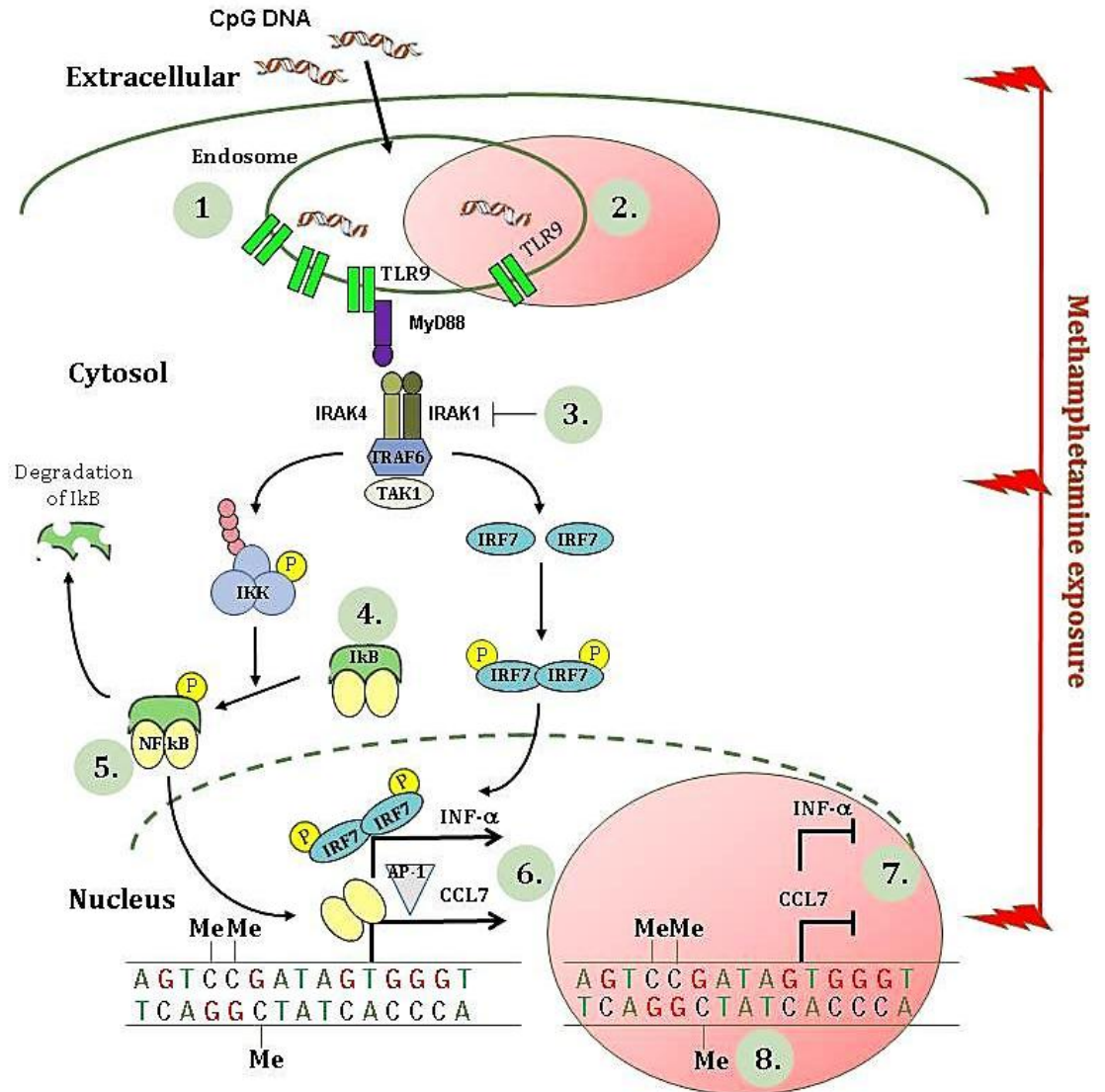
Figure 2.8. Signaling pathway of TLR9 by CpG activation and summary of results.
Single stranded unmethylated CpG (cytosine phosphate guanine) is endocytosed and stimulates TLR9 (Toll-like receptor 9) signaling. Macrophages were treated with CpG or Meth and CpG for two hours. Numbers in this figure indicate a description for each experiment. (1) TLR9 mRNA and protein was up-regulated after CpG treatment. (2) Meth decreased the CpG induction of TLR9 back to control levels. (3) Activation of TLR9 in combination with an IRAK1/4 chemical inhibitor leads to the inhibition of CCL7

transcription. Although it shows that the regulation of CCL7 is utilizing IRAK1/4 as intermediate, we found no evidence of Meth effecting the overall protein expression of IRAK1 or the phosphorylation of IRAK1 at Thr387. (4) Total levels of IkB protein did not decrease after 1 hour of Meth exposure nor up to 24 hours. This, however, was similar to other studies where degradation of IkB was found as early as 15 min for certain treatments. (5) Meth does not change the overall levels of NF-κB in the cell over time, however one possibility is that Meth prevents the translocation of NF-κB thus making it less available at the promoter. (6) CpG treatment moderately (5-10 fold) up-regulated the expression of CCL7 and IFN-α when compared to mock treatment. (7) Yet, Meth and CpG together down-regulated both cytokines. (8) Pyrosequencing results of either treatment, CpG or CpG and Meth, showed no change in DNA methylation at either CpG island of the CCL7 promoter region excluding this as mechanism of transcription regulation.

2.4.   Discussion

The effects of Meth could be acting on the extracellular receptors, intracellular signaling molecules, or in the nucleus. We focused these studies on one signaling pathway, the MyD88-mediated TLR9 signaling pathway. The investigation started at the utmost upstream location, examining changes in the TLR9 mRNA expression and protein levels. The effects of Meth in conjunction with CpG treatment can be seen in red circles whereas the remaining is of the effects of CpG alone (Fig. 2.8). First, a small down-regulation of TLR9 by Meth was observed. However, it was not sufficient to explain the strong down-regulation of CCL7 and INF-α. This suggested that Meth was affecting signaling mediators or transcription regulation further downstream of TLR9. Therefore, we measured protein of signaling factors such as IRAK1, IκB and IRF7 but found no changes in total levels or phosphorylation at key regulatory sites (data not shown). Next, we found that Meth does not affect the expression of a key transcription factor, NF-κB. Furthermore, the levels of DNA methylation in the promoter region of CCL7 did not change in the presence of Meth and or CpG treatment. Hence, we might expect to see either an absence of enhancing transcriptional complexes or an increase in the silencing transcriptional complexes found around the CCL7 start site. To measure the changes in either the silencing or enhancing transcription complexes, we would first use chromatin immunoprecipitation (ChIP) for either NF-κB or AP-1 transcription factors and PCR for CCL7. Next, use a mass spectrometry approach to identify the differences in Meth exposed macrophages to control treated cells from the ChIP pull down. The exact mechanism of how Meth affects TLR9 or other MyD88-mediated signaling pathways will require more extensive studies.

Macrophages respond rapidly to external stimuli and one such response is the release of cytokines, which plays a critical role in recruiting other immune cells to initiate the innate and adaptive immune response. Changes in the production of cytokines can have autocrine and

paracrine signaling effects as well as, can determine activation and phenotypic polarization of these cells. Generally, polarized macrophages can be classified as an M1, classically activated macrophage or M2, alternatively activated macrophage however, there is a spectrum of activation states in between these two [25, 26]. Thus, the phenotype of macrophage activation under specific pathological condition or stimulation will be best described by profiling cytokine secretion among other factors [27]. Classically activated (M1) macrophages will be polarized in response to stimulation by IFN-γ and LPS and characterized by their ability to secrete pro-inflammatory cytokines such as TNF-α, IL-1β, and IL-12 [28, 29]. On the other hand, the M2 phenotype, which includes the M2b phenotype, is considered immune regulating by expressing high levels of IL-10, CXCL1, and TNF-α and can be induced by TLR ligands [30]. Based on our results, the mRNA profile of cytokine expression in macrophages exposed to Meth most closely fit an M2b phenotype, more so than other types. However, additional cell surface markers and other chemical molecules are needed to completely characterize the phenotype of Meth-exposed macrophage.

One principal finding of the present study is that Meth induces the up-regulation of pro-inflammatory cytokines (Fig. 2.3).The pro-inflammatory effect of Meth has been previously demonstrated in literature by measuring a few pro-inflammatory cytokines like TNF-α, IL-1β, and IL-8; however this is the first study profiling 84 cytokines and chemokines as a systematic study [12, 19, 20]. Also, these studies were focused on the LPS-induced response mimicking bacterial infection and were limited in scope by the number of cytokines measured [12, 31]. Therefore, in our study we profiled 84 cytokines and chemokines, which provided a more comprehensive overview of macrophage polarization. Indeed our results showed that besides IL-10 and the modest expression of three others (CCL19, CCL21, and IL-4), macrophages showed pro-inflammatory phenotype over a 24 hour time frame of Meth exposure. One of most striking

observations resulting from profiling the cytokines over time was the strong down-regulation of CCL7 within 2 hours of Meth treatment indicating TLR9 signaling as a target pathway for this suppression [21]. This notion was reinforced further by our observations that Meth also suppresses the expression of IFN-α upon CpG ODN treatment. The CCL7 response was time- and concentration-dependent and, as anticipated, the onset of the Meth effect is rapid in macrophages.

Many of the pro-inflammatory cytokines such as TNF-α, IL-8, IL-1, and CXCL1 are regulated by NF-κB. In particular, IL-6 and IL-8 expression after Meth have been investigated for the dependence on NF–κB in other model systems. In these experiments, Meth up-regulated IL-8 and IL-6 in astrocyte cell line after 3 days of exposure [32]. The subcellular protein levels of NF-κB was measured over a span of 6 hours and, as expected to induce IL-8 and IL-6, was found to translocate to the nucleus. The authors also reported that PI3K/Akt, which is upstream of the activation of NF-κB, is involved in the Meth-induced expression of IL-6 and IL-8. In a similar study using gp120 transfected astrocytes, Meth was found to synergistically increase IL-6 and IL-8 mRNA and protein [33]. In our study, we found a concentration dependence effect of Meth on IL-8 but we did not measure IL-6 since it was not found statistically significant in the initial mRNA screening of time-dependent Meth exposed macrophages. Overall, the induction of cytokines is initiated by multiple pathways depending on the stimulus and even overlap by using the same signaling factors in different pathways thus, adding to the complexity of delineating the pathway for Meth-induced alterations of cytokine expression.

Since Meth users show increased susceptibility to various infections, we posit that the TLR signaling pathways, which orchestrate the clearance of infections, is hindered under Meth exposure [1, 34]. The significance of our results is further reinforced by previous studies showing that the expression of CCL7 is critical for immunity against cryptococcosis [7, 21]. While

infections with this fungus are rarely seen in those with fully functioning immune systems, it is the most common cause of fungal meningitis in AIDS patients, killing more than half a million people worldwide per year [35]. After the fungi, cryptococcus neoformans, are phagocytosed by alveolar macrophages it disseminates from the lungs to other parts of the body, including the brain regions to give rise to fungal encephalitis and meningitis [36]. Thus, the Meth-induced inhibition of CCL7 would prevent the recruitment of monocytes and eosinophils that facilitate the clearance of the fungal infection [21].

In summary, we conclude that Meth is immunosuppressive and inhibits TLR9 signaling and CCL7 and IFN-α expression. The cytokine environment produced by the Meth-exposed macrophage can induce a T-cell response and change the phenotype of naïve T-cells to regulatory T-cells, Th17, Th1, or Th2 helper cells [37-39]. Changes in the ratios or balance of supportive and detrimental T-cells subtypes can be pathological [40, 41]. In addition, the other aspect of the adaptive immune response, antibody production, is also impaired by Meth. In mice, the levels and the type of Ig antibodies produced were hindered in mice that were given increasing doses of Meth [8]. Lastly, Meth hinders several roles of macrophage function particularly cytokine expression and thus, greatly prevents the macrophage's ability to respond for proper innate and adaptive immunity.

2.5. References

1.   Kawasaki, T. and T. Kawai, *Toll-like receptor signaling pathways.* Front Immunol, 2014. 5: p. 461.

2.   Buxton, J.A. and N.A. Dove, *The burden and management of crystal meth use.* CMAJ, 2008. 178(12): p. 1537-9.

3.   Cohen, A.L., et al., *Methamphetamine use and methicillin-resistant Staphylococcus aureus skin infections.* Emerg Infect Dis, 2007. 13(11): p. 1707-13.

4.   Molitor, F., et al., *Association of methamphetamine use during sex with risky sexual behaviors and HIV infection among non-injection drug users.* West Journal of Medicine, 1998. 168: p. 93-7.

5.   Forrest, D.W., et al., *Crystal methamphetamine use and sexual risk behaviors among HIV-positive and HIV-negative men who have sex with men in South Florida.* J Urban Health, 2010. 87(3): p. 480-5.

6.   Eugenin, E.A., et al., *Methamphetamine alters blood brain barrier protein expression in mice, facilitating central nervous system infection by neurotropic Cryptococcus neoformans.* J Infect Dis, 2013. 208(4): p. 699-704.

7.   Patel, D., et al., *Methamphetamine enhances Cryptococcus neoformans pulmonary infection and dissemination to the brain.* MBio, 2013. 4(4).

8.   Martinez, L.R., et al., *Methamphetamine enhances histoplasmosis by immunosuppression of the host.* J Infect Dis, 2009. 200(1): p. 131-41.

9.   Potula, R. and Y. Persidsky, *Adding fuel to the fire: methamphetamine enhances HIV infection.* Am J Pathol, 2008. 172(6): p. 1467-70.

10.   Liang, H., et al., *Methamphetamine enhances HIV infection of macrophages.* Am J Pathol, 2008. 172(6): p. 1617-24.

11. Valencia, F., et al., *Influence of methamphetamine on genital herpes simplex virus type 2 infection in a mouse model.* Sexually Transmitted Diseases, 2012. 39(9): p. 720-5.

12. Liu, X., et al., *Methamphetamine increases LPS-mediated expression of IL-8, TNF-alpha and IL-1beta in human macrophages through common signaling pathways.* PLoS One, 2012. 7(3): p. e33822.

13. Talloczy, Z., et al., *Methamphetamine inhibits antigen processing, presentation, and phagocytosis.* PLoS Pathog, 2008. 4(2): p. e28.

14. Cadet, J.L. and S. Jayanthi, *Epigenetics of methamphetamine-induced changes in glutamate function.* Neuropsychopharmacology Reviews, 2013. 38: p. 248-9.

15. Livak, K.J. and T.D. Schmittgen, *Analysis of relative gene expression data using real-time quantitative PCR and the 2(-Delta Delta C(T)) Method.* Methods, 2001. 25(4): p. 402-8.

16. Dinarello, C.A., *Proinflammatory Cytokines.* Chest, 2000. 118: p. 503-8.

17. Opal, S.M. and V.A. DePalo, *Anti-inflammatory Cytokines.* Chest, 2000. 117: p. 1162-72.

18. Zeytun, A., et al., *Induction of cytokines and chemokines by toll-like receptor signaling: strategies for control of inflammation.* Critical Reviews in Immunology, 2010. 30(1): p. 53-67.

19. Tipton, D.A., Z.T. Legan, and M. Dabbous, *Methamphetamine cytotoxicity and effect on LPS-stimulated IL-1beta production by human monocytes.* Toxicol In Vitro, 2010. 24(3): p. 921-7.

20. Wells, S.M., et al., *Acute inhalation exposure to vaporized methamphetamine causes lung injury in mice.* Inhal Toxicol, 2008. 20(9): p. 829-38.

21. Qiu, Y., et al., *Early induction of CCL7 downstream of TLR9 signaling promotes the development of robust immunity to cryptococcal infection.* J Immunol, 2012. 188(8): p. 3940-8.

22. Akira, S. and K. Takeda, *Toll-like receptor signalling.* Nat Rev Immunol, 2004. 4(7): p. 499-511.

23. O'Neill, L.A., D. Golenbock, and A.G. Bowie, *The history of Toll-like receptors - redefining innate immunity.* Nat Rev Immunol, 2013. 13(6): p. 453-60.

24. Lai, R.K., et al., *Genome-wide methylation analyses in glioblastoma multiforme.* PLoS One, 2014. 9(2): p. e89376.

25. Gordon, S. and P.R. Taylor, *Monocyte and macrophage heterogeneity.* Nat Rev Immunol, 2005. 5(12): p. 953-64.

26. Mantovani, A., et al., *Macrophage polarization: tumor-associated macrophages as a paradigm for polarized M2 mononuclear phagocytes.* TRENDS in Immunology, 2002. 23: p. 549-55.

27. Fairweather, D. and D. Cihakova, *Alternatively activated macrophages in infection and autoimmunity.* J Autoimmun, 2009. 33(3-4): p. 222-30.

28. Martinez, F.O., et al., *Macrophage activation and polarization.* Frontiers in Bioscience, 2008. 13: p. 453-61.

29. Martinez, F.O., L. Helming, and S. Gordon, *Alternative activation of macrophages: an immunologic functional perspective.* Annu Rev Immunol, 2009. 27: p. 451-83.

30. Biswas, S.K. and A. Mantovani, *Macrophage plasticity and interaction with lymphocyte subsets: cancer as a paradigm.* Nat Immunol, 2010. 11(10): p. 889-96.

31.   Coelho-Santos, V., et al., *Prevention of methamphetamine-induced microglial cell death by TNF-a and IL-6 through activation of the JAK-STAT pathway.* Journal of Neuroinflammation, 2012. 9(103).

32.   Shah, A., et al., *Involvement of metabotropic glutamate receptor 5, AKT/PI3K signaling and NF-kappaB pathway in methamphetamine-mediated increase in IL-6 and IL-8 expression in astrocytes.* J Neuroinflammation, 2012. 9: p. 52.

33.   Shah, A., et al., *Synergistic cooperation between methamphetamine and HIV-1 gp120 through the PI3K/Akt pathway induces IL-6 but not IL-8 expression in astrocytes.* PLoS ONE, 2012. 7(12): p. e52060.

34.   Boehme, K.W. and T. Compton, *Innate sensing of viruses by toll-like receptors.* J Virol, 2004. 78(15): p. 7867-73.

35.   Roy, M. and T. Chiller, *Preventing deaths from cryptococcal meningitis: from bench to bedside.* Expert Reviews of Anit-infective Therapy, 2011. 9(9): p. 715-7.

36.   Enoch, D.A., H.A. Ludlam, and N.M. Brown, *Invasive fungal infections: a review of epidemiology and management options.* J Med Microbiol, 2006. 55(Pt 7): p. 809-18.

37.   Broere, F., et al., *A2 T cell subsets and T cell-mediated immunity.* 2011: p. 15-27.

38.   Weaver, C.T., et al., *Th17: an effector CD4 T cell lineage with regulatory T cell ties.* Immunity, 2006. 24(6): p. 677-88.

39.   Peck, A. and E.D. Mellins, *Plasticity of T-cell phenotype and function: the T helper type 17 example.* Immunology, 2010. 129(2): p. 147-53.

40.   Merrill, J.E. and E.N. Benveniste, *Cytokines in inflammatory brain lesions: helpful and harmful.* Trends in Neuroscience, 1996. 19: p. 331-8.

41.   Zhao, J., C.M. Lloyd, and A. Noble, *Th17 responses in chronic allergic airway inflammation abrogate regulatory T-cell-mediated tolerance and contribute to airway remodeling.* Mucosal Immunol, 2013. 6(2): p. 335-46.

Chapter 3

Alterations in Expression of HDACs and Levels Post-translational Modifications in HIV-1-infected, Meth-exposed Macrophages Treated with cART

3.1. Introduction

3.1.1. Discovery of HIV and subsequent pandemic

The first official documentation published by the US Centers for Disease Control and Prevention (CDC) on 5th June 1981 entitled "Pneumocystis Pneumonia – Los Angeles" outlined five cases of young gay men hospitalized with pneumonia, cytomegalovirus, and disseminated candida infections [1]. A month later, the New York Times reported that a total of 41 homosexual men had been diagnosed with Kaposi 's sarcoma, a rare skin cancer [2]. This unknown disease was spreading rapidly and at the end of 1981, 5 to 6 new cases of the disease were being reported each week [3]. It was unclear how young and previously healthy individuals were succumbing to such deadly opportunistic infections but assumed the condition was limited to the gay population, hemophiliacs, intravenous drug users, and immunocompromised individuals. In July 1982, at a meeting in Washington, D.C., the condition or disease was termed Acquired Immune Deficiency Syndrome (AIDS) [3, 4]. The CDC reported that the incidence of AIDS had risen from less than 6 per week to an average of one to two cases being diagnosed in the USA every day [5]. By the end of 1983 the number of AIDS diagnoses reported in the USA was 3,064 with an alarming 42.2% of them deceased [6]. In 1984, French scientists isolated the Human Immunodeficiency Virus (HIV) from the lymph node of infected patients that was the causative agent responsible for AIDS pandemic seen in earlier years [7].

HIV infection became a global pandemic with an estimated 35.3 million cases worldwide and 1.4 million people of those infected live in North America as of 2013 (Fig. 3.1.) [8, 9] HIV has since its discovery been subcategorized into two types, HIV-1 and HIV-2. HIV-1 is the most common type of the virus, while HIV-2 is predominately in Western African [10].

Total: 35.3 million [32.2 million – 38.8 million]
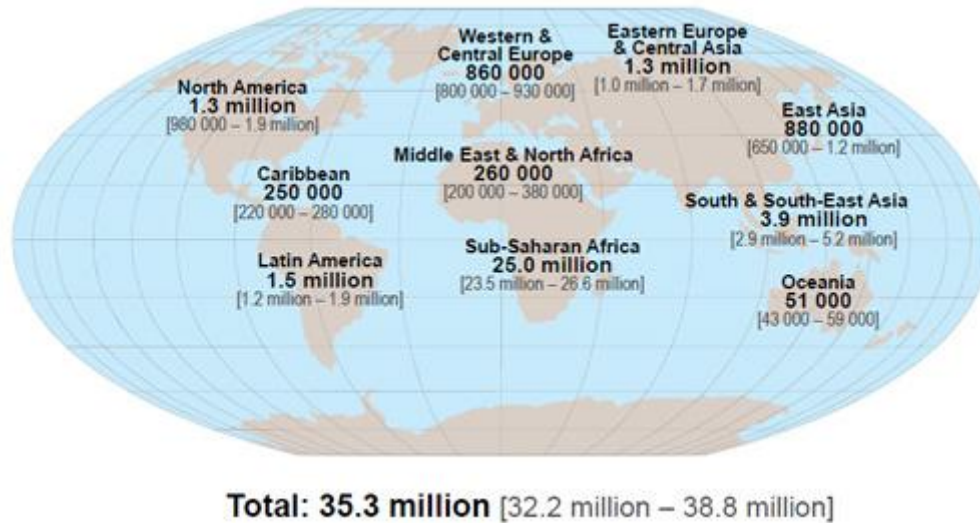
Figure 3.1. Number of People Living with HIV as of 2013 (Source: UNAIDS)

3.1.2. HIV structure and life cycle

HIV is a lentivirus of the *retroviridae* family. *Lenti* or lente translates to 'slow' in Latin and means HIV can be latent for a long period of time before it becomes active and pathogenic. The *retroviridae* family of viruses means the genetic material of HIV is RNA (in the case for HIV, two single stranded RNA molecules) as opposed to DNA. The viral genome consists of 9 genes (*gag*, *pol*, *env*, *tat*, *rev*, *nef*, *vif*, *vpr*, and *vpu*) and 15 distinct proteins [11]. There are six structural proteins: matrix (MA), capsid (CA), nucleocapsid (NC), p6, glycoprotein 120 (gp120) and gp41; three enzymes: protease (PR), reverse transcriptase (RT), and integrase (IN); two essential proteins: Tat, and Rev and four additional proteins called accessory proteins: Vif, Vpr, Vpu, and Nef, of which Rev and Tat are essential since they are compulsory for the transcription of daughter virus particles [12, 13]. The others are accessory as they are dispensible for replication *in vitro*, but required for pathogenesis *in vivo*.

HIV is packaged into virons that contains all necessary components for the virus to travel throughout the bloodstream and infect other cells. The formation of virions can

be divided into three stages: assembly, in which the viral proteins are created and essential components are packaged; budding, wherein the virion crosses the plasma membrane and obtains its lipid envelope; and maturation, where the virion structure changes and becomes infectious [14]. An HIV virion is approximately 100 to 150 nm in diameter and is made up of a viral envelope and viral core. The viral envelope
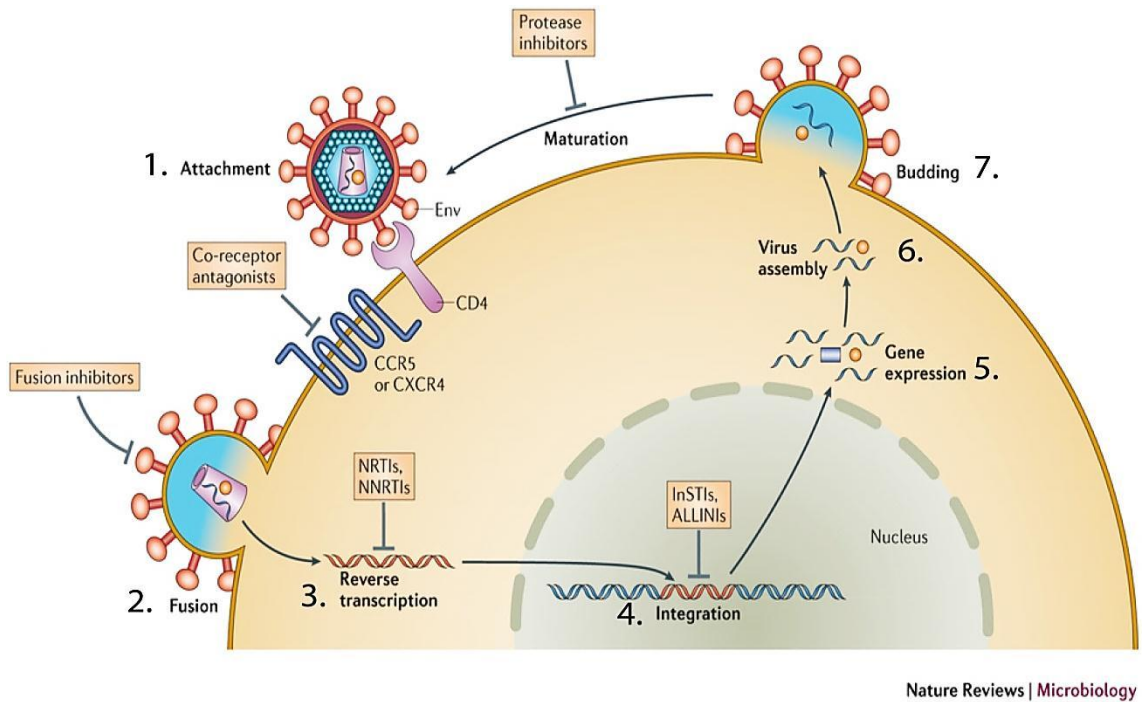
Figure 3.2. The Steps of the HIV Life Cycle. (Source: Adapted from Nature Reviews [15])

is a lipid bilayer derived from host's plasma membrane during budding. A number of host cell proteins and viral specific glycoproteins are associated with the envelope. These viral glycoproteins, both encoded by the HIV *env* gene, are glycoprotein 120 (gp120), which is non-covalently linked to the transmembrane glycoprotein 41 (gp41). The core (or capsid) of the virion consists of a cone-shaped protein p24 and protects the viral genome and the three enzymes RT, PR, and IN that are essential for the survival and infectivity of HIV [16].

The HIV *life cycle* starts with HIV gp120 on the surface of the virion *attaching* to the CD4 co-receptor on the host cell. A conformational change in gp120 allows further interaction with either, CXCR4 (X4) or CCR5 (R5) co-receptors [17]. Once gp120 interacts with both CD4 and either chemokine receptor it results in the insertion of the fusion peptide into the host cell membrane to initiate *fusion* of the viral and host cell membranes. The viral core is then released in to the cytoplasm of the host [18]. Next, the viral RNA is *reversed transcribed* by the prepackaged viral enzyme RT. The cDNA of HIV translocates to the nucleus using a number of host's proteins as chaperones and is *integrated* into the host DNA using IN [19, 20]. When activated, the proviral DNA is *transcribed and translated.* Two of the first viral proteins to be translated to positively regulate transcription are Tat (trans-activator of transcriptional) and Rev (regulator of expression of virion proteins). The large polypeptide chains comprising of viral core envelope (Env) and gag proteins are cleaved in to smaller fractions. HIV RNA, the viral Env protein, the Gag polyprotein, and the three viral enzymes: PR, RT, and IN *assemble* near the host's plasma membrane and results in *budding* of a new infectious particle [15] (Fig. 3.2.).

3.1.3. Common therapy for HIV-1 infection

The treatment strategies for HIV positive individuals are designed to primarily target viral enzymes as well as virus entry to prevent the progression of the various stages of the viral life cycle. The FDA approved drugs for HIV fall in to 6 different classes: non-nucleoside reverse transcriptase inhibitors (NNRTI) nucleoside reverse transcriptase inhibitors (NRTI), protease inhibitors (PI), fusion inhibitors, entry inhibitors (also called chemokine receptor antagonists), and integrase strand transfer inhibitors (INSTI). NRTI were the first class of drug to be approved by the FDA and inhibits RT with modifed nucleosides that bind to viral DNA and halt the elongation by RT. Tenofovir (TDF), trade name Viread, is an FDA approved NRTI and although being synthesized in

1984, it was not approved until 2001. However, TDF is on the World Health Organization's (WHO) List of Essential Medicines for preventing and treating HIV and chronic Hepatitis B, a common co-infection [21-23]. Another common and NRTI is Emtricitabine (FTC) and is available as a monotherapy or as a fixed dose together with TDF, trade names Emtriva and Truvada, respectively [24]. During the mid-90s, the PI class of drug was introduced. As the name indicates, PI prevents viral replication by selectively binding to PR, which is critical for the cleavage of protein precursors into the mature infectious proteins therefore, no active enzymes or budding can occur. Atazanavir (ATV), trade name Reyataz®, was the first approved PI for once daily dosing and is also on the WHO List of Essential Medicines.

Due to HIV mutating and development of drug resistance, the standard regimen of treating HIV is with combinational antiretroviral therapies (cART) using drugs from different classes, two NRTI/NNRTI and one PI/INSTI [25, 26]. The newer classes of drugs that are also useful in cases when drug resistance occurs against PI and RT inhibitors are entry inhibitors and INSTI [27]. The entry inhibitors in particular target the different stages of HIV entry, binding to either the CD4 or CCR5 receptors, or fusion of gp41, onto CD4+ cells. Maraviroc and Enfuviritide are currently approved members in this group. Following the success of triple combination therapy, morbidity and mortality decreased drastically, making what was once a death sentence into a chronic condition where the life expectancy is now almost equal to healthy averages (~70%) [28, 29].

3.1.4. Meth use and HIV risk

HIV-1 infection and Meth addiction are serious and common comorbidities [30, 31]. Prevalence of both comorbidities is hard to determine since the prevalence is reliant on the region, the person's sexual orientation, whether or not the use of Meth is chronic or sporadic, and whether or not Meth is injected [32, 33]. Regardless of why HIV positive patients abuse Meth, it is often accompanied with unsafe sex practices as the effects of

Meth result in increases in sexual libido while decreasing judgment and inhibition, thereby increasing risk for HIV transmission [34]. Another issue with concurrent Meth use and positive HIV status is a decrease in adherence to HIV treatment and medical visits [35]. Frequent Meth use has also been associated with increased risk for antiretroviral resistance, particularly to NNRTIs and possible fatal interactions when used with PI [36-38]. All the risk factors taken together is shocking as Meth use can increase the risk for new HIV transmission cases through sexual activity and also contribute to poorer health outcomes in HIV-infected individuals.

Meth can be smoked, ingested (orally or anally), or injected, though the latter holds an increased risk in the case of sharing needles to spread HIV and other blood borne viruses [21, 39]. An estimated 20-40% of injecting drug users are HIV positive equating to about 3·0 million (range 0·8–6·6 million) people worldwide [33]. Although the percentage of injecting drug users includes other types of illicit drugs besides Meth, the astounding number is a major issue and risk to global public health.

3.1.5. HIV-1 latency and role of epigenetics

Epigenetics is the study of cellular factors and the mechanisms that help control gene expression that are not caused by the changes in DNA sequence. Research shows that epigenetics is, at least partially, contributes to inheriting addictive behaviors, aging, neuronal plasticity, and memory formation [40-43]. Post-translational modifications (PTM) to the histone N-terminal ("histone tails") and DNA methylation are the two epigenetic mechanisms that regulate gene expression. The number and type of PTM (acetylation, methylation, phosphorylation, and mono- di-, or tri-) as well as location (which residue), and combination can indicate gene transcription or repression. This is referred to as the histone code [44, 45]. For example, methylation of histones can occur on lysine or arginine residues and can be mono- (Me), di- (Me2), or trimethylated (Me3). Acetylation (Ac) occurs on lysines but due to the neutralization of ε-amino group, only

one acetyl moiety can occur per lysine. Phosphorylation (P) occurs on serine and threonine residues and similar to acetylation can occur only once but for a different reason, the presence of one hydroxyl group. Ubiquitination (Ub) can occur on lysines and is complex because there can be one (mono-) or long chains of Ub (polyubiquitinated). Given the number of different types of PTM and number of amino acids they may or may not occur on and considering them occurring on multiple residues simultaneously, the number of possibilities to decipher the histone code is extensive. However, using a reductionist approach, the fundamentals have begun to be determined, including how a single PTM alters transcription, or if enzymes demonstrate specificity to which histone substrate [46-48]. For example, acetylation of lysine residues, although not always, will activate transcription whereas, a non-modified lysine inhibits transcription as well as DNA methylation [49, 50].

Of particular interest are the epigenetic mechanisms regulating HIV expression. The most studied PTM and mechanism in regards to HIV transcription is acetylation and deacetylation. The enzymes that accomplish the addition and removal of acetyl groups are called histone acetyltransferases (HAT) and histone deacetylases (HDAC), respectively. HDACs are classified as Class I or Class II. HDACs are divided and grouped together based on the sequence homology to the yeast counterparts however, a big difference between the localization of the two classes. Class I HDACs (HDAC1, 2, 3, and 8) are primarily found in the nucleus whereas, Class II HDACs (HDAC4, 5, 7, and 9) shuttle between the cytosol and nucleus. One HDAC in particular, HDAC1, was found to silence HIV expression but when incorporated into virions help facilitated entry of HIV into other cells [51, 52]. Even though cART has been able to control the virus to below detection levels, latent HIV exists in long-lived memory CD4+ T-cells and macrophages and prevents complete eradication of infection [53, 54]. Therefore, studies have used

HDAC inhibitors (HDACi) to open the chromatin and reactivate the expression of viral genes so that new therapies can target latently infected cells [55-57].

Epigenetic mechanisms are not only of interest to the field of HIV research but as mentioned previously, studied in the cases of drug addiction by itself or with both comorbidities (HIV and addiction) [40, 58]. Changes in gene transcription in the midbrain seen after chronic Meth exposure have been correlated with increases in the histone PTM acetylation as well as a decrease in HDAC1 protein [59-62]. There is evidence that epigenetic mechanisms regulate the viral genome and how that is altered in Meth abusers still needs to be determined so that reservoirs can be depleted and HIV finally eradiated. Therefore, the goal of our study is to identify the key factors involved in affecting HIV transcription using macrophages as a model of the immune function dysregulation in Meth abusers on cART.

3.2. Materials and Methods

3.2.1. Cell culture and sample preparation

Primary human monocytes were obtained through leukophoresis from donors who were seronegative for HIV-1, HIV-2, and hepatitis B virus. These monocytes were purified using counter-current centrifugal elutriation and cultured at a final concentration of 1 million per mL in macrophage serum-free medium (MSFM) (Invitrogen; Carlsbad, CA)[63]. MSFM was supplemented with a 1% HEPES buffer (4-(2-hydroxyethyl)-1-piperazineethanesulfonic acid)) (Invitrogen); 1% Nutridoma (Roche Diagnostics GmbH; Indianapolis, IN), and 10 ng/mL Macrophage-colony stimulating factor (MCSF) (PeproTech; Rocky Hill, NJ). Half of the media volume was exchanged every other day. After seven days of differentiation monocytes are considered monocyte-derived macrophages (MDM) and no longer require MCSF and therefore, HIV-1$_{ADA}$ infection was

diluted in new MSFM at a multiplicity of infection of one (MOI:1) for 4 h at 37°C. After, virus media is removed and replaced with fresh MSFM with the above defined supplements. On day 10, Meth (Sigma-Aldrich; St. Louis, MO) added at a concentration of 100 µM. Two days later on day 12, full media was removed and ATV, TDF, and FTC (henceforth referred to as cART) was added to fresh media, each at an efficacious concentration of 5 µM. All media was removed and cells were washed three times with phosphate buffered saline (PBS; HyClone; Logan, UT) before conditions were harvested on day 17 (Fig. 3.3.). Macrophages were lysed for RNA, whole cell lysates (WCL), or fractionated into subcellular parts using the Qproteome Nuclear Protein Kit (Qiagen; Germantown, MD) according to manufacturer's protocol (Fig. 3.4.). To obtain protein from WCL, cells were scraped in PBS and pelleted by centrifugation at 1000 x g for 5 min at 4°C and re-suspended in 300 µL per 10^6 cells of lysis buffer. Lysis buffer contained 4% (w/v) SDS (Bio-Rad; Hercules, CA), in 0.1 M Tris-HCl (Fisher Scientific; Fair Lawn, NJ), 0.1 M DTT (Promega; Madison, WI) and 1X Protease Inhibitor Cocktail (Sigma-Aldrich). Cells were boiled at 95°C for 5 min, allowed to cool, and 100 units/mL Benzonase Nuclease (Merck KGaA; Darmstadt, Germany) was added. All protein samples were quantified using Pierce 660 Assay as per the manufacturer's protocol using 50 mM ionic detergent compatible reagent (Thermo Scientific; Rockford, IL).

3.2.2. Quantification of HDAC levels and histone PTMs by Western blot

Five micrograms of cytosolic, nuclear, or WCL proteins were loaded onto Tris-Glycine gels (Invitrogen) and separated using one-dimensional electrophoresis. Proteins were immediately transferred to a PVDF membrane (Bio-Rad; Hercules, CA) and blocked overnight at 4°C in 5% milk in Tris-Buffered Saline supplemented with 0.2% Tween 20 (TBST) (both from Fisher Scientific). Nuclear fraction was used to blot for HDAC antibodies that were from a commercial source: HDAC1-6 (1:1000) for 1 h and horseradish peroxidase (HRP) secondary (1:1000) at room temperature for 1 h (Cell

Signaling Technologies; Beverly, MA). Washes were performed after primary and secondary antibodies using TBST three times for 5 min each. Three PTMs were studied, acetylation on lysine 5 histone 4 (H4K5ac), acetylation on lysine 9 histone 3 (H3K9ac), and acetylation on lysine 18 histone 3 (H3K18ac) (all from Abcam; Cambridge, UK) all at 1:1000. Each of the three PTM primary antibodies were incubated at 4°C overnight. Three washes for 5 min each were performed with TBST before and after adding HRP secondary antibody (Jackson ImmunoResearch; West Grove, PA) at 1:20000 at room temperature for 30 min. Each blot was incubated at a 1:1 ratio with TMA-6 Solution A and B enhanced chemiluminescence (Lumingen; Southfield, MI) in the dark for 1 min and exposed for 3 seconds. The density of the band was calculated on the Kodak CareStream Imaging System Image. Three biological replicates/donors were used for quantifying HDACs. Student's t-test was performed on the intensity valued after normalization to the intensity of actin.

3.2.3. RNA extraction and relative quantitative PCR

Cells were lysed directly in the culture dish with Trizol Reagent (Life Technologies; Carlsbad, CA). RNA was resuspended in 10 mM Tris (Pro-Pure, Solon, OH) and 1 mM EDTA (Fisher Scientific), pH 8.0 in RNase free water. One microgram of RNA was converted to cDNA using the High Capacity cDNA Reverse Transcription Kit (Life Technologies) per the manufacturer's protocol. The primers used were human HDAC1 and HDAC6 (both Integrated DNA Technologies; Coralville, IA) and human GAPDH primers were used for normalization (Applied Biosystems; Warrington, UK). The relative abundance of each gene was calculated using the comparative CT method [64]

3.2.4. Imaging of HDAC1 colocalization by confocal microscopy

Primary human MDM were cultured in 8-well chamber slides at a density of 500,000 cells per well. Cells were exposed to either MSFM for control or 100 µM Meth for 24 h at 37°C. Wells were washed 3 times with Tris-buffered saline (TBS, Sigma-

Aldrich), fixed with 4% paraformaldehyde (PFA, Sigma-Aldrich) for 30 min, permeabilized and blocked simultaneously with 0.1% Triton (Thermo Fisher; Waltham, MA) and 10% normal goat serum (NGS, Vector Laboratories; Burlingame, CA) in TBS and then quenched with 50 mM NH_4Cl (Sigma-Aldrich) for 15 min. The cells were washed with 0.5% Tween (Thermo Fisher) in TBS (TTBS) and incubated at (1:100) for the primary antibodies rhodamine-conjugated phalloidin (Life Technologies) and 1 µg/mL of HDAC1 (Abcam) in 10% NGS for 1 h at 37°C. The cells were then washed with TTBS and incubated with the secondary antibody conjugated to Alexa Fluor 488 for 45 min at 37°C. One µg/mL of DAPI (Invitrogen) for 5 min was used to stain nuclei and after one wash with water and one wash with TBS, one drop of Prolong Gold (Invitrogen) was added before the slides were cover slipped. Images were captured using the Zeiss Meta 510 confocal microscope (Carl Zeiss, Inc., Thornwood, NY, USA) and Zen lite Imaging software (version 2011). Ten parallel replicates were measured for each condition using ImageJ software.

3.3. Results

3.3.1. Quantification of HDACs

Given the ambiguity for the roles of HDACs in HIV or Meth use in macrophages, we measured the protein levels of some HDACs from Class I and Class II in an unbiased manner in all 8 conditions (Fig. 3.4). Cells were fractionated into nuclear and cytoplasmic proteins to decipher the localization of each. HDAC1-4 were detected in both the cytosol (Fig. 3.6.) and the nucleus (Fig. 3.7.). Surprisingly, HDAC5 and 6 were never detected in any of the three donors. The only HDAC with a statistical difference in expression compared to control cells was HDAC1 in Meth treated MDM, although there was also a trend for decreased HDAC1 in the nucleus (Fig. 3.8.). To confirm the localization of

HDAC1 protein, we used confocal microscopy to visualize and quantify HDAC1 in Meth exposed MDM. In the previous quantitative Western blot experiments MDM were exposed for 48 h, the confocal images were taken after only 24 h of exposure. Even so, HDAC1 was found to be decreased significantly compared to control (or mock treated macrophages) (Fig. 3.9.). Next, we sougt to determine the mechanism of decreased HDAC1 protein either decreased transcription, altered PTMs, increased degradation, or both altered PTMs and degradation [66]. To do this we first isolated the total RNA and performed RT-qPCR on HDAC1 and HDAC6. We observed that HDAC1 was highly expressed in control cells (data not shown) but drastically decreased in Meth treated MDM. In contrast, HDAC6 levels barely increased compared to control cells (Table. 3.1.). In order to overcome the donor to donor variability in the Western blots from all 8 conditions, separate cell cultures were conducted with fewer treatments and instead of fractionation we performed a WCL to extract all the proteins and reblotted for HDAC1. Much to our surprise, HDAC1 was no longer decreased in Meth treated MDM compared to control (Fig. 3.10.). In fact, no treatments reached significance for HDAC1 in WCL.

3.3.2. Consequences of decreased HDAC1 is changes in the histone acetylation

Decreases in HDAC1 would be expected to lead to increases in HDAC1-specific acetylation sites. Some PTMs that have been reported to be specific to HDAC1 by ChIP are histone 4 lysine 5 (H3K5), histone 3 lysine 18 (H3K18), and histone 3 lysine 9 (H3K9) [67, 68]. As expected with decreased HDAC1, we observed a large increase of H3K18 and H4K5 due to Meth but not H3K9 (Fig. 3.11.).

Gene	HDAC1		HDAC6	
Treatment	CONTROL	METH*	CONTROL	METH[ns]
Fold Expression	1.0 ± 0.0	-8.0 ± 1.8	1.0 ± 0.0	1.7 ± 0.6

Table 3.1. Expression levels of HDAC1 and HDAC6. MDM were cultured with 100 µM Meth or control (MSFM) for 48 hours. Total mRNA was extracted and PCR was performed. Relative to control Meth caused a significant decrease of HDAC1 mRNA but not HDAC6. Data are represented as the mean±SD fold expression of 3 independent experiments. An asterisk (*) indicates $p<0.05$ by a Student's t-test whereas, 'ns' is not statistically significant. Fold changes are normalized to the housekeeping gene GAPDH.
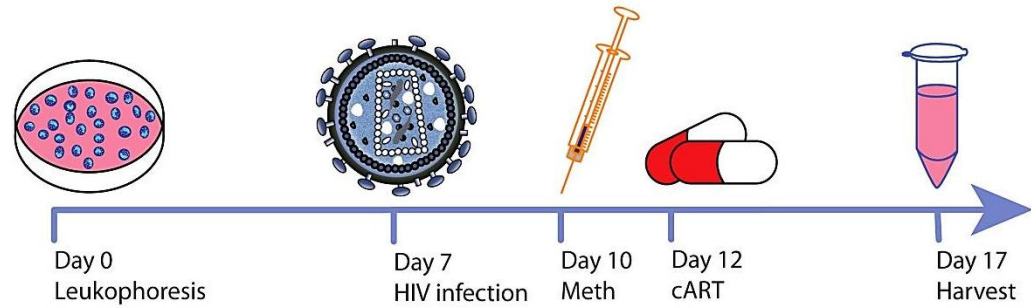
Figure 3.3. Timeline for treatments. Monocytes are differentiated in the presence of MCSF for 7 days. On day 7, MDM are infected with HIV-1$_{ADA}$. Three days post-infection, MDM are exposed to 100 μM Meth and maintained for 48 h. On day 12 days post-plating or 5 days post-infection MDM are treated with cART (ATV, FTC, and TDF) at 5 μM each until day 17.
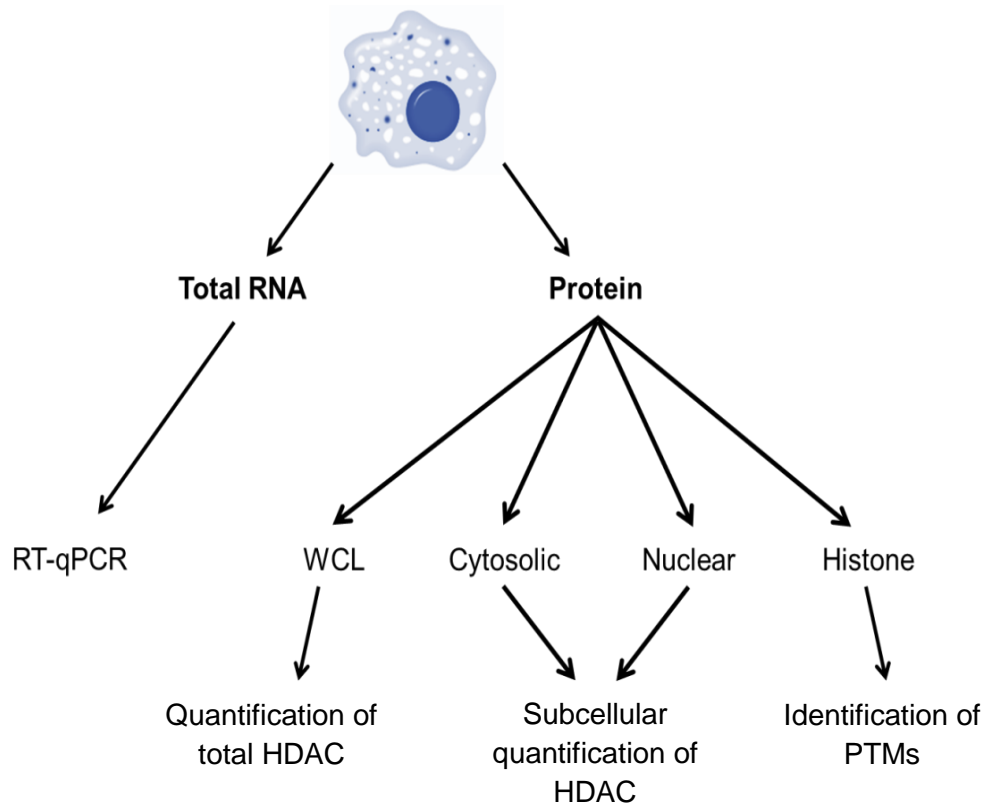
Figure 3.4. Schematic of sample preparation. A diagram of how the macrophages will be processed and the corresponding methods.
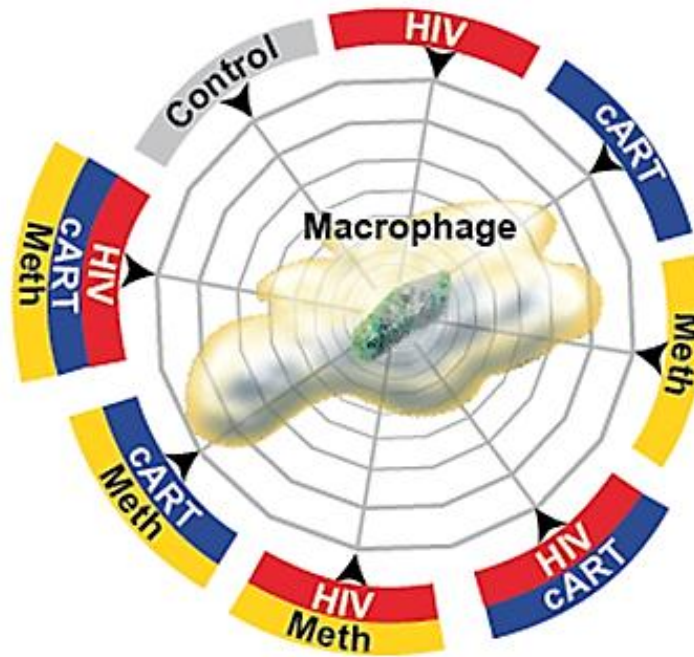
Figure 3.5. Experimental conditions for elucidating the effects of HIV infection, Meth abuse, and antiretroviral therapy on the transcriptional machinery in macrophages. Macrophages will be infected, exposed to Meth and/or treated with cART constituting a total of 8 experimental conditions to determine the individual and compounded effects of each treatment on the macrophage proteome.
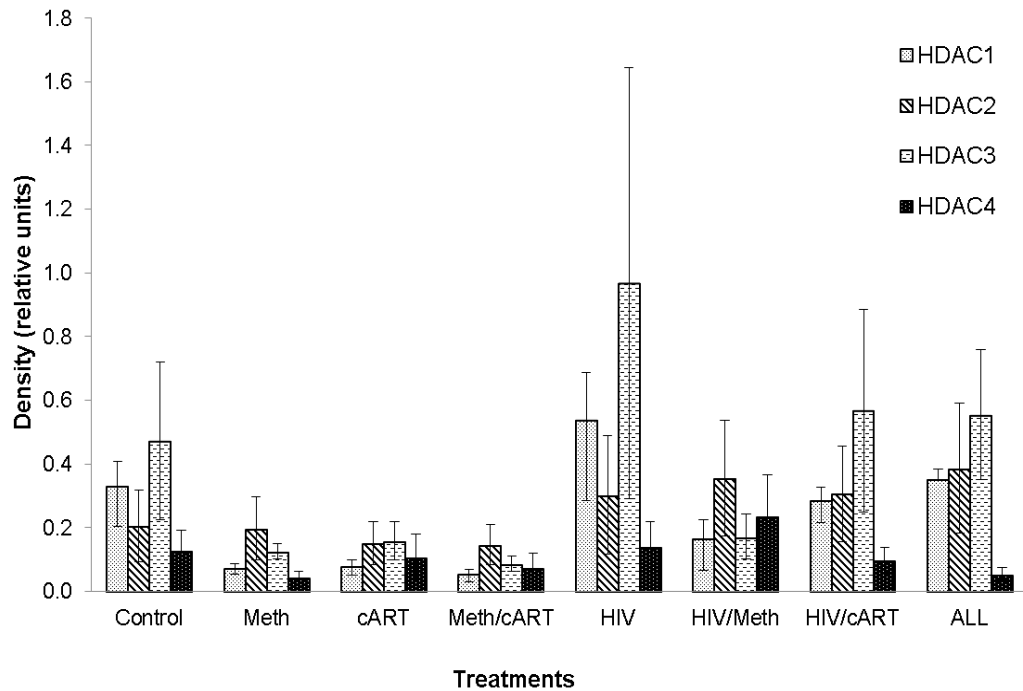
Figure 3.6. Protein levels of HDACs in the cytosol. Description of treatments and timeline refer to Figure 3.3. Proteins extracted from the cytosol of MDM and levels of HDAC1-6 were quantified Densities of HDAC1 were normalized to actin using ImageJ software. Data are represented as the mean±SE fold expression of 3 independent experiments.
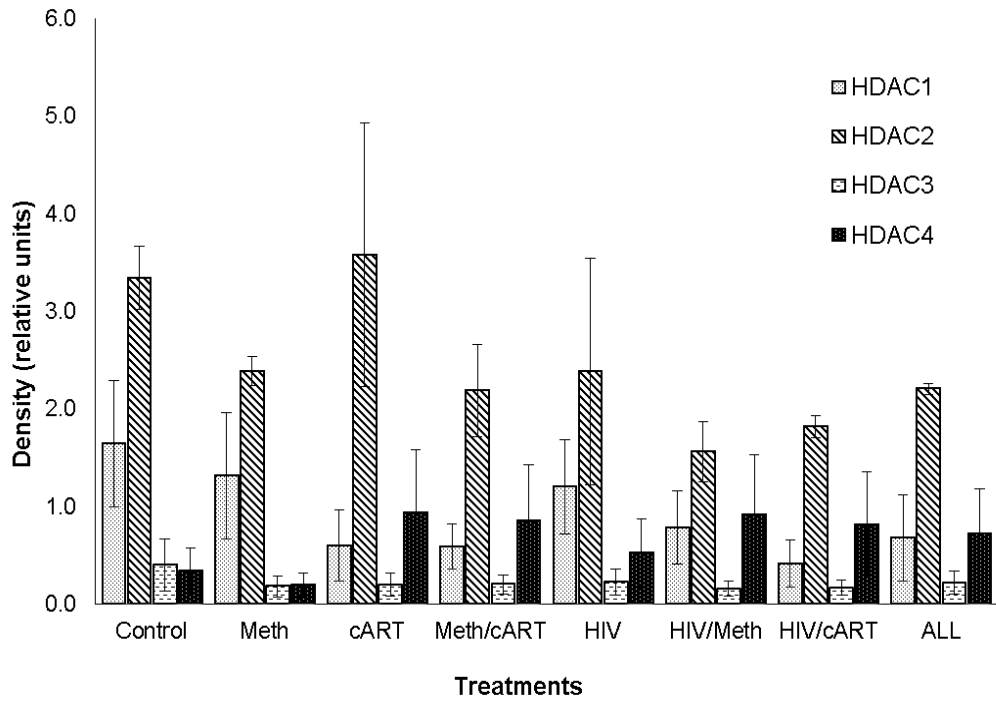
Figure 3.7. Quantification of HDAC protein levels in the nuclear fraction. Description of treatments and timeline refer to Figure 3.3. Densities of HDAC1 were normalized to actin using ImageJ software. Data are represented as the mean±SE fold expression of 3 independent experiments.
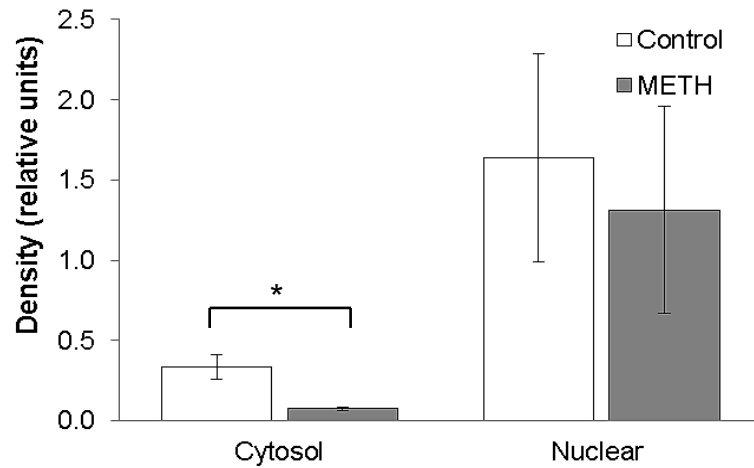
Figure 3.8. Protein levels of HDAC1 from the cytosol and nucleus in control and Meth treated human macrophages. Plot re-represents the samples juxtaposed for HDAC1 from the levels in the cytosol and nucleus (Fig. 3.5. & 3.6). MDM were either mock treated (control media) or with 100 µM Meth for 48 h and then maintained for 5 days with no other treatments. MDM were fractionated and HDAC1 protein was detected by Western blot. An asterisk (*) indicates $p < 0.05$ by a Student's t-test. Densities of HDAC1 were normalized to actin using ImageJ software, n=3.
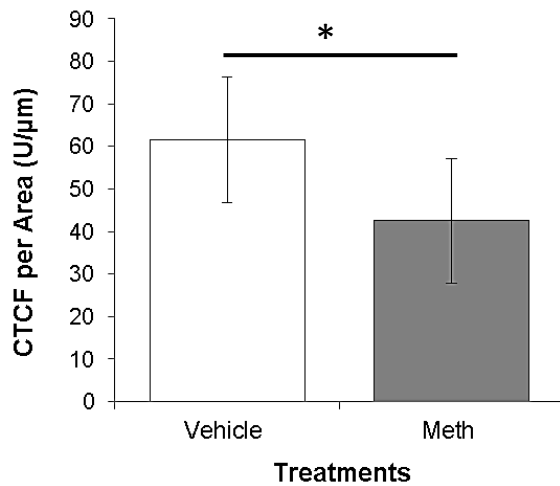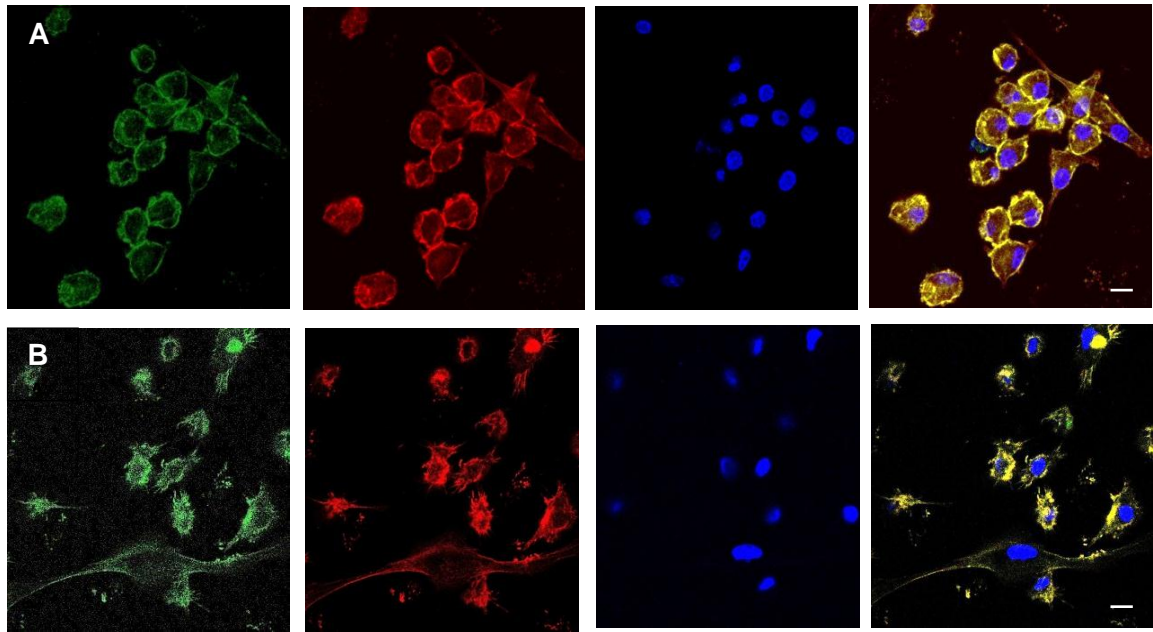
Figure 3.9. Confocal images of MDM stained for HDAC1. MDM were cultured on glass chamber slides with 100 µM Meth or control (MSFM) for 24 h. HDAC1 antibody (green), actin (red), and Dapi (blue). Merged images show the co-localization of HDAC1 with actin (yellow). Row (a) Control MDM. Row (b) Meth exposed MDM. Bar graph is the average quantification of the green channel (HDAC1) intensity corrected per area using

ImageJ software. Single image capture at 63X oil immersion objective. An asterisk (*) indicates p<0.05 by a Student's t-test. Scale bar is 20 μm.
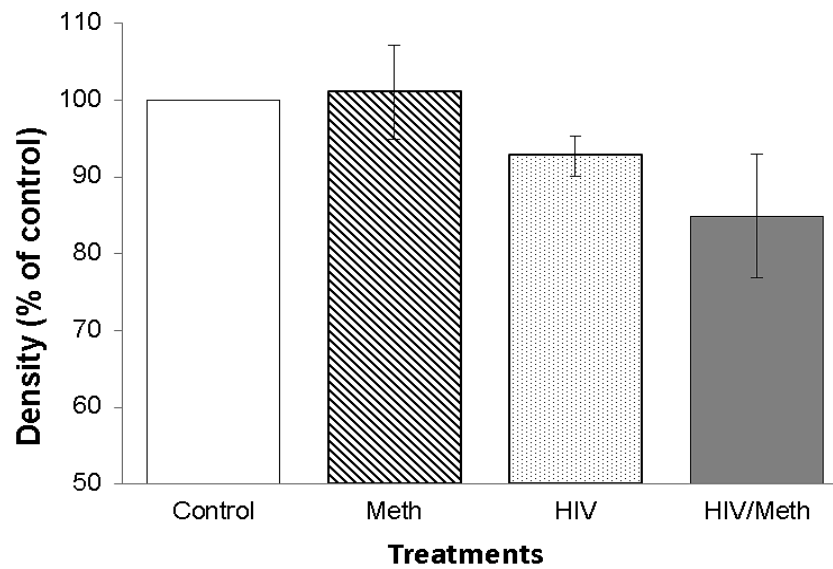
Figure 3.10. HDAC1 levels in WCL. In a separate experiment, MDM were either mock treated (control media), exposed to 100 µM Meth, or infected with HIV-1. Keeping with a similar timeline when there was 8 conditions, MDM were infected on day 7 and exposed to Meth on day 10, then maintained for 48 hours before being lysed and proteins extracted. Quantitative Western blot analysis of HDAC1 from 5 µg of each sample. of HDAC1 were normalized to actin using ImageJ software, n=4.
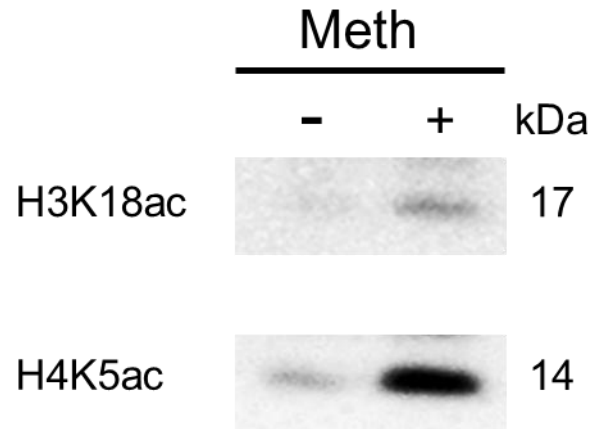
Figure 3.11. Western blot analysis of acetylation of H4K5 and H3K18. Two known targets for HDAC1 are H4K5 and H3K18 and changes in HDAC1 will effect acetylation at these sites. Control and Meth MDM treatment was described in Cell Culture and Sample Preparation (section 4.2.1). Five µg of histones from each sample were loaded and incubated at 1:1000.

3.4. Discussion

In this study, we found that Meth decreases HDAC1 at the protein level. This was explained by the corresponding decrease in mRNA levels. A decrease in HDAC2-6 protein levels or a decrease in HDAC6 mRNA would have been an indicator that Meth exacerbates the degradation pathway or inhibits translation, respectively. Our conclusion from not detecting HDAC5 and 6 by Western blot is that the antibodies were not specific enough considering HDAC6 was quantified using the more sensitive technique, RT-qPCR. In addition, the low number of cell cultures or high variability of HDAC levels among healthy donors might have contributed to HDAC2-4 being inconclusive. Therefore, more studies need to be done with more donors to verify that Meth, HIV-1 infection, and/or cART do not have an effect on HDAC2-6 levels. The confocal images, relative quantification of HDAC1 by RT-PCR and the correlation between the increases in acetylation and HDAC1, allowed us to conclude that Meth induces a decrease in both the protein and RNA level. This is analogous to other reports on Meth addict brains suggesting a similar mechanism in macrophages [61, 62].

The rationale that HDACs result in gene silencing is twofold: one, because of the biochemistry between the histone tails and DNA and two, because of *in vitro* data. Non-acetylated (or deacetylated by HDACs) lysine residues on the N-terminal histone tails are positively charged and electrostatically attracted to the negatively charged phosphate backbone of DNA. This interaction between DNA and histones tails keep chromatin in a closed formation and inaccessible for transcription. Another reason HDAC is associated with gene repression is treatment with HDACi resulted in the abrogation of gene repression [69, 70]. However more recently, it has been found that HDAC1 is present at many transcriptionally active genes [71]. Therefore, whether the downstream effect of the Meth-induced decrease of HDAC1 is gene silencing or activating still needs to be explored.

The rapid decreases of HDAC1 within 24 h of Meth exposure was expected because Meth increases cytokine production and HDAC1 suppresses the NF-κB-dependent genes like TNF-α, IFN-β and other cytokines in macrophages and T-cells [72-77]. However, it was surprising to see no changes in HDAC1 in the HIV or HIV/Meth samples and especially, HIV/Meth not having an additive effect on HDAC1. Literature would suggest that HIV dysregulates HDAC1 to allow for the expression of viral genes and our macrophages are actively producing HIV (p24 ELISA not shown). One explanation is, again, that the number of cell cultures was not robust enough to demonstrate statistical significance as there is a trend of decreased HDAC1 in the cytosol, nucleus, and whole cell lysates in Meth and HIV/Meth MDM compared to control.

3.5. References

1. Prevention, C.f.D.C.a., *Pneumocysitis pneumonia -- Los Angeles*, in *Morbidity and Mortality Weekly Report*1981. p. 250-2.

2. Altman, L.K., *Rare cancer seen in 41 homosexuals*, in *The New York Times*1981.

3. International, U.P., *Homosexuals found particularly liable to common viruses*, in *The New York Times*1981.

4. Grmek, M., *History of AIDS: emergence and origin of a modern pandemic*: Princeton University Press. 290.

5. Prevention, C.f.D.C.a., *Current trends update on Acquired Immune Deficiency Syndrome (AIDS) -- United States*, in *Morbidity and Mortality Weekly Reports*1982. p. 507-8.

6. Control, A.A.C.f.I.D.C.f.D., *Acquired Immunodeficiency Syndrome (AIDS) weekly surveillance report -- United States*, 1983.

7. Barre-Sinoussi, F., et al., *Isolation of a T-lymphotrophic retrovirus from a patient at risk for acquired immune deficiency syndrome (AIDS).* Science, 1983. **220**(4599): p. 868-71.

8. UNAIDS, *Core Epidemiology* 2013.

9. Organization, W.H., *Global update on the health sector response to HIV, 2014*, 2014: WHO Press.

10. Clavel, F., *HIV-2, the West African AIDS virus.* AIDS, 1987. **1**(3): p. 135-40.

11. Frankel, A.D. and J.A.T. Young, *HIV-1: Fifteen proteins and an RNA.* Annual Review of Biochemistry, 1998. **67**(1-24).

12. Strebel, K., *Virus-host interactions: role of HIV proteins Vif, Tat, and Rev.* AIDS, 2003. **17**: p. S25-S34.

13. Karn, J. and C.M. Stoltzfus, *Transcriptional and posttranscriptional regulation of HIV-1 gene expression.* Cold Spring Harb Perspect Med, 2012. **2**(2): p. a006916.

14.   Sundquist, W.I. and H.G. Krausslich, *HIV-1 assembly, budding, and maturation.* Cold Spring Harb Perspect Med, 2012. **2**(7): p. a006924.

15.   Laskey, S.B. and R.F. Siliciano, *A mechanistic theory to explain the efficacy of antiretroviral therapy.* Nat Rev Microbiol, 2014. **12**(11): p. 772-80.

16.   King, S.R., *HIV: virology and mechanisms of disease.* Annals of Emergency Medicine, 1994. **24**(3): p. 443-9.

17.   Berger, E.A., et al., *A new classification for HIV-1.* Nature, 1998. **391**: p. 240.

18.   Kartikeyan, S., et al., *HIV and AIDS: basic elements and priorities*2007: Springer.

19.   Cheng, X., M. Belshan, and L. Ratner, *Hsp40 facilitates nuclear import of the human immunodeficiency virus type 2 Vpx-mediated preintegration complex.* J Virol, 2008. **82**(3): p. 1229-37.

20.   Schweitzer, C.J., et al., *Proteomic Analysis of Early HIV-1 Nucleoprotein Complexes.* J Proteome Res, 2013.

21.   Rodriguez-Mendez, M.L., et al., *Prevalence, patterns, and course of past hepatitis B Virus infection in intravenous drug users with HIV-1 infection.* American Journal of Gastroenterology, 2000. **95**(5): p. 1316-22.

22.   Scharschmidt, B.F., et al., *Hepatitus B in patients with HIV infection: relationship to AIDS and patient survival.* Annals of Internal Medicine, 1992. **117**(10): p. 837-8.

23.   Organization, W.H., *WHO model list of essential medicines* 2013.

24.   Masho, S.W., C.-L. Wang, and D.E. Nixon, *Review of tenofovir-emtricitabine.* Therapeutics and Clinical Risk Management, 2007. **3**(6): p. 1097-104.

25.   Maenza, J. and C. Flexner, *Combination antiretroviral therapy for HIV infection.* American Family Physician, 1998. **57**(11): p. 2789-98.

26.   Services, D.o.H.a.H., *Guidelines for the use of antiretroviral agents in HIV-1-infected adults and adolescents*, 2015.

27. Biswas, P., G. Tambussi, and A. Lazzarin, *Access denied? The status of co-receptor inhibition to counter HIV entry.* Expert Opinion on Pharmacology, 2007. **8**(7): p. 923-33.

28. Samji, H., et al., *Closing the gap: increases in life expectancy among treated HIV-positive individuals in the United States and Canada.* PLoS one, 2013. **8**: p. e81355.

29. Palella, F.J., et al., *Declining morbidity and mortality among patients with advanced human immunodefiency virus infection.* New England Journal of Medicine 1998. **338**: p. 853-60.

30. Buchacz, K., et al., *Amphetamine use is associated with increased HIV incidence among men who have sex with men in San Francisco.* Aids, 2005. **19**(13): p. 1423-4.

31. Molitor, F., et al., *Association of methamphetamine use during sex with risky sexual behaviors and HIV infection among non-injection drug users.* West Journal of Medicine, 1998. **168**: p. 93-7.

32. Strathdee, S.A. and J.K. Stockman, *Epidemiology of HIV among injecting and non-injecting drug users: current trends and implications for interventions.* Curr HIV/AIDS Rep, 2010. **7**(2): p. 99-106.

33. Mathers, B.M., et al., *Global epidemiology of injecting drug use and HIV among people who inject drugs: a systematic review.* Lancet, 2008. **372**: p. 1733-45.

34. Forrest, D.W., et al., *Crystal methamphetamine use and sexual risk behaviors among HIV-positive and HIV-negative men who have sex with men in South Florida.* J Urban Health, 2010. **87**(3): p. 480-5.

35. Reback, C.J., S. Larkins, and S. Shoptaw, *Methamphetamine abuse as a barrier to HIV medication adherence among gay and bisexual men.* AIDS Care, 2003. **15**(6): p. 775-85.

36.   Antoniou, T. and A.L.-i. Tseng, *Interactions between recreational drugs and antiretroviral agents.* Infectious Diseases, 2002. **36**(10): p. 1598-1613.

37.   Hales, G., N. Roth, and D. Smith, *Possible fatal interaction between protease inhibitors and methamphetamine.* Antiviral Therapy, 2000. **5**(1): p. 19.

38.   Ellis, R.J., et al., *Increased human immunodeficiency virus loads in active methamphetamine users are explained by reduced effectiveness of antiretroviral therapy.* J Infect Dis, 2003. **188**(12): p. 1820-6.

39.   Brecht, M.L., et al., *Predictors of Intention to Change HIV Sexual and Injection Risk Behaviors among Heterosexual Methamphetamine-Using Offenders in Drug Treatment: A Test of the AIDS Risk Reduction Model.* J Behav Health Serv Res, 2008.

40.   Renthal, W. and E.J. Nestler, *Epigenetic mechanisms in drug addiction.* Trends Mol Med, 2008. **14**(8): p. 341-50.

41.   Pollina, E.A. and A. Brunet, *Epigenetic regulation of aging stem cells.* Oncogene, 2011. **30**: p. 3105-126.

42.   Woldemichael, B.T., et al., *Epigenetics of memory and plasticity*, in *Progress in Molecular Biology and Translational Science*2014, Elsevier. p. 305-40.

43.   Turner, B.M., *Cellular memory and the histone code.* Cell, 2002. **11**: p. 285-291.

44.   Jenuwein, T. and C.D. Allis, *Translating the histone code.* Science, 2001. **293**(5532): p. 1074-80.

45.   Strahl, B. and C.D. Allis, *The language of covalent histone modifications.* Nature, 2000. **403**(6765): p. 41-5.

46.   Smolle, M. and J.L. Workman, *Transcription-associated histone modifications and cryptic transcription.* Biochim Biophys Acta, 2012.

47.   Musselman, C.A., et al., *Perceiving the epigenetic landscape through histone readers.* Nat Struct Mol Biol, 2012. **19**(12): p. 1218-27.

48.   Bedford, D.C., et al., *Target gene context influences the transcriptional requirement for the KAT3 family of CBP and p300 histone acetyltransferases.* Epigenetics, 2010. **5**(1): p. 9-15.

49.   Sandoval, J., et al., *Validation of a DNA methylation microarray for 450,000 CpG sites in the human genome.* Epigenetics, 2011. **6**(6): p. 692-702.

50.   Saunders, K., et al., *Epigenetic regulation of CD8+ T-lymphocyte mediated suppression of HIV-1 replication.* Virology, 2010. **405**: p. 234-42.

51.   Tripathy, M.K., W. Abbas, and G. Herbein, *Epigenetic regulation of HIV-1 transcription.* Epigenomics, 2011. **3**(4): p. 487-502.

52.   Sorin, M., et al., *Recruitment of a SAP18-HDAC1 complex into HIV-1 virion and its requirement for viral replication.* PLoS Pathogens, 2009. **5**(6): p. e1000463.

53.   Demonte, D., et al., *Administration of HDAC inhibitors to reactivate HIV-1 expression in latent cellular reservoirs: implications for the development of therapeutic strategies.* Biochem Pharmacol, 2004. **68**(6): p. 1231-8.

54.   Colin, L. and C.V. Lint, *Molecular control of HIV-1 postintegration latency: implications for the development of new therapeutic strategies.* Retrovirology, 2009. **6**(11).

55.   Verdin, E., P.P. Jr., and C.V. Lint, *Chromatin disruption in the promoter of human immunodeficiency virus type 1 during transcriptional activation.* EMBO Journal, 1993. **12**(8): p. 3249-59.

56.   Wightman, F., et al., *HDAC inhibitors in HIV.* Immunol Cell Biol, 2012. **90**(1): p. 47-54.

57.   Hakre, S., et al., *Epigenetic regulation of HIV latency.* Current Opinion in HIV and AIDS, 2011. **6**: p. 19-24.

58.   Buch, S., et al., *Cocaine and HIV-1 interplay: molecular mechanisms of action and addiction.* J Neuroimmune Pharmacol, 2011. **6**(4): p. 503-15.

59.   Cadet, J.L. and S. Jayanthi, *Epigenetics of methamphetamine-induced changes in glutamate function.* Neuropsychopharmacology Reviews, 2013. **38**: p. 248-9.

60.   Cadet, J.L. and I.N. Krasnova, *Interactions of HIV and methamphetamine: cellular and molecular mechanisms of toxicity potentiation.* Neurotox Res, 2007. **12**(3): p. 181-204.

61.   Cadet, J.L., et al., *Genome-wide profiling identifies a subset of methamphetamine induced genes associated with Meth-induced increased H4K5Ac binding in the rat striatum.* BMC Genomics, 2013. **14**(545).

62.   Martin, T.A., et al., *Methamphetamine causes differential alteration in gene expression and patterns of histone acetylation/hypoacetylation in the rat nucleus accumbens.* PLoS One, 2012. **7**(3): p. e34236.

63.   Gendelman, H.E., et al., *Efficient isolation and propagation of human immunodeficiency virus on recombinant colony-stimulating factor 1-treated monocytes.* J Exp Med, 1988. **167**(4): p. 1428-41.

64.   Livak, K.J. and T.D. Schmittgen, *Analysis of relative gene expression data using real-time quantitative PCR and the 2(-Delta Delta C(T)) Method.* Methods, 2001. **25**(4): p. 402-8.

65.   Olszowy, P., et al., *Profiling post-translational modifications of histones in human monocyte-derived macrophages.* Proteome Sci, 2015. **13**: p. 24.

66.   Segre, C.V. and S. Chiocca, *Regulating the regulators: the post-translational code of class I HDAC1 and HDAC2.* J Biomed Biotechnol, 2011. **2011**: p. 690848.

67.   Reynolds, N., et al., *NuRD-mediated deacetylation of H3K27 facilitates recruitment of Polycomb Repressive Complex 2 to direct gene repression.* EMBO J, 2012. **31**(3): p. 593-605.

68.   Ma, P. and R.M. Schultz, *Histone deacetylase 1 regulates histone acetylation, development and gene expression in preimplantation mouse embryos.* Developmental Biology, 2008. **319**(1): p. 110-20.

69.   Hassig, C., et al., *A role for histone deacetylase activity in HDAC1-mediated transcriptional repression.* Proceedings of the National Academy of Science, 1998. **95**: p. 3519-24.

70.   Lu, J., et al., *Interleukin-12 p40 promoter activity is regulated by the reversible acetylation mediated by HDAC1 and p300.* Cytokine, 2005. **31**(1): p. 46-51.

71.   Wang, Z., et al., *Genome-wide mapping of HATs and HDACs reveals distinct functions in active and inactive genes.* Cell, 2009. **138**(5): p. 1019-31.

72.   Liu, X., et al., *Methamphetamine increases LPS-mediated expression of IL-8, TNF-alpha and IL-1beta in human macrophages through common signaling pathways.* PLoS One, 2012. **7**(3): p. e33822.

73.   Burns, A. and P. Ciborowski, *Acute exposure to methamphetamine alters TLR9-mediated cytokine expression in human macrophage.* Immunobiology, 2015.

74.   Falkenberg, K.J. and R.W. Johnstone, *Histone deacetylases and their inhibitors in cancer, neurological diseases and immune disorders.* Nat Rev Drug Discov, 2014. **13**(9): p. 673-91.

75.   Grabiec, A.M., et al., *Histone deacetylase inhibitors suppress inflammatory activation of rheumatoid arthritis patient synovial macrophages and tissue.* J Immunol, 2010. **184**(5): p. 2718-28.

76.   Ashburner, B.P., S.D. Westerheide, and A.S. Baldwin, Jr., *The p65 (RelA) subunit of NF-kappaB interacts with the histone deacetylase (HDAC) corepressors HDAC1 and HDAC2 to negatively regulate gene expression.* Mol Cell Biol, 2001. **21**(20): p. 7065-77.

77.   Grausenburger, R., et al., *Conditional deletion of histone deacetylase 1 in T cells leads to enhanced airway inflammation and increased Th2 cytokine production.* J Immunol, 2010. **185**(6): p. 3489-97.

Chapter 4

Method Development: Pressure Assisted Digestion of

Proteins Using a Barocycler

4.1. Introduction

Sample preparation for high-throughput analyses of proteins is at the center of proteomic profiling experiments [1-4]. The multi-step nature of proteomic studies makes reproducibility, standardization, and normalization key to reducing analytical variability. Other than intact protein analysis and the rarely used chemical methods for protein digestion, the majority of proteomic experiments contain a step involving the enzymatic digestion of proteins for mass spectrometry (MS)1-based protein identification and quantitation. It is important to note that each type of proteolytic digestion can yield a different number and type of peptides, thereby limiting the scope of information related to the structure and function of the protein of interest [4]. Therefore, the concept of a universal sample preparation method has several limitations, thereby driving technological and methodological development to create new avenues for enhancing sample preparation.

Conventional enzymatic digestion protocols typically employ an overnight reaction to ensure complete digestion of peptides. Still, samples can contain cleavage sites that are missed during digestion. Namely, a reduced rate of specific peptide bond hydrolysis and/or the presence of posttranslational modifications (PTMs) contribute to this effect [5]. Several techniques, such as high-intensity focused ultrasound (HIFU), microwave radiation, and performing the digestion under conditions of high pressure, have been developed and modified to overcome these digestion shortcomings and to decrease the time needed for complete digestion of the protein [6-11]. The technique involving high-pressure conditions applies pressure up to 40 kpsi and appears to provide improved results as compared with HIFU and microwave radiation. HIFU is based on precise modulation of ultrasound, which was a significant problem in the past; however, current ultrasound techniques have found application (e.g., electrical impedance tomography, optical tomography) [12]. On the other hand, reactions controlled by

microwave radiation are so rapid that the generated reaction heat can lead to by-product formation and, in some cases, to degradation. The limitations of HIFU and microwave radiation have prompted us to test whether pressure cycling technology (PCT) can be used sufficiently for accelerated enzymatic digestion and be applicable in proteomics.

The use of PCT for enhancing enzyme activity was introduced during the early 1990s. However, the development of new instrumentation resulted in more user-friendly methods, leading to development of new applications [13, 14]. Here, we evaluate the Barocycler NEP 2320 (Pressure Biosciences, South Easton, MA, USA) as a platform for analyzing the enzymatic digestion of proteins under high pressure. The Barocycler NEP 2320 applies PCT to accelerate enzymatic digestion of samples, which in turn are used for analytical purposes. In the current study, histone H4 is used as the model protein. Histones, in addition to their functions in epigenetic regulation, represent a class of proteins that can carry multiple homo and heterogeneous PTMs, thereby altering susceptibility for enzymatic digestion, which subsequently causes additional difficulties in profiling studies. Using PCT, we were able to reduce the time of enzymatic digestion of histone H4 from 18 h to 120 min while maintaining 100% of sequence coverage identified by tandem MS (MS/MS) after digestion under atmospheric pressure.

4.2. Materials and Methods

4.2.1. Reagents

High-performance liquid chromatography (HPLC) gradient-grade acetonitrile (ACN) and water were purchased from Fisher Scientific (Fair Lawn, NJ, USA). Trifluoroacetic acid (TFA, Reagent-Plus, 99%), urea, ammonium bicarbonate (ReagentPlus, 99%), iodoacetamide (IAA, Sigma Ultra), and α-cyano-4-hydroxycinnamic acid (CHCA) were purchased from Sigma–Aldrich (St. Louis, MO, USA). Molecular-

grade dithiothreitol (DTT) and sequencing-grade chymotrypsin were purchased from Promega (Madison, WI, USA). Recombinant human histone H4 (P62805) was purchased from New England Biolabs (Ipswich, MA, USA). Primary human monocytes, obtained by elutriation from healthy donors, were used to isolate histone fractions using a Qproteome Nuclear Protein Kit (Qiagen, Hilden, Germany) [15, 16]. The protein fractions obtained using Qproteome were quantitated using a Pierce 660-nm protein assay and prediluted protein standards (bovine serum albumin, Thermo Scientific, Rockford, IL, USA).

4.2.2. Histone fractionation

The histones were isolated from the primary human monocytes using the Qproteome kit from Qiagen. The isolated histones were further fractionated using a reversed phase HPLC (RP–HPLC) system (Shimadzu Scientific Instruments, Columbia, MD, USA), which was equipped with an ultraviolet (UV) detector and Shimadzu LC Solution software for data acquisition. Chromatographic separations of 100 µg of proteins per injection were performed using an analytical HPLC C4 column (250 × 4.6 mm, dp = 5 µm, 300 Å) from Advanced Chromatography Technologies (Aberdeen, Scotland). Mobile phase A was 5% ACN in water plus 0.1% TFA, and mobile phase B was 90% ACN plus 0.1% TFA. Fractionation was initiated with 100% mobile phase A for 5 min. From 5 to 15 min, mobile phase B was ramped up to 35% and then held continuously for 10 min. From 25 to 100 min, the amount of solvent B was increased to 65%, followed by ramping up to 100% in 20 min. This condition was maintained for 5 min, and then the amount of solvent B was decreased to 0% in 5 min and held for 145 min.

4.2.3. Enzymatic protein digestion

Proteolytic digestion under atmospheric conditions was performed for at least 18 h but no longer than 24 h. In this article, enzymatic digestion under atmospheric pressure is referred to as the "conventional method." In this study, we compared

digestion assays of recombinant and native human histone H4 using the conventional method compared with PCT using a Barocycler NEP 2320. After completing digestions of recombinant protein, an AB SCIEX 4800 matrix-assisted laser desorption/ionization–tandem time-of-flight (MALDI–TOF/TOF) mass spectrometer (Framingham, MA, USA) was used to analyze resulting peptides. A nano liquid chromatography (nanoLC) LTQ-Orbitrap mass spectrometer was used to analyze peptides from digestions of native histone H4 isolated from human monocytes.

4.2.4. Conventional method of proteolytic digestion

Dried human histone H4 was dissolved in 20 µl of 8 M urea and 0.4 M NH_4HCO_3, and the pH was adjusted to between 7.5 and 8.5. Proteins were reduced by the addition of 5 µl of 45 mM DTT and incubated for 15 min at 50 °C. After cooling to room temperature, the sample was alkylated through the addition of 5 µl of 100 mMIAA and incubated in the dark at room temperature for 15 min. Following alkylation, the digestion buffer was diluted with water to a final concentration of 2 M urea and 0.1 M NH_4HCO_3. Chymotrypsin was added to the sample in a ratio of 1:4 (w/w) enzyme to protein. Digestion occurred at 37 °C for 18 h. Next, the reaction was quenched by acidifying the sample through the addition of 50 µl of TFA.

4.2.5. PCT digestion

All steps of the tryptic digestion protocol preceding incubation (ambient or high pressure) were identical for the Barocycler NEP 2320 and conventional methods. However, after the sample was alkylated, in the case of using the Barocycler NEP 2320, samples were transferred to PCT MicroTubes and placed in the metal holder component of this instrument. After digestion, samples were acidified using 50 µl of TFA to quench the reaction.

4.2.6. Mass spectrometry

MALDI–TOF/TOF—In preparation for MS analysis, peptides resulting from PCT digestion of recombinant human histone H4 (1 µg) were desalted using reversed phase ZipTip pipette tips with 0.2 µl of C18 resin (Millipore, Billerica, MA, USA). For sample analysis, an AB SCIEX 4800 MALDI–TOF/TOF mass spectrometer was used. First, 1 µl of digested sample was spotted onto a MALDI plate and co-crystallized with 1 µl of CHCA matrix (5 mg/ml in 50% ACN and 0.1% TFA). The droplets were dried in a desiccator under decreased pressure. Spectra acquisition and data processing were performed using 4000 series Explorer software version 3.5.1 (AB SCIEX); the software settings were in a reflectron-positive mode at fixed laser intensity with a low-mass gate and delayed extraction. Peptide masses were acquired for m/z values ranging from 800 to 2500 Da. MS spectra were summed from 1000 laser shots by an Nd-YAG laser operating at 355 nm and 200 Hz. MS/MS spectra were acquired in 1 kV positive mode. The 1000 shots were summed in increments of 50. Database searches were performed on the SwissProt database using Mascot MS/MS Ion Search (http://www.matrixscience.com). The search parameters were as follows: (i) carbamidomethylation on cysteine and oxidation on methionine were variable modifications; three missed chymotrypsin cleavage sites were permitted; the mass accuracy tolerance for the peptide (MS) was set at 15 ppm and for fragments (MS/MS) was set at 0.5 Da.

ESI–LC–MS/MS—Histone H4 isolated and fractionated from human monocytes was digested using both conventional and PCT methods. After digestion, and prior to analysis, samples were desalted using reversed phase ZipTip pipette tips with 0.2 µl of C18 resin as per the manufacturer's protocol (Millipore). Next, samples were analyzed using a high resolution mass spectrometry electrospray ionization (ESI)–LC–MS/MS system in a nanospray configuration (LTQOrbitrap, Thermo Scientific, West Palm Beach,

FL, USA) coupled with a nanoLC system (TEMPO nano MDLC System, AB SCIEX) and using a microcapillary RP-C18 column (New Objectives, Wo-burn, MA, USA). The database search was performed using Proteome Discoverer 1.2 software (Thermo Scientific). The search parameters were as follows: (i) carbamidomethylation on cysteine and oxidation on methionine were variable modifications; three missed chymotrypsin cleavage sites were permitted; the mass accuracy tolerance for the peptide (MS) was set at 15 ppm and for fragments (MS/MS) was set at 0.5 Da.

4.3. Results

4.3.1. Pressure optimization

To optimize the pressure and time for the digestion for recombinant human histone H4, we performed multiple digestions at different pressures and for different time points (see Tables 4.1 and 4.2 below). Experiments were performed in triplicate. Based on manufacturer recommendations, we selected the following three pressure settings: 10, 15, and 25 kpsi. Cycling consisted of 30 cycles at 1 min each; each cycle was run for 50 s at the pressure setting of interest, followed by 10 s of stabilization at atmospheric pressure. The temperature was ambient, and chymotrypsin was used at a concentration of 0.5 µg/µl. The resulting digest of the protein was analyzed using an AB SCIEX 4800 MALDI–TOF/TOF mass spectrometer for the recombinant histone H4. The digest of recombinant histone H4 revealed seven peptides and constituted a nearly full sequence except for the first amino acid and the C-terminal fragment, a 100GFGG103 (MW = 336.14) tetrapeptide. The peak list, created by 4000 series Explorer software, was used in parallel to acquire MALDI–TOF/TOF data. This data consisted of (i) the m/z ratio (including an average mass with lower and higher m/z recordings), the peak height (peak intensity), the signal/noise ratio, (iv) resolution, and (v) the area under the peak. The peak with highest intensity represents 100%. Considering that in each experiment

the only variable parameter is the applied pressure, we theorized that peak intensity would reflect the relative change in the amounts of each peptide generated by such digestion, thereby more of any given peptide in the mixture. The m/z peak of such a peptide is expected to have higher intensity. Therefore, we elected to demonstrate pressure optimization based on the relative comparison of peak intensities for each peptide generated using pressures of 10, 15, and 25 kpsi. Results for all peptides are summarized in Table 4.1, and Fig. 4.1 is a bar graph comparing the changes in peak intensity for the two N-terminally located peptides that are postulated to be of the greatest biological importance. In all three samples (10, 15, and 25 kpsi), the peptide 90ALKRQGRTLY99 showed the highest intensity, thereby setting up 100%, which were 0.24 1.2, and 1.3 × 104, respectively. Based on these data, we postulated that we did not reach the signal saturation for this mixture of peptides under our experimental conditions, thereby allowing us to make relative comparisons. Comparisons should be performed with caution and can be performed for only a single peptide at three digestion conditions (horizontally, e.g., for one given peptide), assuming that the rate of ionization remains constant and signal suppression from other peptides is negligible. Based on the data presented, it was determined that a pressure of 10 kpsi was too low, as reflected by the low signal intensity overall and for each of the seven peptides. When comparing peak intensities for pressures of 15 and 25 kpsi, results indicate that 15 kpsi was beneficial for the signal intensity of peptides 1, 2, and 5 (see Table 4.1), which were further digested and/or degraded at 25 kpsi. If low-specificity chymotrypsin was used, we would expect that the peptide 74TEHAKRKTVTAMDVVY89 would be further fragmented into the following three peptides: 74TEH76, 77AKRKTV-TAM85, and 86DVVY89. This fragmentation is expected to result in a drop in the peak intensity for this particular intact peptide. For example, when low-specificity chymotrypsin is used, the peptide 2SGRGKGGKGLGKGGAKRHRKVL23 could be further fragmented at 25 kpsi into the

following three peptides: 2SGRGKGGKGL11, 12GKGGAKR18, and 19HRKVL23. Because this was not observed, we conclude that susceptibility of peptide bonds cleaved under PCT conditions is, to some extent, selective. This selective cleavage could be advantageous if one investigates proteins with point mutations, splice variants, and/or isoforms and when the aim of the experiment is not only to have maximal sequence coverage but also to have overlapping sequences. For other peptides, a pressure of 25 kpsi appears to be optimal. It has been postulated that, from a biological point of view, the most important part for all histones is the N-terminus end (also called the "histone tail") [17]. This end is arbitrarily set to be approximately 30% of sequence from the N-terminal end of histones; in histone H4, this would be the first 38 amino acids [18]. The N-terminus portion of histone has been shown to play an important role in chromatin remodeling and transcription regulation. In summary, we conclude that 15 kpsi is the optimal pressure to digest histones for further studies.

4.3.2. Time optimization at 15 kpsi

Based on reasoning presented above with respect to fragmentation and pressure, we attempted to optimize digestion time at a pressure of 15 kpsi. For this part of data analysis and interpretation, we used the same criteria as we used for analysis applied to pressure optimization as described in the previous section. Results for all peptides are presented in Table 4.2, and Fig. 4.2 is a bar graph comparing the changes in peak intensity for the two N-terminally located peptides that are postulated to be of the greatest biological importance. For peptides 1, 2, 3, and 5, the optimal time appears to be 120 min; when extended, this leads to a decrease in the signal intensity. The decrease in the peak intensity for the peptides shown in Table 4.2 would again suggest that a longer period of time pushes the digestion reaction to yield smaller peptides. In summary, we optimized the conditions for chymotrypsin digestion of recombinant human

histone H4 as 15 kpsi for 120 cycles. Each cycle was 1 min long and consisted of 50 s of high pressure and 10 s of atmospheric pressure.

4.3.3   Summary of PCT using chymotrypsin

Fig. 4.3 shows a representative spectrum of MALDI–TOF/TOF spectrometric analysis of fragments generated from chymotrypsin digestion of recombinant histone H4 using the optimal conditions established by this study. Table 4.3 shows sequences of peptides, which provide nearly complete sequence coverage. It is important to note that we were able to sequence the entire N-terminal end (histone tail) of histone H4. We also performed MS/MS analysis of five minor peaks with m/z 864.9, 1021.5, 1798.3, 2108.0, and 2331.1, but we were unable to assign them to any part of the histone H4 sequence, concluding that they are most likely part of contamination.

4.3.4.   RP–HPLC fractionation of intact histones

After optimization of the PCT method using recombinant histone H4, we moved to the next step involving intact histones isolated from biological material. The source of histones used for this study was human monocytes obtained from elutriated blood of healthy donors (see Materials and methods). For preparation, histones were subjected to RP–HPLC fractionation (Fig. 4.4), followed by identification of collected fractions using MS. Histones H2B, H4, H2A, and H3 were eluted as separate peaks between 50 and 70 min (Fig. 4.4 inset). Peaks appear to be broad, which is likely due to small differences in the elution time for post-translationally modified forms rather than due to chromatographic conditions. Histone H1 was eluted prior to the 50-min time point; however, it was not collected for the purpose of this study. A relatively broad fraction containing histone H4 was collected, as shown in the box in the Fig. 4.4 inset, and used for further experiments.

4.3.5. Chymotryptic digestion of native histone H4 using conventional and PCT methods

Equal amounts of the HPLC fractions containing histone H4 were digested using either optimized PCT or the conventional method (i.e., atmospheric pressure). Peptides resulting from these digestions were analyzed using an LTQ-Orbitrap in a nanoLC–ESI–MS/MS configuration. The reason we used MALDI–TOF/TOF for digested recombinant histone H4 and used ESI–MS/MS for histone H4 purified from monocytes was because we expected a higher complexity in histone H4 from monocytes compared with the recombinant sample. Both digestion conditions yielded 75% sequence coverage (Fig. 4.5), with [2]SGRGKGGKGLGKGGAKRHRKVL[23] being the only missing peptide. This was expected, to some extent, because the N-terminal tail of histone H4 is extensively post-translationally modified. Such modifications can lead to a digestion that differs from non-modified proteins.

Number	Molecular mass (Da)	Peptide and its position in protein sequence	Peak height (peak intensity)		
			10 kpsi	15 kpsi	25 kpsi
1	2203.08	[2]SGRGKGGKGLGKGGAKRHRKVL[23]	129 ± 3.88	120 ± 6.21	23 ± 1.53
2	1750.86	[24]RDNIQGITKPAIRRL[38]	637 ± 17.53	1749 ± 172.21	918 ± 47.33
3	1268.78	[39]ARRGGVKRISGL[50]	13 ± 0.67	26 ± 1.07	47 ± 1.51
4	1078.56	[51]IYEETRGVL[59]	19 ± 1.60	23 ± 1.45	39 ± 2.46
5	1666.74	[60]KVFLENVIRDAVTY[73]	131 ± 8.99	1275 ± 118.96	553 ± 32.57
6	1848.77	[74]TEHAKRKTVTAMDVVY[89]	230 ± 14.28	1458 ± 119.70	1549 ± 148.86
7	1205.57	[90]ALKRQGRTLY[99]	2320 ± 277.70	11139 ± 1474.80	12241 ± 1221.65

Table 4.1. Optimization of PCT pressure based on relative intensity of MALDI-TOF/TOF peptide peaks.

Number	Molecular mass (Da)	Peptide and its position in sequence	Peak height (peak intensity)		
			30 min	120 min	200 min
1	2203.08	^{2}SGRGKGGKGLGKGGAKRHRKVL^{23}	120 ± 6.21	454 ± 22.84	23 ± 2.00
2	1750.86	^{24}RDNIQGITKPAIRRL^{38}	1749 ± 172.21	5126 ± 472.10	2606 ± 144.99
3	1268.78	^{39}ARRGGVKRISGL^{50}	26 ± 1.07	93 ± 2.04	44 ± 1.42
4	1078.56	^{51}IYEETRGVL^{59}	23 ± 1.45	29 ± 1.53	41 ± 2.60
5	1666.74	^{60}KVFLENVIRDAVTY^{73}	1275 ± 118.96	2612 ± 111.01	1996 ± 148.70
6	1848.77	^{74}TEHAKRKTVTAMDVVY^{89}	1458 ± 119.70	2590 ± 212.12	5276 ± 508.08
7	1205.57	^{90}ALKRQGRTLY^{99}	11139 ± 1474.80	9013 ± 1080.66	13520 ± 1781.94

Table 4.2. Optimization of PCT time based on relative intensity of MALDI-TOF/TOF peptide peaks.

Number	Peptide sequence	Position	Molecular mass (Da)
1	SGRGKGGKGLGKGGAKRHRKVL	2–23	2203.08
2	RDNIQGITKPAIRRL	24–38	1750.86
3	ARRGGVKRISGL	39–50	1268.78
4	IYEETRGVL	51–59	1078.56
5	KVFLENVIRDAVTY	60–73	1666.74
6	TEHAKRKTVTAMDVVY	74–89	1848.77
7	ALKRQGRTLY	90–99	1205.57
8 [*]	RDNIQGITKPAIR	24–36	1481.80
9 [*]	ARRGGVKRISGLIY	39–52	1523.66
10 [*]	LENVIRDAVTY	63–73	1292.53

[*] Overlapping peptides.

Table 4.3. Peptides generated using conventional chymotrypsin digestion of recombinant human histone H4.
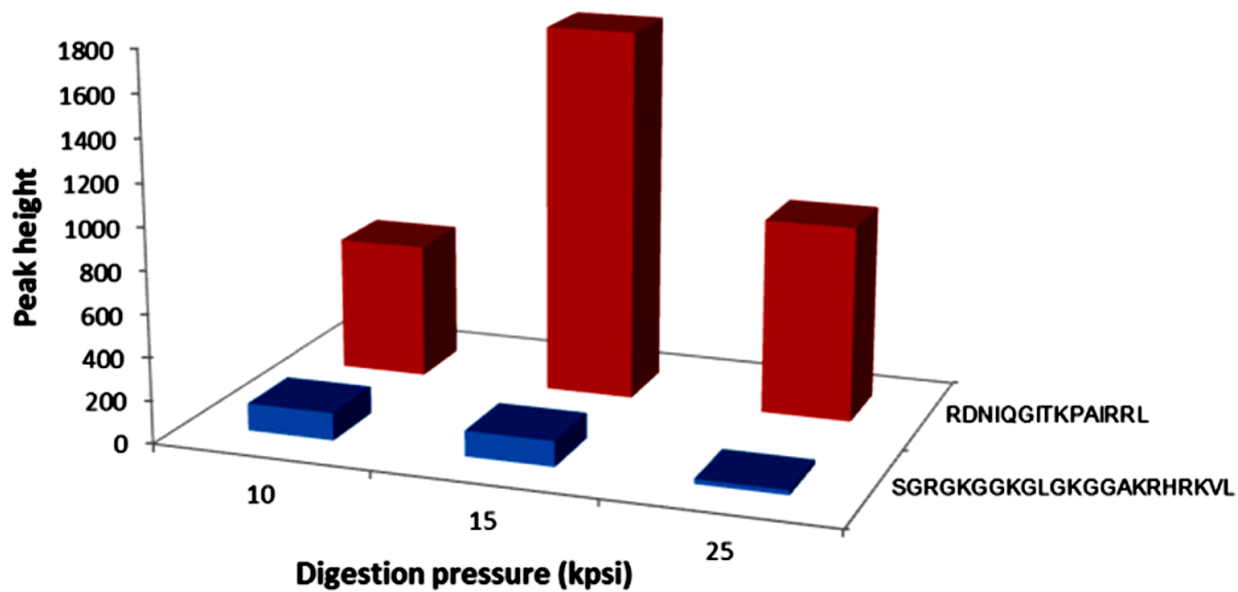
Figure 4.1. Pressure optimization for two peptides from the N-terminal tail portion of recombinant human histone H4. Pressure setting was varied for 10, 15, or 25 kpsi at a constant 30 min digestion.
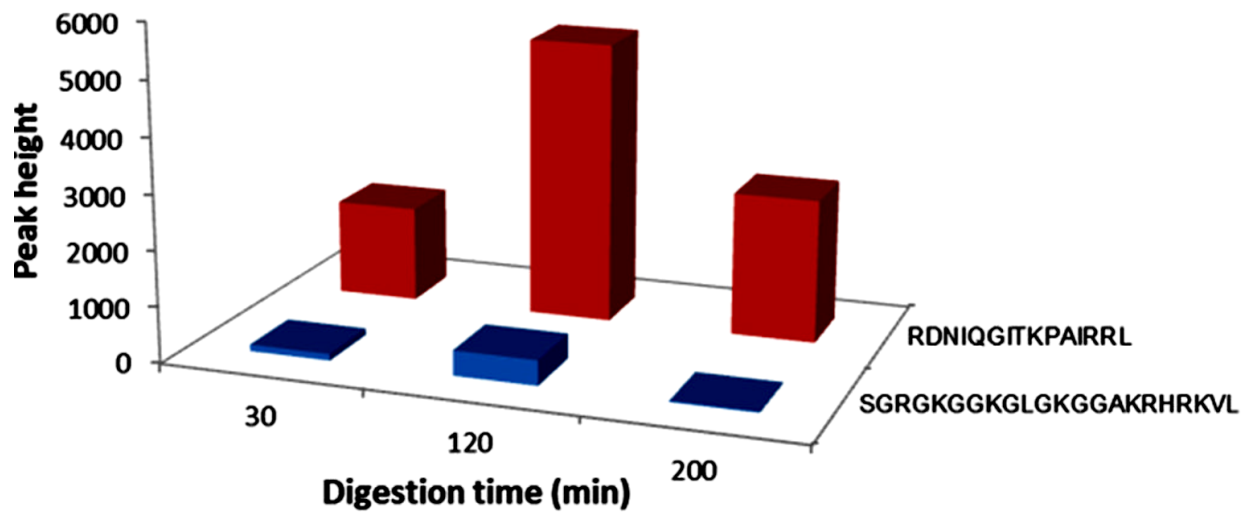
Figure 4.2. Time optimization for two peptides from the N-terminal tail portion of recombinant human histone H4. The amount of time the Barocylcer digested was either 30, 120, or 200 min at a constant15kpsi.
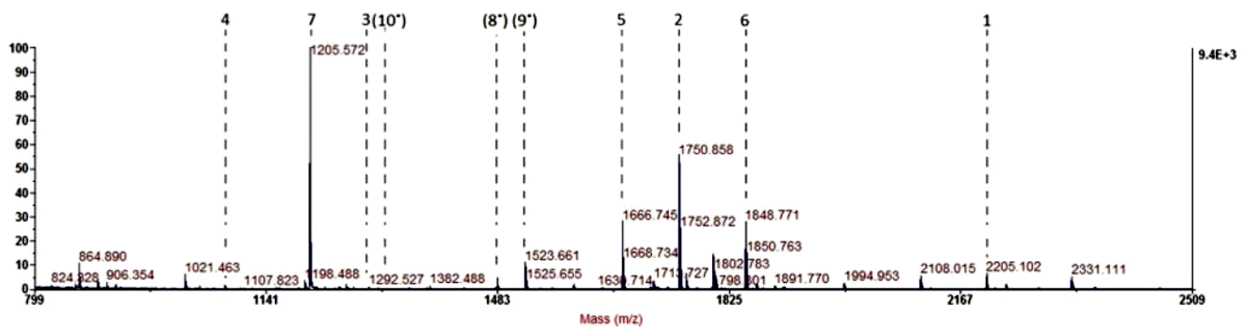
Figure 4.3. MALDI–TOF mass spectrum of recombinant human histone H4 digested using the PCT method. The numbered peaks match those generated by conventional chymotrypsin digestion, providing 95% sequence coverage, and are listed in Table 4.3.
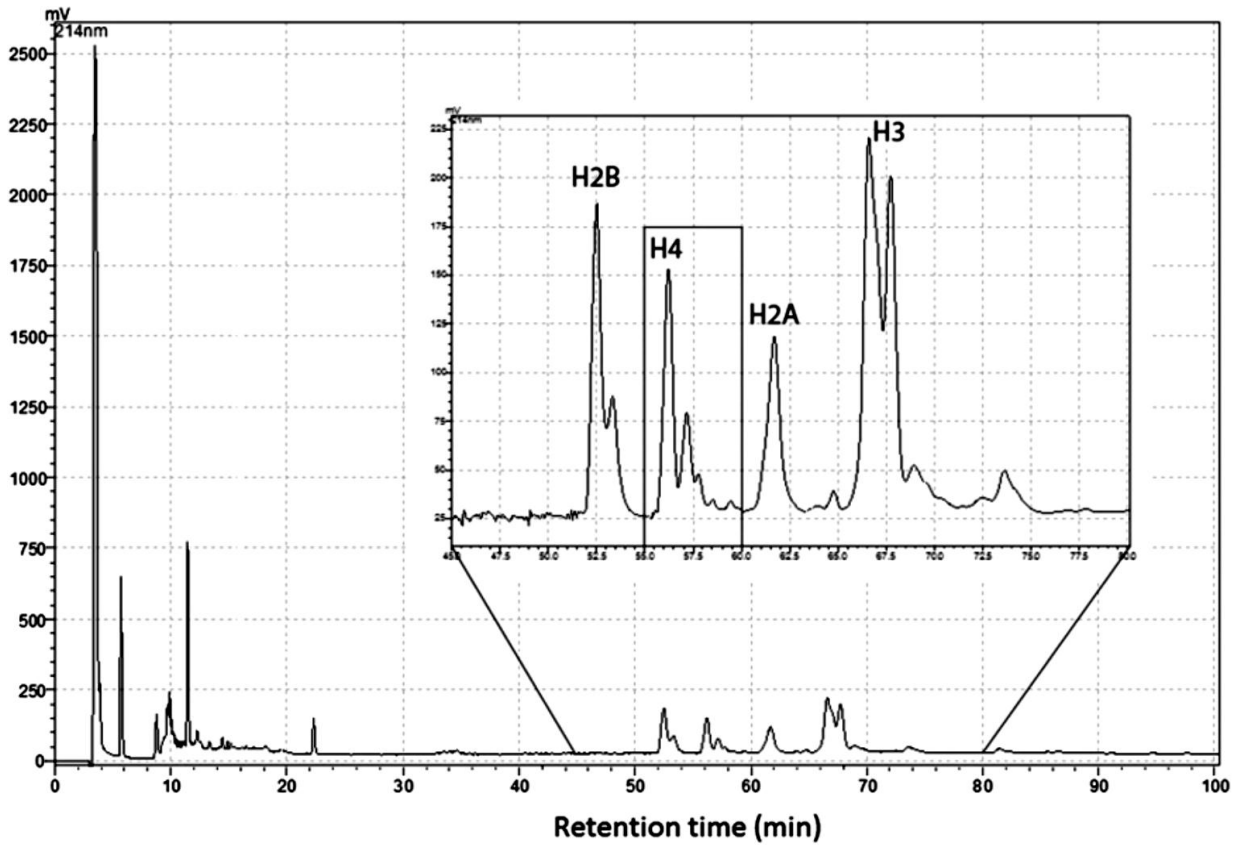
Figure 4.4. RP–HPLC chromatogram showing fractionation of histones using UV detector set at 214 nm. The inset shows an enlarged range of the peptides containing peaks assigned to respective histones.

Figure 4.5. Comparison of peptide identification using digestion on high pressure and atmospheric (conventional) pressure. (A) conventional digestion; (B) histone H4 sequence (P62805 H4_HUMAN); (C) PCT digestion.

4.4. Discussion

The major advantage of the PCT method using the Barocycler NEP 2320 is that it significantly reduces the time necessary to proteolytically digest proteins. For example, using the PCT method, proteins can be digested in 120 min at 15 kpsi instead of 18 h at atmospheric pressure. It is important to note that our experimental approach focused on only one protein, and not additional proteins that are difficult for proteolytic digestion, thereby limiting the scope of this study. For example, this technology may be beneficial for tests involving highly glycosylated proteins such as mucins. Another limitation in our study is that the only proteolytic enzyme tested was chymotrypsin. Additional proteolytic enzymes are available and should be tested in the future.

One observation from this study was that PCT using a Barocycler NEP 2320 technology platform did not show a substantial qualitative difference between 10 and 15 kpsi, and if based on peak intensity, 15 kpsi provided a more intact protein to be digested. However, there was a decrease in major peptides measured by peak intensity under 25 kpsi, which may indicate that proteolytic digestion was further forced at this pressure to yield smaller fragments. We find this phenomenon to be interesting for further explorations because it may be very useful in studies where the in-depth analysis of splice variants or isoforms is of interest. Overall, we conclude that PCT is a promising technique for more controlled sample preparation, as compared with arbitrary overnight incubation, and clearly reduces time for this step. However, additional efforts are needed to refine the experimental protocols, and more formal studies need to be performed.

4.5. References

1. Singleton, C., Recent advances in bioanalytical sample preparation for LC-MS analysis. Bioanalysis, 2012. 4(9): p. 1123-40.

2. Finoulst, I., et al., Sample preparation techniques for the untargeted LC-MS-based discovery of peptides in complex biological matrices. J Biotechnol,. 2011: p. 245291.

3. Li, F., D. Fast, and S. Michael, Absolute quantitation of protein therapeutics in biological matrices by enzymatic digestion and LC-MS. Bioanalysis, 2011. 3(21): p. 2459-80.

4. Biringer, R.G., et al., Enhanced sequence coverage of proteins in human cerebrospinal fluid using multiple enzymatic digestion and linear ion trap LC-MS/MS. Brief Funct Genomic Proteomic, 2006. 5(2): p. 144-53.

5. Hamady, M., et al., Does protein structure influence trypsin miscleavage? Using structural properties to predict the behavior of related proteins. IEEE Engineering in Medicine and Biology Magazine, 2005: p. 58-66.

6. Carrera, M., et al., Fast monitoring of species-specific peptide biomarkers using high-intensity-focused-ultrasound-assisted tryptic digestion and selected MS/MS ion monitoring. Anal Chem, 2011. 83(14): p. 5688-95.

7. Carreira, R.J., et al., New findings for in-gel digestion accelerated by high-intensity focused ultrasound for protein identification by matrix-assisted laser desorption ionization time-of-flight mass spectrometry. J Chromatogr A, 2007. 1153(1-2): p. 291-9.

8. Lill, J.R. and V.J. Nesatyy, Microwave-assisted protein staining, destaining, and in-gel/in-solution digestion of proteins. Methods Mol Biol, 2012. 869: p. 521-32.

9. Osula, O., S. Swatkoski, and R.J. Cotter, Identification of protein SUMOylation sites by mass spectrometry using combined microwave-assisted aspartic acid cleavage and tryptic digestion. J Mass Spectrom, 2012. 47(5): p. 644-54.

10. Marshall, P.L., et al., Pressure cycling technology (PCT) reduces effects of inhibitors of the PCR. Int J Legal Med, 2013. 127(2): p. 321-33.

11. Powell, B.S., et al., Pressure cycling technology in systems biology. Methods Mol Biol, 2012. 881: p. 27-62.

12. Bal, G., Cauchy problem for ultrasound modulated EIT. arXiv, 2012. 1.

13. Lee, B., et al., Rapid and efficient protein digestion using trypsin-coated magnetic nanoparticles under pressure cycles. Proteomics, 2011. 11(2): p. 309-18.

14. Gross, V., et al., Tissue fractionation by hydrostatic pressure cycling technology: the unified sample preparation technique for systems biology studies. Journal of Biomolecular Techniques, 2008. 19: p. 189-99.

15. Gendelman, H.E., et al., Efficient isolation and propagation of human immunodeficiency virus on recombinant colony-stimulating factor 1-treated monocytes. Journal of Experimental Medicine, 1988. 167: p. 1428-41.

16. Go, E.P., et al., Glycosylation site-specific analysis of clade C HIV-1 envelope proteins. J Proteome Res, 2009. 8(9): p. 4231-42.

17. Hou, H. and H. Yu, Structural insights into histone lysine demethylation. Curr Opin Struct Biol, 2010. 20(6): p. 739-48.

18. Zheng, C. and J.J. Hayes, Structures and interactions of the core histone tail domains. Biopolymers, 2002. 68: p. 539-46.

Chapter 5

Summary and Conclusions

5.1. Summary and Conclusions

We looked directly at the effects of Meth on a macrophage function, cytokine production, in macrophages and a possible mechanism for the observed effects. Our study was the first exploratory and most comprehensive study for measuring the levels of cytokines in Meth exposed macrophages over time and as a result, determined that Meth increases the production of more pro-inflammatory cytokines than anti-inflammatory cytokines in the first few hours of administration. Cytokines play a large role in chemoattraction, proliferation, programmed cell death, cell phenotype switching, and regulation of inflammation. Further studies are needed to determine which of the cytokines expressed are secreted and the function they will have on surrounding target cells. However, it is clear that the dysregulation caused by Meth in the cytokines expressed in our study can have complex and numerous effects on other cell types and tissue. Another finding was that the cytokine changes are dynamic meaning they change based on concentration of Meth and time of exposure. One cytokine, in particular was strongly down-regulated, CCL7. The significance is CCL7 is it is critical for the clearance of cryptococcal neoformans, a fungal infection common in HIV-1 patients and Meth use exacerbates the pathogenesis. First, we investigated whether the silencing of CCL7 was due to DNA methylation but there was not a large enough increase that would yield gene repression. Therefore, we looked at which mechanisms induce CCL7 and found it is expressed by activation of TLR9 and accordingly, we explored the signaling pathway and the mediators that Meth might be altering to shift the expression. We measured by different means the levels of TLR9, IRAK, the activated state of IRAK, degradation of the inhibitory protein of NF-κB, IκB, and transcription factors such as STAT1, NF-κB, IRF7 and phospho-IRF7. None of these factors seemed to change due to Meth exposure, at least not at the times we measured and under the conditions we measured. Additional and more thorough work needs to be done on how the signaling factors that mediate

125

TLR9 signaling change due to Meth. But in conclusion Meth affects cytokine production in macrophages and is mediated, at least in part, by TLR9 signaling.

In the other study, we looked at HDAC1-6 and found that HDAC1 was significantly decreased in Meth exposed macrophages. There was a trend of decreased HDAC1 in HIV and HIV/Meth macrophages. The next step is to determine the effects of decreased HDAC1 on the functions of macrophages. Predictably, expression of viral loads would increase since HDAC1 is allows HIV to remain in a latent state [1]. Interestingly though, decreased HDAC1 in has been implicated in Meth-induced alterations of gene expression in the nucleus accumbens, a brain region responsible for feeling pleasure and reward, exacerbating addiction to Meth [2] These results suggest that the alterations in gene expression by HDAC1 can simultaneously worsen addiction and HIV infection.

5.2. Challenges and Future Directions

For our study we detected and measured levels of HDAC1 by three methods: densiometric quantification of immunoblots, qRT-PCR and confocal imaging. The biggest challenge came from quantitative Western blots of HDAC1. Despite including multiple donors, resulted in inconclusive data due to the large standard deviation preventing the statistical significance of the data. Although quantitative Western blots are common in the field, they are done improperly, regularly. Variability of densiometric analysis can be from differences in the most upstream step of processing cell cultures or lack of complete lysis of cells. Next, improper quantitation can result in differences due to the type of protein concentration method used for example: Pierce 660 versus Bradford versus absorbance at 280 nm, since each method exploits different properties of proteins. In conjunction with the protein concentration issue, is the oversaturation of a loading control like actin. Actin is so abundant in cells that it can easily reach the

detection limits of X-ray films and imaging softwares if loading more than 3 µg of cell lysate whereas, that amount is sometimes not enough to detect the protein of interest [3]. Other common loading controls like GAPDH are often used without first verifying that there is no effect on the expression with different treatments. Use of positive controls for Western blotting could significantly improve the quantitation for the protein of interest and a good positive control is a lysate that over expresses the gene interest. Incomplete separation of samples using SDS–PAGE usually comes from interfering reagents in the lysis buffer. To this end, there are commercial kits that remove the restricting chemical(s) but will most definitely cause a loss of proteins when purifying the sample. Thus, if blotting for more than one protein of interest with similar molecular weights one must decide if this cleaning up step is essential or overcome it by running two membranes, but both options result in loss or use of additional sample. Next, incomplete transfer of proteins to the PVDF membrane can occur to contribute to variations of densiometric analyses but the loss can easily be determined by staining the gel with Coomassie Brillant Blue. However, even if the step is not 100% efficient, Western blot is most likely not sensitive enough to detect the small difference in incomplete transfer of proteins. After transfer, membranes will be ready for primary antibodies but not all antibodies are not created equal thus giving rise to less than specific detection of the protein of interest and false positives or difficult time quantifying [4]. Running serial dilutions of the antibody control with different amounts of the positive control cell lysate can help you assess the quality of the antibody and can also prevent the oversaturation of the signal thus solving two problems at once. The issues mentioned were not known or foreseen when conducting the experiments and have taught me a lot.

In conclusion, Western blots should be used only for the detection of proteins in a sample or used in a semi-quantitative manner meaning the only conclusion is less or more due to a treatment. The alternative and always better approach to Western blot is

an enzyme-linked immunosorbent assay (ELISA) for detection and quantification of proteins and with recent advanced can be multiplexed with decreased variability, higher reproducibility (intra-variability versus inter-variability), and increased confidence (or decrease in false positives). However, the price of ELISA is positively correlated to the number of proteins desired to be quantified. Future work should therefore always utilize ELISA for protein quantification when available, otherwise implement a positive control between donors, preferably more than three donors or replicates and a lysate of commercial grade so that quality control has been performed and reproducibility is similar between lots. Also, running a separate blot with far less protein loaded for actin normalization simultaneously with samples so variability due to the electrophoresis apparatus is minimized including separation of proteins and protein transfer to membranes. Finally, the antibody quality and optimized concentration should be determined before being used on the membranes by doing serial dilutions with the positive control samples. This ensures linearity of signal and prevention of signal saturation.

Another challenge encountered with the conclusion of the Meth-induced up-regulation of acetylation on H3 lysine 18 and H4 lysine 5 is related to quantitative Westerns since there was no normalization of PTMs to the total protein. Therefore, all histone blots should have been normalized to the corresponding unmodified histone otherwise, it is unknown whether Meth-induced an up-regulation of total histone or just the PTM.

Future directions should incorporate the use of chromatin immunoprecipitation with qPCR for both HDAC1 and specific histone acetylation sites to determine the genes affected by the absence of HDAC1 in Meth exposed macrophages and crossed referenced to the genes associated with the increase of acetylation due to Meth. This will identify genes linked to HDAC1 but more importantly, can use bioinformatics on the data

to understand how the genes correlate to function(s) of the macrophage that make it more susceptible to infections, which is the ultimate goal of the study. Further investigation needs to go into the trend of decreased HDAC1 in the HIV and HIV/Meth treatments that never reached statistical significance in our experiments but are confident from literature and our preliminary results that HDAC1 is involved in HIV transcription and altered due to Meth.

5.3. References

1. Keedy, K.S., et al., *A limited group of class I histone deacetylases acts to repress human immunodeficiency virus type 1 expression.* J Virol, 2009. **83**(10): p. 4749-56.

2. Martin, T.A., et al., *Methamphetamine causes differential alteration in gene expression and patterns of histone acetylation/hypoacetylation in the rat nucleus accumbens.* PLoS One, 2012. **7**(3): p. e34236.

3. Hammond, M., et al., *A method for greater reliability in Western blot loading controls: stain-free total protein quantitation*, BioRad, Editor.

4. Haverland, N., et al., *Immunoreactivity of anti-gelsolin antibodies: implications for biomarker validation.* J Transl Med, 2010. **8**: p. 137.

ELSEVIER LICENSE
TERMS AND CONDITIONS

Oct 01, 2015

This is an Agreement between Ariel Burns ("You") and Elsevier ("Elsevier"). It consists of your order details, the terms and conditions provided by Elsevier, and the payment terms and conditions.

All payments must be made in full to CCC. For payment instructions, please see information listed at the bottom of this form.

Supplier	Elsevier Limited The Boulevard,Langford Lane Kidlington,Oxford,OX5 1GB,UK
Registered Company Number	1982084
Customer name	Ariel Burns
Customer address	985800 Nebraska Medical Center OMAHA, NE 68198
License number	3712101024997
License date	Sep 18, 2015
Licensed content publisher	Elsevier
Licensed content publication	Analytical Biochemistry
Licensed content title	Pressure-assisted sample preparation for proteomic analysis
Licensed content author	Pawel P. Olszowy,Ariel Burns,Pawel S. Ciborowski
Licensed content date	1 July 2013
Licensed content volume number	438
Licensed content issue number	1
Number of pages	6
Start Page	67
End Page	72
Type of Use	reuse in a thesis/dissertation
Intended publisher of new work	other
Portion	full article
Format	electronic
Are you the author of this Elsevier article?	Yes
Will you be translating?	No
Title of your thesis/dissertation	Effects of Methamphetamine, HIV-1, or Combination Antiretroviral Therapy on Macrophages
Expected completion date	Dec 2015
Estimated size (number of pages)	140
Customer Tax ID	USNebraska
Elsevier VAT number	GB 494 6272 12

131

Price	0.00 USD
VAT/Local Sales Tax	0.00 USD / 0.00 GBP
Total	**0.00 USD**

This is a License Agreement between Ariel Burns ("You") and Elsevier ("Elsevier") provided by Copyright Clearance Center ("CCC"). The license consists of your order details, the terms and conditions provided by Elsevier, and the payment terms and conditions.

All payments must be made in full to CCC. For payment instructions, please see information listed at the bottom of this form.

Supplier	Elsevier Limited The Boulevard,Langford Lane Kidlington,Oxford,OX5 1GB,UK
Registered Company Number	1982084
Customer name	Ariel Burns
Customer address	985800 Nebraska Medical Center
	OMAHA, NE 68198
License number	3720320118769
License date	Sep 18, 2015
Licensed content publisher	Elsevier
Licensed content publication	Immunobiology
Licensed content title	Acute exposure to methamphetamine alters TLR9-mediated cytokine expression in human macrophage
Licensed content author	Ariel Burns,Pawel Ciborowski
Licensed content date	Available online 8 September 2015
Licensed content volume number	n/a
Licensed content issue number	n/a
Number of pages	1
Start Page	None
End Page	None
Type of Use	reuse in a thesis/dissertation
Intended publisher of new work	other
Portion	full article
Format	electronic
Are you the author of this Elsevier article?	Yes
Will you be translating?	No
Title of your thesis/dissertation	Effects of Methamphetamine, HIV-1, or Combination Antiretroviral Therapy on Macrophages

Expected completion date	Dec 2015
Estimated size (number of pages)	
Customer Tax ID	USNebraska
Elsevier VAT number	GB 494 6272 12
Permissions price	0.00 USD
VAT/Local Sales Tax	0.00 USD / 0.00 GBP
Total	0.00 USD